UNIVERSITY OF CALIFORNIA
SANTA BARBARA

Mechanisms underlying behaviors in *Drosophila* and *Aedes*: lessons from circadian rhythms, taste and touch

A dissertation submitted in partial satisfaction of the requirements for the degree Doctor of Philosophy in Molecular, Cellular & Developmental Biology

by

MENGLIN LI

Committee in charge:
Professor Craig Montell, Chair
Professor Sung Soo Kim
Professor Denise J. Montell
Professor Julie H. Simpson

December 2023

The dissertation of Menglin Li is approved.

_____

Sung Soo Kim

_____

Denise J. Montell

_____

Julie H. Simpson

_____

Craig Montell, Chair

July 2023

Mechanisms underlying behaviors in *Drosophila* and *Aedes*: lessons from circadian rhythms, taste and touch

by

Menglin Li

ACKNOWLEDGEMENTS

I would like to express my deepest gratitude to my mentor, Dr. Craig Montell, for his guidance, support and encouragement throughout my PhD journey. He has been a great source of inspiration and motivation for me, and has taught me how to think critically, communicate effectively and conduct high-quality research. I am honored to have been his student and to have learned from his expertise and wisdom.

I would like to thank my committee members, Dr. Denise Montell, Dr. Julie Simpson and Dr. Sung Soo Kim, for their valuable feedback and guidance through the years and on my final dissertation. They have challenged me to improve my research questions, methods and interpretations, and have provided me with constructive criticism and suggestions. I appreciate their time, expertise and support throughout my PhD program.

I am also very thankful to my lab mates, Angela, Dhananjay, Ryan, Geoff, Jiangqu, Zijing, Anindya, Raman, Pratik, David, Nick, Avinash, Xiaodong, Izel, Declan, Emma, Arumoy and Subash, for their friendship, collaboration and assistance. They have made the lab a fun and stimulating environment to work in and have helped me with various aspects of my projects. I enjoyed our discussions and celebrations, and I have learned a lot from their diverse perspectives and experiences. I would like to express my appreciation especially to Angela, Dhananjay and Ryan as they are my best friends in lab and have always been supporting me not only in research but also in personal life.

I would like to acknowledge the contributions of the rotation students Nikola and Annalise, who have worked with me on some experiments and data analysis. I appreciate their enthusiasm, curiosity and diligence. I would also like to thank the undergraduates who have

assisted me in the lab, especially Kara, Anvitha and Yiqin. They have shown great interest and potential in research, and I hope they will pursue their scientific passions in the future.

I am grateful to my parents for their unconditional love and support throughout my life. They have always believed in me and encouraged me to pursue my dreams. They have also sacrificed a lot for me to have the opportunities that I have today. I dedicate this dissertation to them.

I would like to thank my boyfriend Jiawei for his love, patience and understanding. He has been my best friend and partner in crime for the past six years. He has always been there for me through thick and thin and has made me laugh even in the most stressful times. I am lucky to have him by my side.

I would also like to thank my best friends Nan, Yuerou and Naixin for their friendship and support. They have been with me since middle school and have witnessed my growth as a person and a researcher. They have always listened to me venting about my frustrations and celebrating my achievements.

Finally, I would like to thank all the friends that I met at UCSB, especially Yichen, Ming, Yue, Weiyi, Xiaofan and Yi. They have enriched my life with their kindness, generosity and fun. They have made my time at UCSB memorable and enjoyable.

I am truly blessed to have all these wonderful people in my life. Without them, this dissertation would not have been possible.

Curriculum Vitae

MENGLIN LI

October 2023

EDUCATION

9/2017 – 10/2023	**Ph.D.**, Molecular, Cellular and Developmental Biology University of California, Santa Barbara
9/2017 – 6/2020	**M.A.**, Molecular, Cellular and Developmental Biology University of California, Santa Barbara
9/2013 - 7/2017	**B.S.**, Biology, College of Life Sciences Nankai University, Tianjin, China

FELLOWSHIPS AND GRANTS

2021-22	2021-2022 Doctoral Student Travel Grant
2022	MCDB/Shing and Sheng-Yung Chang Graduate Student Travel Award

AWARDS AND HONORS

2022	63rd Annual Drosophila Research Conference Poster Presentation Award
2022	UCSB Grad Slam Competition - Finalist
2022	2nd place in 2022 New Venture Competition, UCSB
2022	Impact Award in 2022 New Venture Competition, UCSB
2017	Undergraduates Research Activities "100 Projects" of Nankai University

RESEARCH EXPERIENCE

2017-23	**Graduate Student Researcher** (Dr. Craig Montell lab) Department of Molecular, Cellular and Developmental Biology University of California, Santa Barbara
2014-17	**Undergraduate Research Assistant** (Dr. Jintang Dong lab) College of Life Sciences, Nankai University
2016	**Summer Research Intern** Winship Cancer Institute, Emory University

ADDITIONAL COURSEWORK AND EDUCATION

2021-2023 The Graduate Program in Management Practice Certificate

TEACHING EXPERIENCE

2018 Teaching Assistant, Intro Bio Lab MCDB 1BL, UCSB
2019 Teaching Assistant, Concepts of Biology MCDB 20, UCSB
2020 Teaching Assistant, Developmental Biology MCDB 112, UCSB
2021 Teaching Assistant, Developmental Biology MCDB 112, UCSB
2022 Teaching Assistant, Developmental Biology MCDB 112, UCSB

PUBLICATIONS

- **Li, M.**, Meyerhof G., *et al*. (2023), Night owl chronotype caused by disruption of a distinct subset of photoreceptor cells. ***Cell Reports***. In revision
- Kaduskar, B., Kushwah, R., Auradkar, A., Guichard, A., **Li, M.**, *et al*. (2022), Reversing insecticide resistance with allelic-drive in Drosophila melanogaster. ***Nature Communications***, 13, 291.
- Hodge, B.A., Meyerhof, G.T., Katewa, S.D.,Lian, T., Lau, C., Bar, S., Leung, N., **Li, M.**, *et al.* (2022), Dietary restriction and the transcription factor *clock* delay eye aging to extend lifespan in *Drosophila Melanogaster*. ***Nature Communications***, 13, 3156.
- Zhang, B., Li, Y., Wu, Q., Xie, L., Barwick, B., Fu, C.,Li, X., Wu, D., Xia, S., Chen, J., Qian, W., Yang, L., Osunkoya, A., Boise, L., Vertino, P., Zhao, Y., **Li, M.**, *et al.* (2021), Acetylation of KLF5 maintains EMT and tumorigenicity to cause chemoresistant bone metastasis in prostate cancer. ***Nature Communications***, 12, 1714.
- Wu, Q., Fu, C., **Li, M.**, *et al*. (2019), CINP is a novel cofactor of KLF5 required for its role in the promotion of cell proliferation, survival and tumor growth. ***International journal of cancer***, 144: 582-594.

ORAL PRESENTATIONS

1. **Li M.,** Meyerhof, G.T., Simones K., Aluri A., Montell C., Regulation of chronotype in fruit flies. UCSB Grad Slam Preliminary Round 2022, Santa Barbara, CA.
2. **Li M.,** Meyerhof, G.T. Simones K., Aluri A., Montell C., Sleep chronotype: from fruit flies to humans. UCSB Grad Slam Final Round 2022, Santa Barbara, CA.

POSTER PRESENTATIONS

1. **Li M.,** Meyerhof, G.T. Simones K., Aluri A., Shen Y., Montell C., Regulation of chronotype in fruit flies. Presented at 25th Annual MCDB-BMSE Retreat and Symposium, UC Santa Barbara, 2022.

2. **<u>Li M.,</u>** Meyerhof, G.T., Simones K., Aluri A., Montell C., rhodopsin 3 regulates circadian periodicity. Presented at 63rd Annual Drosophila Research Conference, San Diego, 2022.

ABSTRACT

Mechanisms underlying behaviors in *Drosophila* and *Aedes*: lessons from circadian rhythms, taste and touch

by

Menglin Li

The five classical senses including vision, taste, smell, hearing, and touch, are being used by us humans and all the living organisms in the world constantly. These senses help us perceive signals from the environment around us like colors, flavors, aromas, sounds and textures. Most importantly, these senses are essential for us to survive. In this dissertation, we will describe the mechanisms underlying behaviors like circadian rhythms, taste, and touch in *Drosophila* and *Aedes aegypti*. We will describe the discovery of the importance of a minor group of rhodopsins in regulating sleep chronotype in *Drosophila*. Essentially, we identified that a small subset of *Drosophila* photoreceptor cells that express *rhodopsin 3* (*rh3*) is required for regulating sleep chronotype. *rh3* mutants displayed an evening chronotype with delays in sleep, activity, feeding, and core clock gene expression. The *rh3* mutants possessed a longer internal periodicity than control flies. And importantly, we found that the evening chronotype in *rh3* mutants could be rescued by the alignment of external and internal periodicities or restricted time of feeding.

In this study, we also explored the taste preferences of mosquitoes for different carboxylic acids as acid taste is important for their host seeking behavior and nectar feeding behavior. We found that mosquitoes are aversive to low pH food and have specific preferences for the carboxylic bone of lactic acid. Additionally, we also investigated the function of a mechanosensor, *tmem63*, in texture detection during blood and nectar feeding

behavior of mosquitoes. We verified its expression in the proboscis of mosquitoes and also observed that this receptor was involved in the detection of food texture.

This dissertation combined research from both *Drosophila* and *Aedes aegypti* as they share homolog genes and similar sensory organs that are important for specific behaviors and enable them to survive and thrive in their habitats. Studies in *Drosophila* advanced and accelerated our research in *Aedes aegypti*, which is the most dangerous animal in the world. Through this research, we hope to provide a better understanding of their circadian rhythm, taste perception and mechanosensation, which can shed light on finding solutions for sleep disorders treatments and suppressing the spreading of infectious diseases by mosquitoes.

TABLE OF CONTENTS

INTRODUCTION

Humans and all living organisms rely on their five classical senses, namely vision, taste, smell, hearing, and touch, to interact with the environment around them to survive and thrive. We accept environmental cues through distinct types of receptors and convert them into electrical signals in specific neurons which eventually project to different areas of our brains and result in various behavior decisions.

One of the most important environmental cues to humans is the daily light. The lights on and lights off timing regulate our circadian rhythm which aligns all our other physiological behaviors like sleeping, exercising, feeding and memory formation, etc. Sleep disorders have been commonly found in modern society. People with delayed sleep phase syndrome or evening sleep chronotype especially correlates with increased risk of getting metabolic diseases like diabetes, neural degeneration diseases like Alzheimer's or mental health issues like depression in humans. Thus, it is critical to understand the regulation of delayed sleep or evening sleep chronotype. Likewise, *Drosophila* accepts environmental cues like light through their vision system and displays a similar circadian rhythm as humans. They also have a 24-hour pattern of activity and sleep which is regulated by circadian clocks in their brains. *Drosophila* sleeps in ways that is comparable to mammalian sleep that they meet a whole set of criteria that characterize sleep including a stereotyped sleep posture, an increased arousal threshold, reduced brain neurons activity, a homeostatic response to sleep deprivation and is regulated by circadian rhythm. *Drosophila* has been used as one of the most important model organisms to study sensory biology due to its small size, quick

generation period, easy-manipulated genetics, and well-established tool libraries. Thus, we used Drosophila to study the mechanisms underlying sleep chronotypes in this study. So far, all the genes that are known to regulate sleep chronotypes are involved in the central clocks. However, rhodopsins, which are the light sensors expressed in *Drosophila*'s compound eyes, have been shown to be important for regulating the circadian rhythm. Our research explored whether rhodopsins are required for regulating sleep chronotypes. We identified that a minor group of *Drosophila* photoreceptor cells expressing rhodopsin 3 (*rh3*) play a pivotal role in determining the chronotype. *rh3* mutants exhibited an evening chronotype, characterized by delays in sleep onset, activity patterns, feeding habits, and the expression of core clock genes. Importantly, these mutants exhibited a prolonged internal periodicity compared to control flies. Intriguingly, we demonstrated that the evening chronotype in *rh3* mutants could be rescued through the alignment of external and internal biological rhythms or by restricting their feeding time. Thus, we hope to provide a novel idea for sleep disorder treatments.

Drosophila and *Aedes aegypti*, despite their differences, share homologous genes and possess similar sensory organs that are essential for their physiological behaviors, enabling them to survive and thrive in their respective habitats. The knowledge derived from our studies on *Drosophila* greatly accelerated our research on *Aedes aegypti*, which is the most dangerous animal on the planet due to its role in spreading infectious diseases.

The mosquitoes, *Aedes aegypti*, spread infectious diseases like Zika, dengue and yellow fever in the world and put billions of people in danger each year. Female mosquitoes specifically need to feed on blood for their egg development. *Aedes* mosquitoes are more attractive to

humans than other animals and they use a whole set of sensory cues to target the host including CO2, heat, human odors and vision, etc. After landing on a host, mosquitoes use their proboscis and tarsi to detect the tastants of the food resources and decide to feed or not. However, little is known about their taste preferences. Thus, we focused on investigating their taste preferences for various carboxylic acids. Our findings unveiled the mosquitoes' aversion to low pH food and their specific attraction for the lactate. In addition to our explorations into taste, we also studied the function of a mechanosensory receptor, *tmem63*, in texture detection during blood and nectar feeding behaviors in mosquitoes. We verified the expression of *tmem63* in the proboscis of mosquitoes and also found its involvement in detecting food texture during blood feeding behaviors.

This dissertation aims to provide a deeper understanding of the mechanisms underlying circadian rhythms, taste perception, and mechanosensation in insects. We hope to contribute to the development of novel treatments for sleep disorders and to find innovative strategies that can mitigate the transmission of infectious diseases by mosquitoes.

I. NIGHT OWL CHRONOTYPE CAUSED BY DISRUPTION OF A MINUTE SUBSET OF PHOTORECEPTOR CELLS

This chapter is adapted from an unpublished manuscript: Menglin Li, Geoff Meyerhof, Nicolas Debeaubien, Kara Simones, Anvitha Aluri, Yiqin Shen and Craig Montell. "Night owl chronotype caused by disruption of a minute subset of photoreceptor cells."

ABSTRACT

Chronotype is the proclivity to engage in behaviors at certain times of the day, such as when to sleep or wake up. However, the mechanisms regulating chronotype are elusive. Here, we identified a small subset of *Drosophila* photoreceptor cells that express *rhodopsin 3* (*rh3*), and regulate chronotype. *rh3* mutants adopt an evening chronotype characterized by delays in sleep, activity, feeding, and clock gene expression. In addition, they display a long internal periodicity. If they are housed under an extended circadian cycle that matches their long periodicity, or subjected to time-restricted feeding, they exhibit an intermediate chronotype. Mutations in the clock gene *period* that extend or shorten periodicity, adopt a morning or evening chronotype, respectively. However, under circadian cycles matching their internal periodicity, they show an intermediate chronotype. We conclude that *rh3* photoreceptor cells regulate chronotype, and altered chronotypes can result from mismatch between the periodicities of internal and external clocks.

INTRODUCTION

Humans and other animals have a strong propensity to fall asleep and wake up at particular times of the day. People with a morning preference, or morning chronotype, are often referred to as "early birds" or "morning larks," because they fall asleep and wake up early, and are most energetic in the morning. Those with the opposite chronotype are "night owls," and sleep and wake up later in the day. The effects of chronotype on behavior extend beyond just sleep, as chronotype also impacts the timing of feeding, cognition, and sociability.[1] Furthermore, chronotype can affect health. In humans, an evening chronotype is associated with an increased risk for several metabolic and mental disorders, including type 2 diabetes and depression.[2-5] Chronotype is thought to be influenced by an animal's circadian rhythm—the endogenously generated ~24-hour cycle that aligns behavior, metabolism, and physiology with predictable changes in the environment caused by the rising and setting of the sun.[3,6-8] Chronotype can differ significantly among individuals, and is in part genetically determined.[9-17]

Like humans, the fruit fly, *Drosophila melanogaster,* also exhibits a chronotype as well as a robust circadian rhythm, the latter of which is set by endogenous circadian clocks.[14,18-22] The fly's ~24-hour pattern of activity and sleep is regulated by clocks in ~150 pacemaker neurons in the brain.[23,24] The pacemaker neurons entrain to environmental lighting cues, both directly, via light-sensing proteins, and indirectly, via the compound eye, ocelli, and Hofbauer-Buchner eyelets.[25-27] Similarly, clocks in the mammalian suprachiasmatic nucleus, a population of hypothalamic neurons, set sleep and activity rhythms, and are also entrained from light sensed by the eye.[28]

Light is the strongest zeitgeber for setting circadian rhythms, and in flies, different classes of photoreceptor cells have distinct impacts on circadian biology.[29-32] In this work, we

employed *Drosophila* as an animal model to test whether light sensing by a specific class of photoreceptor cells in the eye plays a role in regulating chronotype. Each of the ~800 repeat units in a compound eye harbor eight photoreceptor cells, six of which (R1 to R6) extend the full depth of the retina and express the rhodopsin Rh1.[33,34] The remaining two photoreceptor cells, R7 and R8, extend only through the distal and proximal halves of the retina, respectively.[35] Different subsets of the R7 photoreceptor cells express either Rh3 or Rh4,[36,37] while the R8 cells express either Rh5 or Rh6.[38-40] Thus, Rh1 is the major rhodopsin as it is expressed at much higher overall levels in the compound eyes than the other four rhodopsins combined. Three small light-sensitive organs (ocelli) atop the head express Rh2,[41,42] the extraretinal Hofbauer–Buchner eyelet beneath the posterior margin of the compound expresses Rh6,[43] while a subset of neurons in the brain express Rh7,[32,44] and in R8 photoreceptor cells and the Hofbauer–Buchner eyelet.[44]

We found that mutation of *rhodopsin 3* (*rh3*), which inactivates only ~30% of the R7 photoreceptor cells in the compound eyes, profoundly shifts the sleep patterns to later times, causing the flies to adopt an evening chronotype. In contrast, mutations disrupting other rhodopsin genes had either no or minor effects on chronotype. Inactivating just a portion of the neurons that are downstream of *rh3*–those in the dorsal rim area of the eye (Dm8 neurons), is sufficient to recapitulate the evening chronotype of the *rh3* mutant. The *rh3* mutant flies also exhibit delays to the timing of their feeding, shifted expression of central and peripheral core-clock-genes, and an elongated circadian periodicity. We found that optogenetic activation of *rh3*-positive R7 cells with CsChrimson, or activation with Rh5, restored a normal chronotype and circadian rhythm to *rh3* mutants, indicating that this subset of photoreceptor cells rather than Rh3 per se contributes significantly to the phase of

circadian behaviors. Moreover, our data indicate that differences in chronotype can stem from the misalignment of external and internal periodicities, and can be suppressed by behavioral modifications, such as time-restricted feeding.

RESULTS

Loss of *rh3* sets an evening chronotype in sleep and feeding

In order to determine whether which if any of the photoreceptor cells in the compound eyes, ocelli, Hofbauer-Buchner eyelets or the brain affect chronotype, we took advantage of the differential expression of rhodopsins in different classes of photoreceptor cells, and the availability of a full set of rhodopsin (*rh1–rh7)* mutants. To screen the rhodopsin mutations for their effects on chronotype, we recorded the locomotor patterns of wild-type and rhodopsin mutant flies using the *Drosophila* Activity Monitoring (DAM) system,[45,46] which is performed by placing individual flies in clear glass vials, and recording their activities in one minute bins via an infrared sensor. We scored sleep as five consecutive minutes of inactivity, as described previously.[47-49] Female wild-type control flies (w^+,w^{1118}: Canton-S flies outcrossed to w^{1118} but retained the w^+ gene) display maximum activities at dawn and dusk, while sleep is at its nadir at these times.[49,50] (Figures 1A and S1A) In the middle of the day, there is a peak in sleep, known as the "daytime siesta" (Figures 1A and S1A), which is regulated in part by circadian pacemaker neurons.[51,52]

To quantify the effects of the rhodopsin mutations on chronotype, we considered both the daytime and nighttime components of sleep. We defined evening chronotype as a delay in the average time of the daytime siesta peak, as well as a reduction in early nighttime sleep (early-night sleep index, ENSI), which we quantified by dividing the total sleep from the first four hours of night (A = ZT 12–16; ZT 0 indicates lights on; ZT 12 indicates light off) by the total

nighttime sleep (B = ZT 12–24; Figures 1A, 1B and S1A–1C). Conversely, morning chronotype is an advance in the timing of the daytime siesta peak and an increase in early nighttime sleep (Figure S1B). Null mutations in six out of the seven rhodopsin genes did not have major effects on chronotype (Figures S1A and S1C). These include mutations disrupting the major rhodopsin, Rh1 (Figures S1A and S1C).

In contrast to all of the other rhodopsin mutations, null mutations eliminating a minor rhodopsin (Rh3) expressed in only a minority (30%) of one out of eight photoreceptor cells (R7), displayed an evening chronotype (*rh3*^{2}, *rh3*^{L}, or transheterozygous *rh3*$^{2/L}$; Figures 1A and S1A). The *rh3* mutants exhibited a nearly 2-hour delay in the peak of their daytime siesta (1.7 ±1.1 h), as well as a delay in the onset of nighttime sleep (Figures 1A, 1B, S1A and S1C; ENSI: control, 0.32 ± 0.03; *rh3*$^{2/L}$. 0.15±0.05). Concordant with their delay in nighttime sleep, *rh3* mutants also had increased early nighttime activity, characterized by an evening activity peak that was extended into the night (early-night activity index, ENAI; Figures 1C and 1D). Because of the limited spatial resolution of the DAM assay, we validated the sleep and activity behavior of *rh3* mutants using video tracking software, which provided results similar to the DAM system (Figure S1D–S1F; see STAR Methods).

Flies that are sleeping exhibit another key sleep behavior, namely a decreased responsiveness to external stimuli.[49] As a consequence, sleeping flies require a greater arousal stimulus to induce activity. To test whether the timing of the peak arousal threshold was delayed in the *rh3* mutants we used a protocol similar to what has been described previously.[53,54] We housed flies in a custom behavioral arena that delivered a set of three gradually-increasing vibration stimuli (0.05–0.38 m/s^2) once every two hours over the course of 24 hours (Figures S1G and S1H). Using video tracking, we determined the arousal

threshold by determining the minimum vibration intensity required to induce locomotion in previously quiescent flies. We found that *rh3* mutant flies had a consistently higher arousal threshold than control flies throughout the day (Figure 1E; ZT 2, 6.2, 8.2, and 10.3), and that their peak daytime arousal threshold was delayed by ~2 hours (ZT 4.1 in control vs. ZT 6.2 in $rh3^{2/L}$ mutants). In the early night (ZT 12.4), *rh3* mutants were more responsive to the vibration stimuli than the control (~0.21 m/s^2 in control vs. ~0.11 in $rh3^{2/L}$; p=0.007), suggesting that the onset of deep nighttime sleep was also delayed in *rh3* mutants.

While there was a delay in the peak of the siesta in the *rh3* mutants, there was little if any delay in the onset of the siesta, resulting in an increased duration of the siesta. However, if the *rh3* mutants exhibited an evening chronotype, we would expect a delay in the initiation of the siesta. An abrupt change in lighting conditions can startle animals and induce locomotion that is not necessarily governed by the circadian clock (a masking effect).[55] Indeed, during the night period (ZT 12–24), the onset of sleep was greatly delayed in the $rh3^{2/L}$ flies (Figure 1A). Therefore, we wondered whether the lack of delay in the daytime siesta in the mutant flies was due to a startle effect resulting from the sudden onset of light at ZT 0.

To reduce or remove the startle effect, we conducted two types of analyses. First, we compared the activity patterns of control and *rh3* mutants under conditions in which the light intensity gradually increased in the morning, and gradually decreased in the evening. To accomplish this, we exposed flies housed with light that ramped up in intensity from ZT 0–6 and ramped down from ZT 6–12 (Figure 1F and 1I). This revealed that the onset of both the morning and evening activity peaks were delayed significantly in the *rh3* mutants (Figures 1F–1H). In addition, using the ramping paradigm, we found that the *rh3* mutation caused the daytime siesta to be delayed by ~1 hour (Figures 1I and 1J).

Second, to fully eliminate any startle effect from light, we examined the timing of the morning peak and the siesta during the first subjective day after shifting from light-dark to dark-dark conditions. We found that in the *rh3* mutant, the subjective morning activity peak was delayed (Figures 1K and 1L) as well as the daytime siesta (Figures S1I and S1J). The results from the ramping light conditions, and from the subjective day during the dark-dark period indicate that the light-induced startle response masks the delay in siesta and morning activity in the *rh3* mutants. These data support the conclusion that mutation of *rh3* delays the phase of morning and evening locomotion and sleep, thereby displaying an evening chronotype.

In addition to activity and sleep, variations in chronotype have also been reported to impact the timing of feeding, which is in part set by central and peripheral circadian clocks.[56-58] To monitor the daily feeding of *rh3* mutant flies, we used the Fly Liquid Interaction Counter (FLIC) assay.[57] In this assay, flies are individually housed with *ad libitum* access to a liquid food source. Interaction of the proboscis with the food completes an electrical circuit, which serves as the basis for scoring feeding intention. Consistent with previous reports,[57,59] wild-type flies display a pronounced evening peak in feeding intention, while a morning peak is much more difficult to assign (Figure 1M). Therefore, we focused on the timing of the evening peak, and found that it was greatly delayed in $rh3^{2/L}$ (Figures 1M; control, ZT 11.7; $rh3^{2/L}$, ZT 15.5), and that the total amount of nighttime food interactions was also significantly increased in the mutant (Figure 1N; control, 31.0 ± 6.0 s; $rh3^{2/L}$, 61.4 ± 12.0 s). These results indicate that loss of *rh3* delays the phase of multiple circadian behaviors, creating an evening chronotype that profoundly affects the timing of sleep, activity, and feeding.

Circadian activation of *rh3*-positive neurons restores chronotype in *rh3* mutants

To validate the role that *rh3* plays in setting chronotype, we first tested whether we could rescue a normal chronotype in $rh3^{2/L}$ transheterozygous mutants by expressing a wild-type *rh3* transgene (*UAS-rh3*) under the control of an *rh3-Gal4* (*rh3>rh3;*$rh3^{2/L}$). We found that introducing the *rh3* transgene in the mutant flies restored a normal chronotype (Figures 2A and 2B). It advanced the peak of the daytime siesta (Figure 2A) and increased the early-night sleep index (Figure 2B). Furthermore, the *rh3* transgene also suppressed nighttime activity (Figures 2C and 2D) and feeding (Figures 2E and S2A) in $rh3^{2/L}$ mutant flies. To address whether the rescue transgene advanced the morning peak and onset of the siesta in the *rh3* mutants, we analyzed the onset of activity and the onset of the siesta in flies expressing the *rh3* transgene during the subjective first day under dark-dark conditions. This revealed that the *rh3* transgene advanced the morning activity peak (Figures 2F and 2G) as well as the siesta (Figures S2B and S2C).

The maximum light sensitivity of Rh3 is in the near ultraviolet (UV) range (330 nm).[60,61] Therefore, we examined whether the UV-light sensitivity of Rh3 was critical for its role in regulating chronotype. To test this, we expressed one of two non-UV light sensors in place of *rh3.* Namely, we expressed either the red-light sensitive channelrhodopsin, CsChrimson, in place of Rh3 (*rh3>CsChrimson;*$rh3^{2/L}$*),* or the blue light sensor, Rh5, and measured these flies' chronotype. We housed *rh3>CsChrimson;*$rh3^{2/L}$ flies under a 12 hour:12 hour light/dark cycle and activated CsChrimson during the light phase with a narrow-peak red light (592 nm). We found that optogenetically activating *rh3* neurons in *rh3* mutant flies (*rh3>CsChrimson;*$rh3^{2/L}$) recovered an intermediate chronotype. Relative to the *rh3* mutant

(*rh3-Gal4*/+;*rh3*$^{2/L}$), it increased the early-nighttime sleep index, and decreased early-nighttime locomotor activity (Figures S2D—S2G). It may have also advanced the daytime siesta, although we cannot exclude that this may be due to a shortening of the duration of the siesta (Figure S2D). Additionally, optogenetic activation of *rh3* neurons also suppressed nighttime feeding (Figures S2H and S2I). However, expressing the blue-light sensitive rhodopsin Rh5 in place of Rh3 only partially restored a normal chronotype. It increased early nighttime sleep, but did not significantly change the timing of the daytime siesta (Figures S2J and S2K). These results reveal that the evening chronotype exhibited by *rh3* mutants does not result from an inability to sense UV light per se, as CsChrimson can substitute for Rh3. However, not all light receptors fully recapitulate the effect of Rh3 in *rh3*-expressing cells, as Rh5 only partially suppressed the evening chronotype of *rh3* mutants.

Given that some rhodopsins function in tissues outside of the eye,[32,62-66] we next sought to verify that Rh3 functions in R7 photoreceptor cells to regulate chronotype. To this end, we used a *Gal4* driver that is only expressed in the R7 photoreceptors (*inaF-C-Gal4*)[67] to restore expression of *rh3* in a *rh3* mutant background. Compared to the *rh3* mutant (*UAS-rh3*/+;*rh3*$^{2/L}$), the early-night sleep index was increased in *inaF-C>rh3*;*rh3*$^{2/L}$ flies (Figure S3A and S3B), the early-night activity index was also significantly decreased (Figures S3C and S3D), although it is not clear if there was an effect on the timing of the daytime siesta rather than a shortening of the daytime siesta (Figure S3A), since during the first day of dark-dark conditions, the *inaF-C>rh3* rescue transgene did not cause the initiation of the siesta to significantly advance (Figures S3E and S3F). However, using *inaF-C-Gal4* to drive expression of Rh4 (*inaF-C>rh4*;*rh3*$^{2/L}$) in an *rh3* mutant background only partially restored a normal phenotype. It advanced the midpoint of the peak of the daytime siesta (Figures S3A

and S3B), decreased early-night activity (Figures S3C and S3D), but failed to increase early-nighttime sleep (Figures S3A and S3B). Thus, we conclude that *rh3* is required in a subset of the R7 photoreceptors for a normal chronotype, but Rh4 cannot completely suppress the evening chronotype phenotype of *rh3* mutants.

Contribution of Dm8 neurons to chronotype

Unlike R1–6 cells, R7 cells project their axons through the lamina portion of the optic lobes, to a deeper optic lobe layer called the medulla, where they couple to specific Dm8 neurons depending on whether the R7 cell expresses *rh3* or *rh4*, and whether it is located in the dorsal rim area (DRA) of the eye.[68-70] Therefore, we characterized the role of Dm8 neurons in regulating chronotype. Although R7 photoreceptors inhibit downstream Dm8 neurons, there is a mutual inhibition between neighboring Dm8 cells.[71,72] We tested whether activating or inhibiting all Dm8 neurons would recapitulate the evening chronotype of *rh3* mutants. To this end, we used the *Ort-C2b-Gal4* to drive expression of either a bacterial depolarization-activated Na^+ channel, NaChBac, (*Dm8>NaChBac*)[73] or tetanus toxin (*Dm8>TNT*) in all Dm8 neurons and measured the flies' sleep and activity. Surprisingly, the timing of the circadian activity profile of these flies was relatively unperturbed (Figures S3G and S3H), suggesting that mutual inhibition or activation of *rh4*- and *rh3*-expressing photoreceptor cells may result in a normal chronotype. To address this possibility, we first examined the chronotype of flies devoid of all R7 cells by assaying the sleep and activity patterns of *sevenless (sev^{14})* mutant flies, which lack R7 cells.[74] Similar to *Dm8>NaChBach* and *Dm8>TNT* flies, the *sev^{14}* mutant also displayed a normal chronotype (Figures S3I and S3J). We also tested the chronotype of *rh4,rh3* double mutants, which lack signaling from all

R7 cells. Unlike flies singly mutant for *rh3,* the *rh4,rh3* double mutants displayed a normal chronotype (Figures S4A and S4B).

Our results with the *sev*^{14} mutant and the *rh4,rh3* double mutant are consistent with the model that simultaneous inhibition of *rh4*- and *rh3*-expressing photoreceptor cells restores the timing of sleep and activity. To further probe this possibility, we selectively inhibited the Dm8 neurons (DRA1 neurons) downstream of just the R7 cells in the DRA ($_{DRA}$R7 cells), all of which express Rh3.[69,75,76] Blocking signaling from DRA1 neurons, using a *DRA1-GAL4* to drive expression of tetanus toxin (*DRA-Dm8>TNT*), caused the flies to adopt an evening chronotype that was reminiscent of the *rh3* mutant phenotype–i.e. delayed timing of sleep and increased nighttime activity (Figures 2H-2K). In total, these results demonstrate that inactivating signaling emanating from $_{DRA}$R7 cells is sufficient to cause flies to adopt an evening chronotype, which can be restored by simultaneously blocking the signaling from *rh4*-expressing R7 cells.

Rh3 regulates the phase and amplitude of central and peripheral circadian clock gene expression

Given that *rh3* mutants showed a phase delay in their sleep, activity, and feeding patterns, we wondered whether interrupting the signaling from *rh3* photoreceptor cells might affect the expression of peripheral and central core-clock genes. On the molecular level, endogenous circadian rhythms in flies, mammals, and other animals are set by transcriptional-translational negative feedback loops with 24-hour periodicities.[6,28,77] While the central circadian clock in the brain is primarily entrained to light, peripheral circadian clocks can be entrained to additional time-giving cues (zeitgebers), including the time of feeding.[78]

To test the requirement for *rh3* photoreceptor cells for the timing of expression of peripheral core-clock genes, we performed real-time PCR (RT-qPCR) experiments to measure the oscillations in relative mRNA levels of *clock* (*Clk*), *par-domain protein-1 epsilon* (*Pdp1ε*), *period* (*per*), and *timeless* (*tim*).[79-83] To conduct this analysis, we used whole flies since we were interested in clock expression in the periphery, and the contribution of the pacemaker neurons is even smaller in whole flies versus heads. We collected flies at four-hour intervals over the span of 24 hours and extracted mRNA from whole-fly homogenates. Because only ~150 central pacemaker neurons exist in the brain, clock gene expression from these homogenates primarily reflects peripheral oscillators.

We found that the *rh3* mutant exhibited pronounced changes in the amplitudes and peaks of mRNAs corresponding to peripheral core clock genes. In control flies, *Clk* expression peaked at ZT 20 (Figure 3A), as previously reported.[84] However, in the *rh3* mutant, *Clk* expression peaked at ZT 4, indicating that it was greatly delayed by 8 hours (Figure 3A). Expression of *Pdp1ε*, *per*, and *tim* reached their zenith at ZT 16 (Figures 3B–3D). However, in the *rh3* mutant, expression of these mRNAs was delayed by ~4 hours, peaking at ZT 20 (Figures 3B–3D). Thus, for all four clock genes examined the peak expression was delayed. Additionally, loss of *rh3* blunted the peak amplitudes of *Pdp1ε*, *per*, and *tim* in the periphery (Figures 3B–3D).

Next, we examined Per protein expression in the pacemaker neurons from control and *rh3* mutant flies whose endogenous Per protein was tagged with mNeonGreen.[85] Per protein expression peaks in the pacemaker neurons at ZT 0 and is substantially diminished by ZT 4.[85] Therefore, we chose these two timepoints to examine the expression of Per in the *rh3* mutant. We focused on three groups of lateral pacemaker neurons (LNs; Figure 3E), as we could

consistently identify these populations of neurons from sample to sample based on their location and morphology. At ZT 0, Per expression was significantly reduced in the s-LNvs, LNds, and l-LNvs of *rh3* mutant flies compared to the control (Figures 3F–3I). Expectedly, in control flies, the expression of Per was reduced by ZT 4 (Figures 3F–3I). However, between ZT 0 and ZT 4, Per expression was largely unchanged in the LNs of the *rh3* mutant (Figures 3F–3I), and at ZT 4 was significantly higher than the control in the LNds (Figures 3F and 3H), and trending towards significance in the s-LNvs (Figures 3F and 3G; p=0.061 for s-LNvs). By ZT 8, we were unable to detect Per expression in the control or *rh3* mutant. Together, these experiments demonstrate that *rh3* impacts Per expression in LNs. However, from these results alone we are unable to conclude whether *rh3* impacts the phase of Per in LNs. Notably, the s-LNvs and LNds, which showed higher Per expression at ZT 4 in the *rh3* mutant than the control, play a fundamental role in pacemaker neuron synchronization as well as the phase of morning and evening activity peaks.[86,87]

Loss of *rh3* greatly extends circadian periodicity

Variations in chronotype are known to be correlated with changes in several behaviors, including differences in the ability to entrain to light/dark cycles.[88] Animals with normal light entrainment can quickly adjust their locomotor rhythms to synchronize with a sudden shortening of a light cycle (phase advance), or an unanticipated lengthening of a light cycle (phase delay).[89,90] For example, as previously observed,[91] control flies rapidly adjust their activity rhythms (within 1–2 days) in response to an eight-hour phase advance (Figures S4C and S4D) or a phase delay to the light/dark cycle (Figures S4E and S4F). However, flies with defects in light entrainment typically take longer to adjust to these changes.[90,92] We found

that the *rh3* mutant showed comparably rapid shifts to a phase advance (Figures S4C and S4D) or a phase delay (Figures S4E and S4F), indicating that impaired entrainment to phase shifts does not underlie the behavioral phase delay of the *rh3* mutant.

In humans, there is evidence that chronotype or sleep timing can vary both with the seasons and with the distance one lives from the equator, suggesting that the length of daily light exposure can impact the phase of behaviors.[93-95] Furthermore, lengthening or shortening of the photoperiod at the time of birth has been reported to affect chronotype, although the effect is small.[96] To test the contribution of photoperiod length on chronotype, we measured sleep in wild-type and *rh3* mutant flies housed under light:dark cycles that were either extended or shortened (i.e, 14 hour:10 hour light/dark cycles or 10 hours:14 hours light/dark cycles). We observed that the evening chronotype of *rh3* persisted in both shorter and longer photoperiods, and that the chronotype of control flies was also not changed (Figures S5A–S5H). Therefore, defects in photoperiod entrainment are unlikely to contribute to the behavioral delays exhibited by the *rh3* mutant.

Morning and evening chronotypes have been correlated with internal periodicities that are shorter or longer than 24 hours, respectively.[12,13,17,97] Therefore, we used DAM assays to determine the endogenous circadian periodicities of the *rh3* mutant during seven days of constant darkness after entraining the flies under light/dark cycles for four days. For the first three days, we used 12 hour light/12 hour dark dark cycles. Then, on the fourth day, we varied the light duration (4, 8, 12 and 16 hours) by turning off the lights at either ZT 4, ZT 8, ZT 12, or ZT 16 and then maintained the flies in the dark for an additional seven days. When we turned off the lights at ZT 12, control flies had a locomotor rhythm in the dark with a ~24-hour periodicity (23.9 ± 0.04 hours; Figures 4A and 4B), as shown many times

previously.[18,19,21,22] Turning off the lights at other times (ZT 4, ZT 8 or ZT 16) prior to the seven days of darkness did not have a significant effect on the periodicities, although 16 hours of light marginally extended the rhythm of the control flies to 24.4 ± 0.08 hours (Figures 4A and 4B).

In contrast to the ~24 hour periodicity of control flies, the periodicity of *rh3* mutants was expanded. The periodicity of the *rh3* mutants was extended to 25.2 ± 0.12 hours, which was significantly greater than the 23.9 ± 0.04 hours exhibited by control flies (Figures 4A and 4B). We rescued this mutant phenotype by either expressing *UAS-rh3* under the control of *rh3-Gal4* (S6A–S6C, S6E and S6F; 24.2 ± 0.10 hours) or under the control of *inaF-C-Gal4* (Figures S6D–S6F; 24.5 ± 0.19 hours*)*. Thus, the evening chronotype of *rh3* mutants is correlated with a long internal periodicity that stems from the inactivity of *rh3*-expressing photoreceptors in the eye.

Strikingly, the periodicity of *rh3* mutant flies was impacted significantly by the time that the lights were turned off. Reducing the photoperiod from 12 to 4 hours (turn off at ZT 4) prior to the dark-dark period increased the free-running periodicity of *rh3* mutants to 25.9 ± 0.19 hours (Figures 4A and 4B). Most dramatically, exposing *rh3* mutants to 8 hours of light (turn off at ZT 8) increased the periodicity to 27.2 ± 0.14 hours (Figures 4A–4D). Lengthening the photoperiod from 12 to 16 hours prior to the dark-dark period had little to no effect on the periodicity as compared to 12 hour of light (Figures 4A and 4B; turnoff at ZT 12, 25.2 ± 0.12 hours; turnoff at ZT 16, 25.1 ± 0.13 hours). Because the periodicity of control flies was slightly extended after 16 hours of light, under these conditions the difference in the periodicities of the control and *rh3* mutant flies was relatively small (24.4 versus 25.2 hours,

respectively). This reveals a surprisingly strong relationship between the length of the final light exposure and free-running periodicity in *rh3* mutants.

Similar to the *rh3* mutant, we observed an extension of the free-running periodicity when we inhibited the activity of the DRA1 neurons downstream of *rh3*-expressing R7 cells using tetanus toxin (*DRA-DM8>TNT*; 25.9 h; Figures 4E–4H). The per^L allele of the *per* gene also has a long periodicity (~29 hours) due to a missense mutation causing residue 243 to be changed from a valine to aspartic acid.[19,98] We sequenced the *rh3* genes in the $rh3^2$ and $rh3^L$ mutants and confirmed that neither allele harbors the per^L mutation (data not shown). To determine if the length of the final light exposure affects the free-running periodicity of other mutants with a non-24 hour clock, we also tested per^L and per^s, exposing them to three days of 12 hour light:12 hour dark cycles, and then varied the duration of the final light cycle on day 4, as described above. We found that, unlike *rh3,* the periodicity of both per^L and per^S remained unchanged after varying the duration of the final light cycle between 8–16 hours, with per^L displaying a 29.9±0.1 hour periodicity, and per^S displaying a 19.2 ±0.1 hour periodicity (Figures S6G and S6H).

Circadian alignment restores a normal chronotype in the *rh3* mutant

To test whether the evening chronotype of *rh3* mutants is caused by a mismatch between their internal periodicity (25.2–27.2 hours depending on whether the last light cycle is 4, 8 or 12 hours) and the external periodicity (24 hours), we housed *rh3* mutants under a light:dark cycle that more closely matched the maximum periodicity we observed. Strikingly, maintaining $rh3^{2/L}$ flies under a 14 hour:14 hour light/dark cycle restored the timing of their midday siesta (Figures 5A, 5C, S5I), suppressed their early-nighttime activity (Figures 5B,

5D and 5F), and increased their early-nighttime sleep index (Figures 5E), such that these parameters resembled those of wild-type flies kept under a 24-hour cycle.

In addition to locomotor behavior and sleep, the evening feeding pattern of *rh3*$^{2/L}$ flies was also corrected by housing them under a 28-hour light/dark cycle. Unlike the 24-hour pattern, where the *rh3*$^{2/L}$ evening feeding peak extended into the night (Figures 1M and 1N), the evening *rh3*$^{2/L}$ feeding peak under 28-hour LD cycle was aligned with the transition from lights on to lights off, resulting in *rh3* flies no longer feeding more than the control at night (Figures 5G and 5H). In total, these results indicate that the evening chronotype of *rh3* flies is the result of a circadian misalignment, owing to the elongated circadian periodicity of the *rh3* mutant. Maintaining *rh3* flies under a 28-hour light/dark period, which much more closely mimics their longest internal rhythm, advances the relative timing of sleep and feeding such that these parameters resemble those of control flies housed under a 24-hour light/dark rhythm.

Interestingly, we found that under a 28-hour light/dark period, control flies adopted a morning chronotype, characterized by an advancement of the timing of their midday siesta (Figures 5C and 5E), increased early-night sleep index (Figures 5C and 5E), and decreased early-night activity index (Figures 5D and 5F). This is consistent with the notion that circadian misalignment can result in both morning and evening chronotypes, where an evening chronotype reflects an internal periodicity longer than the external lighting cues and a morning chronotype reflects the opposite.

Elimination of morning and evening chronotypes in *per* mutants by aligning the external clock with the internal clocks

To test the generalizability of the model that mismatch of the internal and external periodicities can result in morning or evening chronotypes, we examined the chronotypes of two additional mutants with defects in their circadian rhythms. Mutations of the classic core-clock gene, *per*, can result in circadian rhythms that are either longer or shorter than 24 hours. Flies with the per^L allele have a ~29-hour circadian rhythm, whereas flies with the per^S allele have a ~19-hour rhythm.[19] Under a light/dark cycle with a 24-hour periodicity (12 hour:12 hour light/dark cycle), the daytime siesta and evening activity peak of per^L flies was significantly delayed, with the siesta peaking at ~ZT 12 (Figure 6A) and the evening activity peaking at ~ZT 16 (Figures 6B and S7A). However, housing per^L mutants on a 30-hour rhythm (15 hour:15 hour light/dark cycles) restored the relative timing of these parameters (Figures 6C–6D and S7A). Conversely, per^S flies displayed a morning chronotype under a 12 hour:12 hour light/dark cycle, indicated by an early onset of sleep (Figure 6E) and activity relative to the control (Figure 6F). The morning chronotype of per^S flies was reversed by maintaining them under a 19-hour circadian schedule that more closely matched their internal rhythm (9.5 hour:9.5 hour light/dark; Figures 6G, 6H and S7B).

The chronotype of control flies was also modified by varying the periodicity of the light/dark cycle to either 19 or 30 hours. The relative timing of their evening activity peak strongly correlated with the periodicity of the environmental lights ($R^2 = 0.84$; Figure S7C). Housing wild-type flies under a 19-hour light/dark cycle delayed the relative timing of the evening activity peak by roughly 4 hours (Figures 6H and S7C), whereas a 30-hour cycle advanced the timing by 5 hours (Figures 6D and S7C). These results strongly support the model that major changes in chronotype can result from circadian misalignment.

Time-restricted feeding restores a normal chronotype in the *rh3* mutant

Although matching the environmental (zeitgeber) periodicity to the internal periodicity can suppress differences in chronotype, this approach is ill-suited for real-world chronotype modification given that the 24-hour rotation of the earth is fixed, and that there are practical constraints to artificially instituting longer and shorter zeitgeber periodicities. Therefore, we attempted to modify the evening chronotype of *rh3* flies housed under a 24-hour light dark cycle by altering an additional time-giving cue—the timing of feeding. We wondered whether the increased nighttime feeding exhibited by *rh3* flies (Figure 1M and 1N) served to delay the onset of their nighttime sleep. To test this, we restricted the mutant flies' access to food (time-restricted feeding; TRF) to just an eight-hour window during the day (ZT 2–10) and monitored their activity and sleep via real-time video tracking. Strikingly, *rh3* mutants maintained on TRF for 48 hours displayed a sleep chronotype that was nearly identical to the control (Figure 7C). TRF advanced the timing of *rh3* mutant's midday siesta by nearly two hours (from ZT 6.8 ± 0.8 hours to ZT 4.9 ± 0.45 hours; Figure 7E) and increased their early-nighttime sleep index (Figure 7E), such that neither of these parameters were significantly different from the control flies ($p = 0.85$ and $p = 0.11$, respectively; Figures 7A, 7C and 7E). Although TRF suppressed the nighttime activity of *rh3* mutant flies (Figures 7B and 7D), the early-nighttime activity index was not significantly changed (Figure 7F), as both early- and total-nighttime activity (measured by distance traveled) were proportionally suppressed (Figures 7G and 7H). These results demonstrate that TRF can advance an evening chronotype resulting from an extended circadian periodicity and suggest that the extended feeding window of *rh3* mutants contributes to their evening chronotype.

Circadian alignment restores the phase of clock genes expression

Chronic circadian misalignment is reported to reduce the peripheral expression of several core-clock genes.[99] Because a 28-hour light/dark cycle restored a normal chronotype to *rh3* flies, we wondered whether there would be an impact on the amplitudes and phases of clock-gene RNA expression in peripheral tissues. To quantitatively measure the expression of several core clock genes (*Clk, Pdp1ε, per* and *tim*), we prepared RNA from whole flies every four hours over the span of a 28-hour day and performed RT-qPCR. We observed that the extended 14 hour:14 hour light/dark cycle partially restored the phase of *Clk* mRNA expression in the *rh3* mutant (Figure S7D). To more clearly compare the phases of peak expression during the 24- and 28-hour cycles, we used a circular plot and normalized the length of each 24 and 28 hour light schedule to 1.0 (Figure S7H; light period is from 0 to 0.5 and the dark period is from 0.5 to 1.0). The mRNA expression peaks are indicated by either solid arrows (24-hour periods) or dashed arrows (28-hour periods). We found that shifting the $rh3^{2/L}$ flies to a 28-hour cycle caused the peak to advance, and therefore reduced the difference in phase between the control and $rh3^{2/L}$ mutant (Figure S7H).

The relative phase of mRNA expression of *Pdp1ε, per and tim in* $rh3^{2/L}$ flies also advanced under 28-hour cycles. The *Pdp1ε, per, and tim* mRNAs peaked at relative times closer to control flies under 24-hour cycles than they did when the $rh3^{2/L}$ flies were maintained under 12 hour:12 hour regimes (Figures S7E–S7G and S7I–S7K). The differences in expression amplitudes between $rh3^{2/L}$ and the control were lower under the 28-hour cycles compared to the 24-hour cycles (Figures S7E–S7G vs. Figures 3B—3D). However, the extended photoperiod did not fully restore circadian amplitude in $rh3^{2/L}$ flies,

as control flies still showed higher expression of *Pdp1ε*, *per* and *tim* (Figures S7E–S7G). In total, these results indicate that changes to the phase of peripheral clock gene expression in the $rh3^{2/L}$ mutant results from circadian misalignment, although circadian misalignment does not fully account for *rh3*-mediated increases in circadian amplitude.

DISCUSSION

Small subset of retinal photoreceptor cells regulates chronotype

The initial hypothesis guiding this work is that light sensing in the eye not only regulates photoentrainment,[27] but also chronotype. To test this, we examined the sleep profile of rhodopsin mutant flies, focusing on impacts to the timing of both daytime and nighttime sleep. However, mutation of six out of seven rhodopsin genes had no or minimal impacts on chronotype, including *ninaE*, which encodes the major rhodopsin (Rh1) functioning in most photoreceptor cells in the eyes.

We discovered that a subset of R7 cells, which constitutes a very small fraction of the photoreceptor cells in the eyes, has a major impact on chronotype. Although Rh3 is only expressed in ~30% of the R7 photoreceptor cells,[36,37,100] it is required for regulating the phase of sleep, locomotor, and feeding rhythms. In addition to *rh3*, a second opsin gene, *rh4*, is also expressed in R7 cells. These two rhodopsins are present in non-overlapping subsets of R7 cells.[36,47] Because *rh4* mutants display a normal chronotype, this demonstrates that only the *rh3*-expressing R7 photoreceptor cells contribute to the daily timing of behavior.

The specific requirement for these photoreceptor cells for a normal chronotype is remarkable because only ~2% of the photoreceptor cells in the compound eyes express Rh3 (see Methods: Estimate of percentage of Rh3-expressing R7 cells in each compound eye**)**. Moreover, since R7 cells have a smaller diameter than R1-6 cells, the Rh3-expressing R7

cells comprise only about 1% of the total surface area of the photoreceptor cells in the compound eyes. Despite their diminutive size and numbers, Rh3-expressing photoreceptor cells have a greater impact on chronotype than any other photoreceptor cell class, including the Rh1-expressing cells (R1-6), which comprise 75% of the photoreceptor cell and >90% of the total surface area.

While we do not know the minimum number of Rh3-expressing R7 cells that need to function to achieve an intermediate chronotype, inactivation of the DRA1 Dm8 neurons, which receive input exclusively from R7 cells in the dorsal rim area (DRA) of the eye, causes an evening chronotype. All R7 cells in the DRA express Rh3.[75] Given that the R7 cells in the DRA comprise just ~0.4% of all photoreceptor cells (see Methods: Estimate of percentage of Rh3-expressing R7 cells in each compound eye), our results demonstrate that disrupting signaling from an exceedingly small subset of photoreceptor cells (~0.4%) is sufficient to alter the sleep and activity patterns, resulting in an evening chronotype. The DRA is important for sensing polarized light,[101-103] which in some insects, such as monarch butterflies, contributes to long-range navigation.[104] However, fruit flies do not travel long distances. These findings raise the intriguing possibility that sensation of polarized light might contribute to chronotype.

Surprisingly, while loss of *rh3* caused an evening chronotype, flies with mutations in both *rh3* and *rh4* display normal activity patterns. Similarly, the *sev* mutant, which is devoid of all R7 cells, also exhibits an intermediate chronotype. One possibility to explain this conundrum is that R7 cells inhibit DM8 cells, and that neighboring Dm8 cells inhibit each other.[71,72] However, in the absence of Rh3-expressing R7 cells, an important source of inhibition in the optic lobes is removed. Nevertheless, our findings could account for the

results of a previous study with *sev* mutants, which did not detect a substantial delay in behavior.[105]

Given that Rh3 is a UV sensing opsin,[60,61] we speculated that this spectral sensitivity might be relevant for setting chronotype. However, we rescued the evening chronotype in *rh3* mutants using a red-light-sensitive channelrhodopsin, CsChrimson. Therefore, it is the activation of Rh3-positive neurons, rather than an ability to sense UV light per se, that is germane to regulating a normal chronotype. CsChrimson does not engage a phototransduction cascade, which couples Rh3 and other *Drosophila* rhodopsins to a trimeric G-protein (Gq) and phospholipase C (PLC), which culminates with activation of the TRP and TRPL channels.[35] Thus, these other signaling proteins, such as Gq and PLC, do not regulate chronotype independent of their roles in transducing light activation of rhodopsins to gating of TRP and TRPL.

Previous work has shown differential roles for rhodopsins under moonlight and twilight conditions. Moonlight promotes nocturnal activity, and depends on Rh1 and Rh6.[106] In addition, the rhodopsins expressed in the R7 and R8 cells (Rh3, Rh4, Rh5 and Rh6) are particularly important in responding to twilight.[107] In the current work, which employs brighter lighting, we did not detect roles for Rh4, Rh5 or Rh6 in chronotype. This highlights the differential roles of rhodopsins in regulating activity under distinct lighting conditions.

It is possible that a similar chronotype-regulating mechanism involving a small subset of photoreceptor cells also exists in the mammalian retina. In mice and humans, the intrinsically photosensitive retinal ganglion cells (ipRGCs), which are blue-light-sensitive photoreceptors, also have a fundamental role in regulating circadian rhythms.[108,109] Behavioral studies in humans suggest that ipRGC function correlates with chronotype,[110] and genetic variations in

melanopsin, the light-sensitive rhodopsin-family member expressed in ipRGCs, are associated with the timing of daily sleep.[111] However, to our knowledge, the current report is the first to experimentally demonstrate that a specific class of photoreceptor cells regulates chronotype.

Early bird and night owl chronotypes caused by misalignment of internal and external circadian periodicities

It has long been posited that circadian periodicity could set chronotype, with early chronotypes ("early birds") resulting from a circadian periodicity that is less than 24 hours and late chronotypes ("night owls") resulting from the opposite.[97,112,113] Recent work in humans has supported this notion for extreme chronotypes. Specific mutations in hPer2 cause Familial Advanced Sleep Phase Syndrome,[16] and decrease circadian periodicity,[12,17] while mutations in Cry1 cause Familial Delayed Sleep Phase Disorder,[13] and increase circadian periodicity. However, the evidence for these sleep disorders resulting from changes to circadian periodicity is only suggestive. Here, we identify a retinal gene that modifies circadian rhythms and provide causal evidence demonstrating that the internal circadian periodicity regulates chronotype. The strong effect of Rh3 on periodicity is surprising since nearly all of the genes that are known to impact on periodicity in flies either disrupts a clock gene directly or a factor that directly affects the activity or expression of a clock gene.[19,114-116]

Unexpectedly, the magnitude of the increased periodicity exhibited by *rh3* mutants was affected by the length of the last light period prior to shifting to dark-dark cycles. In contrast the length of the light period had little impact on wild-type flies or flies harboring the per^L or per^S allele, suggesting that *rh3* has a unique impact on the flies' circadian periodicity.

To establish that chronotype depends on internal periodicity, we used a combination of environmental and genetic approaches. We rescued the evening chronotype resulting from mutation of *rh3* by placing the mutant flies under a light/dark cycle with a longer length that aligns with their internal rhythm. Moreover, placing wild-type flies under a 28-hour light/dark cycle results in these animals adopting a morning chronotype, measured by the relative phase of their daytime siesta, early night sleep, and evening activity peak.

We found that a similar interaction among internal periodicity, zeitgeber periodicity, and chronotype holds for the per^L and per^S mutants, which have longer and shorter circadian rhythms, respectively. The per^L mutant had an evening chronotype reminiscent of the *rh3* mutant, while per^S had a morning chronotype, similar to a wild-type flies maintained under an elongated light/dark cycle. Housing these per^L and per^S mutants under light/dark cycles that match their internal rhythms was sufficient to restore an intermediate chronotype. These data strongly support the model that chronotype is altered by misalignment of internal and external circadian periodicities.

Of note, while we conclude that matching the internal and external periodicities is important for chronotype, there are likely additional mechanisms that impact on chronotype.[117] Experiments performed in mice indicate that there exist clock-independent chronotype-regulating mechanisms. *bmal1* knockout mice, which are arrhythmic and therefore possess no internal periodicity, display a delayed chronotype under light/dark conditions.[118,119] Additionally, in humans, there is a progressive shift toward a morning chronotype that occurs with age. However, this shift is not accompanied by a decrease in circadian periodicity.[113] An additional factor that could regulate chronotype in a clock-independent fashion is the sleep homeostat, the neuronal system monitoring daily energy

expenditure to set total sleep time.[50] However, it is unlikely that the sleep homeostat accounts for changes to the chronotype of *rh3* flies given that circadian alignment fully amended the phase of their sleep.

Regulation of core-clock gene cycles by a small subset of photoreceptor cells

Concordant with delays in the phase of sleep, locomotor, and feeding rhythms in *rh3* mutant flies, the peaks of core-clock gene expression were delayed. These observations are based on a series of RT-qPCR experiments, where we isolated mRNA from whole-fly homogenates throughout a 24-hour cycle. This approach enabled us to ascertain the summation of clock-gene expression across the entire organism. Because the overwhelming majority of clock-expressing cells exist outside of the brain, these data reflect core clock gene expression primarily from peripheral oscillators.[77] Therefore, our data suggest that *rh3,* which is expressed in only ~2% of all photoreceptor cells, is essential for core clock gene expression throughout the entire organism.

Previous work in flies shows that the phase of peripheral oscillators can be set by the time of feeding.[78] Given that *rh3* flies maintained under a 24-hour cycle display abnormal nighttime feeding, it is possible that changes to the time of feeding account for some of the phase delay in peripheral core-clock gene expression. This hypothesis is consistent with our observation that housing *rh3* flies under a 28-hour cycle, which realigns feeding with the transition from daytime to nighttime, partially restored the phase in core-clock gene expression.

In addition to delays in phase, mutation of *rh3* also appears to suppress circadian amplitude—the difference in peak to trough mRNA expression of the core clock genes. Both

chronic circadian misalignment as well as an extended feeding window have been shown to suppress circadian amplitude.[99,120,121] However, neither of these mechanisms seem to account for the reduced amplitude in *rh3* flies, given that housing these flies under a 28-hour light/dark cycle, which re-aligns feeding and locomotor rhythms, fails to restore circadian amplitude.

Unlike circadian clocks in peripheral tissue, clock gene expression in pacemaker neurons in the brain is required for setting both the morning and evening activity peaks of the fly as well as their phase.[86,87,122] Expression of PER proteins expression in s-LNv neurons restores the morning activity, while expression of PER proteins in both the s-LNv and LNd neurons is able to restore the evening activity.[86] Exposure to constant light can induce complete desynchronization between s-LNv and LNd neurons, resulting in distinct free-running periodicity.[123] The unchanged Per expression we observed in the LNd and s-LNv neurons of *rh3* flies between ZT 0 and ZT 4 may disrupt the normal function of these cells, contributing to the *rh3* mutant's evening chronotype and elongated free-running rhythm.

Time-restricted feeding as a chronotype-modifying intervention

Because *rh3* mutants exhibited abnormal levels of nighttime feeding, we wondered whether nighttime feeding contributed to their evening chronotype. To test this, we restricted the *rh3* mutant flies' access to food to just an eight-hour window during the early day, thereby preventing any nighttime feeding. This time-restricted feeding was sufficient to advance the phase of both daytime and nighttime sleep in *rh3* mutants but had a minimal impact on the timing of sleep in wild-type flies, likely because wild-type flies normally consume most of their food during the day.[121]

In mammals, there exists a food-entrainable oscillator that is not reliant on a functional SCN, and which allows animals to anticipate the daily timing of feeding.[124,125] However, previous reports indicate that *Drosophila* are incapable of similar food-anticipatory behavior, but that timed feeding can transiently change the phase of activity without affecting the central clock.[126,127] Consistent with this finding, we found that time-restricted feeding exerts an almost immediate effect on the phase of *rh3* mutants' sleep, observable within the first 24- to 48-hours on the diet. Interestingly, in humans, an evening chronotype can be partially reversed using time-restricted feeding alone[128] or in combination with early-day physical exercise with exposure to light.[129]

Speculation that a subset of photoreceptor cells impacts chronotype in humans

Approximately 50% of humans with blindness or visual impairment report disturbances to their sleep, compared to just 9% in those with normal sight.[130,131] One reason for this could be that blind individuals are unable to adequately reset their circadian clocks each day to light, which is the primary circadian entrainment cue for humans. In extreme cases, blind people can adopt a non-24 hour sleep pattern, which is thought to follow their free running periodicity.[130] Those with this condition often report cyclic disruptions to their sleep, as their rhythm drifts in and out of phase with the solar day.[132] In humans, visual impairment increases with age, and is often accompanied by sleep disorders and a progressive shift towards an earlier chronotype.[133] Whether the inactivation of a particular set of photoreceptor cells contributes to these changes is unknown.

Our work raises the possibility that a small subset of photoreceptors in mammals might have a major impact on chronotype. Intriguingly, there is recent evidence linking the activity

of a very small subset of retinal photoreceptor cells in humans (ipRGCs) to an individual's chronotype.[134] Individuals with a late or night-owl chronotype appear to have lower sensitivities in the short wavelength range that maximally activate ipRGCs, at least before noon.[134] Conversely, early birds or morning larks appear to have greater sensitivity to short wavelengths earlier in the day than individuals with an intermediate chronotype. Finally, it would be of interest to learn if humans with early bird and night owl chronotypes attributable to alterations in sensitivities of the ipRGCs, revert to a more standard chronotype if they are housed under circadian cycles that are shorter or longer than 24 hours, respectively.

Limitations of the Study

Light influences circadian activity and chronotype. Therefore, it is potentially important to simulate natural lighting conditions in order for flies to exhibit normal behavior. However, it is a challenge to devise lighting conditions that recapitulate natural light. In an attempt to do so, we used full spectrum lights with a UV component. Furthermore, since the intensity of sunlight changes over the course of the day, we also tested the effects on activity and sleep resulting from ramping lights that increase and decrease in intensity over the course of hours. Nevertheless, the lighting conditions that we used do not fully simulate natural light, which could impact on chronotype.

This work also raises multiple questions for the future. We showed that disruption of the DRA-DM8 neurons, which express Rh3, recapitulates the *rh3* mutant phenotype, indicating that this very small population of photoreceptor cells plays an important role in regulating chronotype. However, we do not know if activity of these Dm8 neurons is sufficient for a

normal chronotype. The complete circuit regulating chronotype downstream of the Dm8 neurons is also not known. We also do not understand the mechanistic basis through which elimination of the activity of *rh4*-expressing R7 photoreceptor cells suppresses the night owl chronotype caused by mutation of *rh3*, which is expressed in a nonoverlapping subset of R7 cells. Finally, night owl chronotype has been suggested to increase aggression and has been linked to a variety of adverse health issues in people.[3,135] Whether the *Drosophila rh3* mutants exhibit similar problems remains to be determined.

ACKNOWLEDGMENTS

We thank Jiangqu Liu for providing the image of a fly brain in Figure 3E. This work was supported by grants to CM from the National Eye Institute (NEI) (R01EY008117), and the National Institute of Allergy and Infectious Disease (R01AI169386). GM was supported by a predoctoral fellowship from the NEI (F31EY033179).

AUTHOR CONTRIBUTIONS

Conceptualization, M.L., and G.M.; Software, G.M., M.L, and N.D..; Formal analysis, G.M., and M.L.; Investigation, M.L., G.M., N.D., N.S., K.S., A.A., and Y.S.; Visualization, M.L., and G.M.; Writing—original draft, M.L., and G.M., Writing—review and editing, M.L., G.M., and C.M.; Data curation, M.L., and G.M.; Methodology, M.L., and G.M.; Resources, C.M.; Supervision, C.M.; Funding acquisition, C.M.

FIGURES AND TABLES

Figure 1

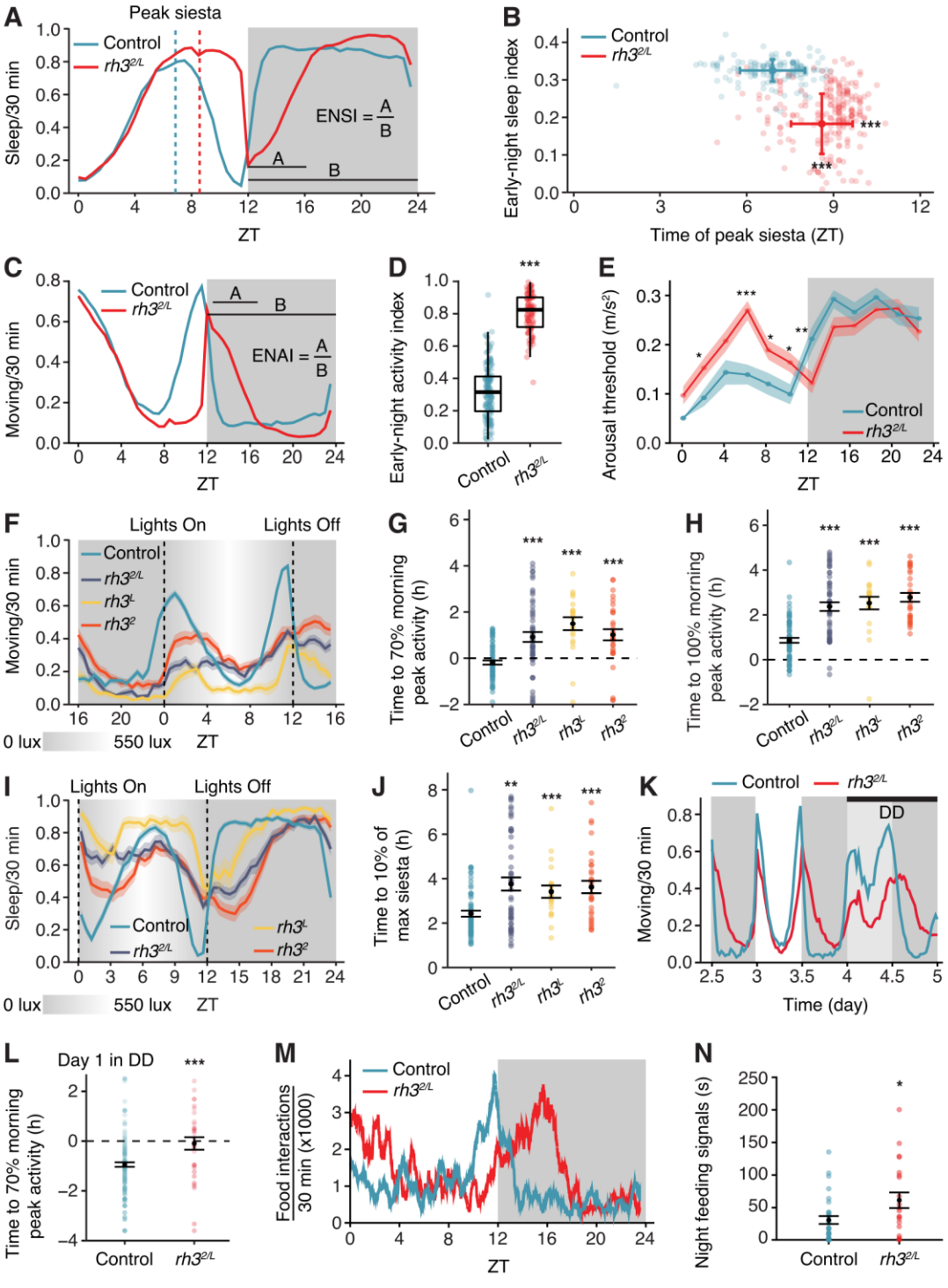

Figure 1. Loss of *rh3* sets an evening chronotype

(A) Sleep profiles of control (w^+,w^{1118}: Canton-S flies outcrossed to w^{1118} but retained the w^+ gene*)* and *rh3* mutants ($rh3^{2/L}$) assayed using the DAM system. Sleep (Y-axis) corresponds to the proportion of time the flies are asleep in a 30-minute bin. Each profile represents the average result from four days of recordings. The lights are on from ZT 1—12 (day) and off from ZT 12—24 (night). The dashed vertical lines show the average calculated time of the midday siesta (see STAR Methods) for each genotype. The horizontal lines (A and B) represent the time intervals used to calculate the early-night sleep index (ENSI). The equation is indicated above. Line A=sleep during ZT 12—16, and line B=total sleep during ZT 12—24.

(B) Bivariate chronotype plots indicating the early-night sleep index versus the time of the daytime siesta peak. See the STAR Methods for the formula used to generate each parameter. The dots represent the mean times for the daytime siesta for each of two fly lines. The error bars represent one standard deviation from the means. Each parameter was compared between genotypes via an unpaired Student's *t*-test.

(C) Activity profiles showing the four-day average movement for control (w^+,w^{1118}) flies and the *rh3* mutant using the DAM system. The horizontal lines (A and B) represent the time intervals used to calculate the early-night activity index (ENAI). The equation is indicated below. Movement (Y axis) represents the proportion of time the flies moved during each 30-minute bin.

(D) Quantification of the early night activity index (ENAI). The box represents the 25th percentile, median, and the 75th percentile. The whiskers represent 1.5 times the interquartile range (IQR), or the min/max values if no data surpass 1.5*IQR.

(E) Average circadian sleep arousal threshold of control (blue) and *rh3*$^{2/L}$ (red) flies. The shaded areas correspond to the SEM. n = 60 flies/genotype. The p values were calculated using a two-way Aligned Rank ANOVA with factors corresponding to genotype and ZT. P values from post-hoc comparisons were adjusted using a Benjamini-Hochberg multiple testing correction. *p<0.05, **p<0.005,***p<0.0005

(F) Activity profiles showing the four-day average movement for control (w^+,w^{1118}) flies and the *rh3* mutants under ramping light using the DAM system. The grayscale gradient indicates the gradual increase of the light intensity after lights on (ZT 0) and the gradual decrease from the peak light intensity at midday (ZT 6) (See STAR Methods).

(G) Quantification of time to 70% of morning peak activity. Dashed line placed at ZT 0. Means ±SEMs. ***p<0.0005

(H) Quantification of time to 100% of morning peak activity. Dashed line placed at ZT 0. Means ±SEMs. ***p<0.0005

(I) Sleep profile for control (w^+,w^{1118}) flies and the *rh3* mutants under ramping light using the DAM system. The grayscale gradient indicates the gradual increase of the light intensity after lights on (ZT 0) and the gradual decrease from the peak light intensity after midday (ZT 6) (See STAR Methods).

(J) Quantification of timing to 10% of the maximum siesta for control (w^+,w^{1118}) flies and the *rh3* mutants under ramping light using the DAM system. Means ±SEMs. **p<0.005, ***p<0.0005.

(K) Activity profiles showing the movement of the control flies and the *rh3* mutant flies transitioning from 12h:12h light:dark cycles (days 2.5–4) to constant darkness (day 4–5 is the first subjective day under constant dark) using the DAM system.

(L) Quantification of the time to 70% of morning peak activity of the first subjective day under constant darkness. Dashed line placed at CT 0. Means ±SEMs. ***p<0.0005

(M) 24-hour food-interaction profile of the control and *rh3* mutant flies, measured using the FLIC assay. The Y axis indicates the total number of feeding signals for 31 control flies and 21 $rh3^{2/L}$ flies.

(N) Night feeding signals by the control and *rh3* mutant flies. The feeding signals were calculated from ZT 12 (lights off) to ZT 24 (lights on) and were measured in seconds. Means ±SEMs. *p <0.05.

For sleep and activity profiles (Figures 1A-1D), n = 148 for control, n = 95 for $rh3^{2/L}$.

For Figures 1F–1J, n = 32 $rh3^{2}$ flies, n = 32 $rh3^{L}$ flies, n = 32 $rh3^{2/L}$ flies, n = 96 control flies. n ≥ 3 independent biological replicates. Unpaired Student's *t*-tests. *p <0.05, **p<0.005, ***p<0.0005 from Wilcoxon signed rank tests with a Benjamini-Hochberg multiple testing correction. See also Figure S1.

Figure 2

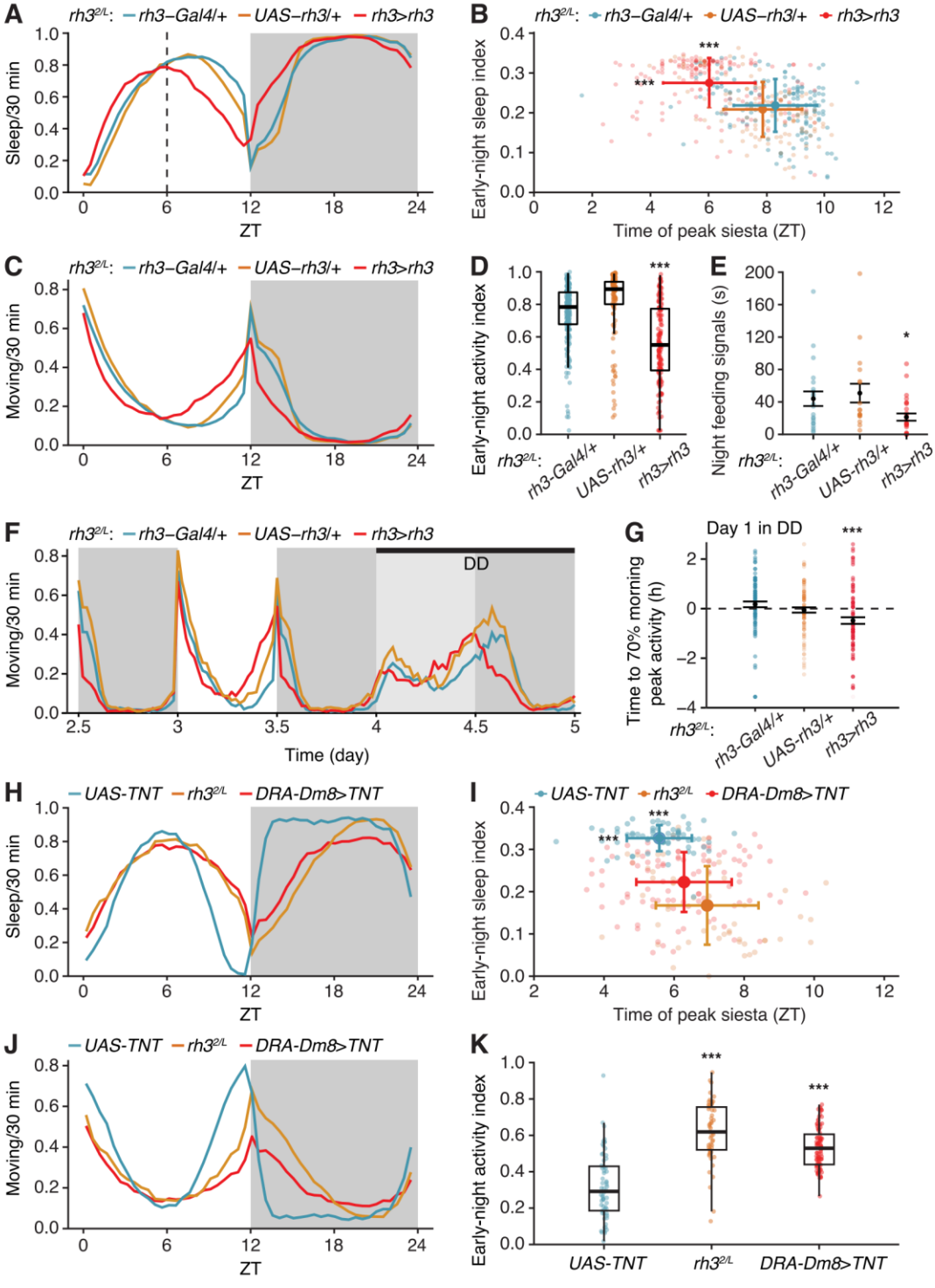
A
rh3²/ᴸ: rh3–Gal4/+ UAS–rh3/+ rh3>rh3
Sleep/30 min
ZT
B
Early-night sleep index
Time of peak siesta (ZT)
C
Moving/30 min
ZT
D
Early-night activity index
rh3²/ᴸ: rh3-Gal4/+ UAS-rh3/+ rh3>rh3
E
Night feeding signals (s)
F
DD
Moving/30 min
Time (day)
G
Day 1 in DD
Time to 70% morning peak activity (h)
H
UAS-TNT rh3²/ᴸ DRA-Dm8>TNT
Sleep/30 min
ZT
I
Early-night sleep index
Time of peak siesta (ZT)
J
Moving/30 min
ZT
K
Early-night activity index
UAS-TNT rh3²/ᴸ DRA-Dm8>TNT

Figure 2. Activating *rh3* neurons rescues evening chronotype

(A) Sleep profiles (assayed using the DAM system) exhibited by the $rh3^{2/L}$ mutant expressing *UAS-rh3* under control of the *rh3-Gal4*. n = 159 for *rh3-Gal4*/+;$rh3^{2/L}$, n = 127 for *UAS-rh3*/+;$rh3^{2/L}$, and n = 155 for *rh3>rh3*;$rh3^{2/L}$.

(B) Bivariate chronotype plots indicating early-night sleep index versus time of daytime siesta. See the STAR Methods for the formula for each parameter. n = 159 for *rh3-Gal4*/+;$rh3^{2/L}$, n = 127 for *UAS-rh3*/+;$rh3^{2/L}$, and n = 155 for *rh3>rh3*;$rh3^{2/L}$.

(C) Activity profiles for flies housed under a 12 h:12 h light/dark cycle. Moving (Y axis) corresponds to the proportion of time the flies that moved during each 30-minute bin. n = 159 for *rh3-Gal4*/+;$rh3^{2/L}$, n = 127 for *UAS-rh3*/+;$rh3^{2/L}$, and n = 155 for *rh3>rh3*;$rh3^{2/L}$.

(D) Reduction in early-night activity index exhibited by $rh3^{2/L}$ flies expressing *UAS-rh3* under control of the *rh3-Gal4*. Boxes represent the 25th percentile, median, and the 75th percentile. The whiskers represent 1.5 times the interquartile range (IQR), or the min/max values if no data surpass 1.5*IQR. n = 159 for *rh3-Gal4*/+;$rh3^{2/L}$, n = 127 for *UAS-rh3*/+;$rh3^{2/L}$, and n = 155 for *rh3>rh3*;$rh3^{2/L}$. Student's *t*-test with Bonferroni multiple testing correction. ***p<0.0005.

(E) Testing for reduction in night feeding behavior in $rh3^{2/L}$ by expressing *UAS-rh3* under control of the *rh3-Gal4*. Feeding behavior was assayed using the FLIC assay. Indicated are the total average times (in seconds) that individual flies showed feeding behavior from ZT 12—24. Mean ±SEMs. n = 21 for *rh3-Gal4*/+;$rh3^{2/L}$, n = 17 for *UAS-rh3*/+;$rh3^{2/L}$, and n = 26 for *rh3>rh3*;$rh3^{2/L}$. Student's *t*-test with Bonferroni multiple testing correction. * p <0.05.

(F) Activity profiles (using the DAM system) showing the movement of $rh3^{2/L}$ flies expressing *UAS-rh3* under control of the *rh3-Gal4* during the transition from 12h:12h

light:dark cycle (day 2.5-4) to constant darkness (day 4–5 is the first subjective day under constant darkness).

(G) Quantification of the time to 70% of the morning peak activity during the first subjective day under constant darkness. Mean ±SEMs. ***p<0.0005.

(H) Four day average sleep profile assayed using DAM for *DRA-Dm8>TNT* flies (red) compared to $rh3^{2/L}$ mutants (orange) and *UAS-TNT* control (blue).

(I) Bivariate chronotype plots indicating early-night sleep index vs. time of daytime siesta. n = 96 flies for *DRA-Dm8>TNT*, n = 53 flies for $rh3^{2/L}$, and n = 64 flies for UAS-*TNT*.

(J) Activity profiles showing four days of activity data for flies housed under a 12 h:12 h light/dark cycle. Moving (Y axis) corresponds to the proportion of time the flies moved during each 30-minute bin. n = 96 flies for *DRA-Dm8>TNT*, n = 53 flies for $rh3^{2/L}$, and n = 64 flies for UAS-*TNT*..

(K) Increase in early-night activity index for *DRA-Dm8>TNT* flies. Boxes represent the 25th percentile, median, and the 75th percentile. The whiskers represent 1.5 times the interquartile range (IQR), or the min/max values if no data surpass 1.5*IQR. n = 96 flies for *DRA-Dm8>TNT*, n = 53 flies for $rh3^{2/L}$, and n = 64 flies for UAS-*TNT*. Pairwise Student's *t* tests with Bonferroni multiple testing corrections. ***p<0.0005.

For A–D and H–K, values were generated from an average over four days in DAM monitors.

Figure 3

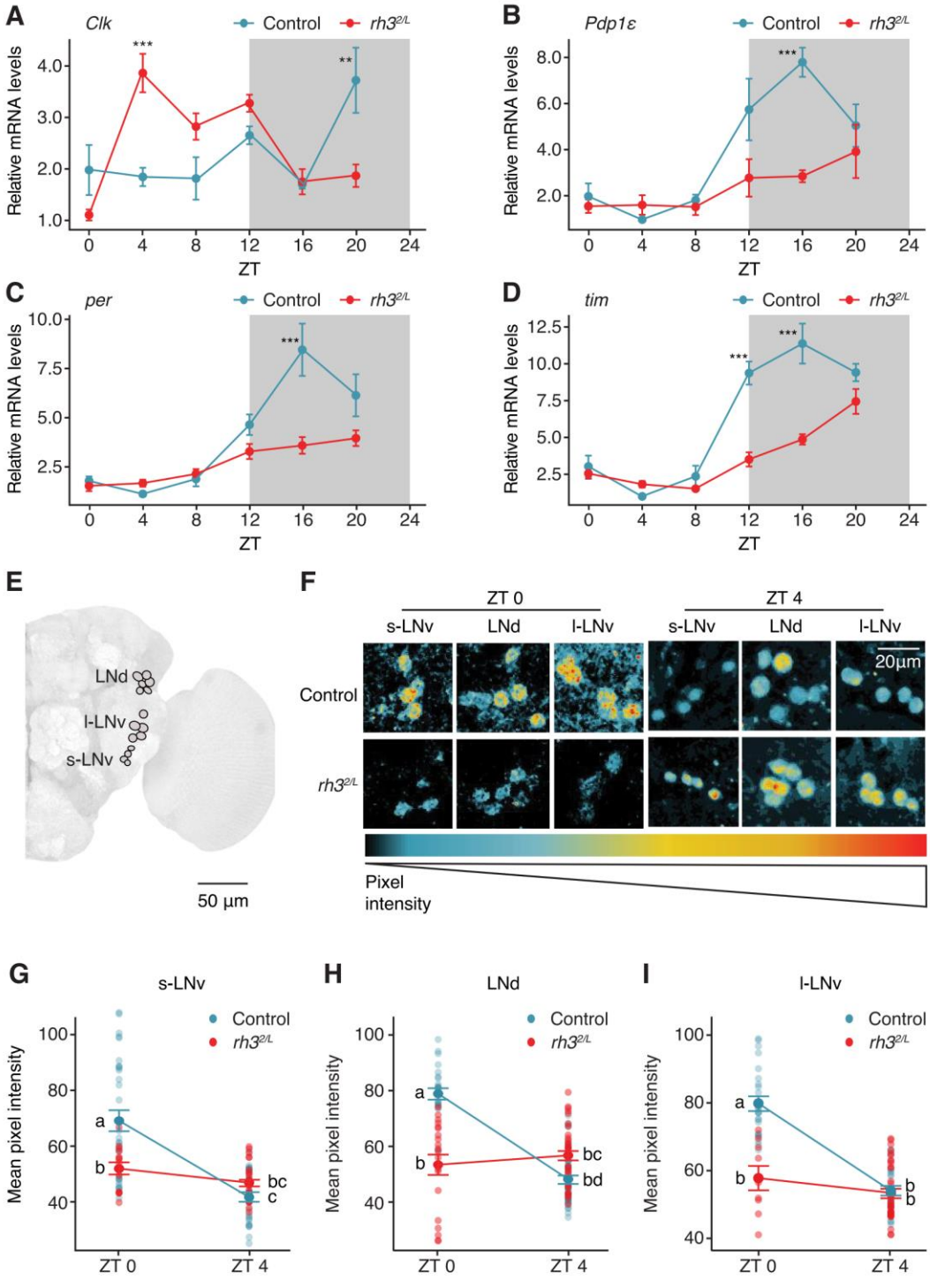
A
Clk
Control
rh3²/ʟ
Relative mRNA levels
ZT
B
Pdp1ε
C
per
D
tim
E
LNd
l-LNv
s-LNv
50 µm
F
ZT 0
ZT 4
s-LNv
LNd
l-LNv
20µm
Control
rh3²/ʟ
Pixel intensity
G
s-LNv
Mean pixel intensity
H
LNd
I
l-LNv

Figure 3. Rh3 enhances circadian amplitude and sets the phase of the molecular clock

RNA was extracted from whole-fly homogenates and each data point represents the mean from three independent RNA samples. Fold changes were calculated using the ΔΔCT method and were normalized to *rp49* as well as to the trough of expression for each gene.

(A–D) Circadian mRNA expression of core-clock genes in control (w^+,w^{1118}) and $rh3^{2/L}$ flies.

(A) Relative *Clk* RNA levels.

(B) Relative *Pdp1ε* RNA levels.

(C) Relative *per* RNA levels.

(D) Relative *tim* RNA levels.

(E) Image of a *Drosophila* brain superimposed with ovals showing the approximate positions of three groups of lateral pacemaker neurons. Scale bar, 50 μm.

(F) Representative images showing Per expression in lateral pacemaker neurons pseudo-colored to visualize pixel intensity. Scale bar, 20 μm.

(G–I) Plots showing average Per expression (Per::mNeonGreen) in lateral pacemaker neurons of control (w^+,w^{1118}) and $rh3^{2/L}$ mutants. The error bars indicate SEMs. Each unique letter (a, b and c) indicates that a group is significantly different ($p \leq 0.05$) from groups labeled with other letters. Groups that share the same letters indicate that there are no significant differences between them.

(G) Per expression in s-LNv neurons (ZT 0: n = 30 control; n = 15 *rh3*. ZT 4: n = 27 control; n = 27 *rh3*).

(H) Per expression in LNd neurons (ZT 0: n = 20 control; n = 26. ZT 4: n = 38 control; n = 38 *rh3*).

(I) Per expression in l-LNv neurons (ZT 0: n = 24 control; n = 10 *rh3*. ZT 4: n = 21 control; n = 38 *rh3*).

For A–D, Error bars represent means ± SEMs. Statistical significance between each genotype was determined using two-way ANOVA (with factors of time and genotype) with Bonferroni multiple testing corrections. ** $p<0.005$. *** $p<0.0005$. For the G–I groups, the means were compared using two-way ANOVA examining the interaction between ZT and genotype, with means compared by Tukey HSD (honestly significant difference) test.

Figure 4

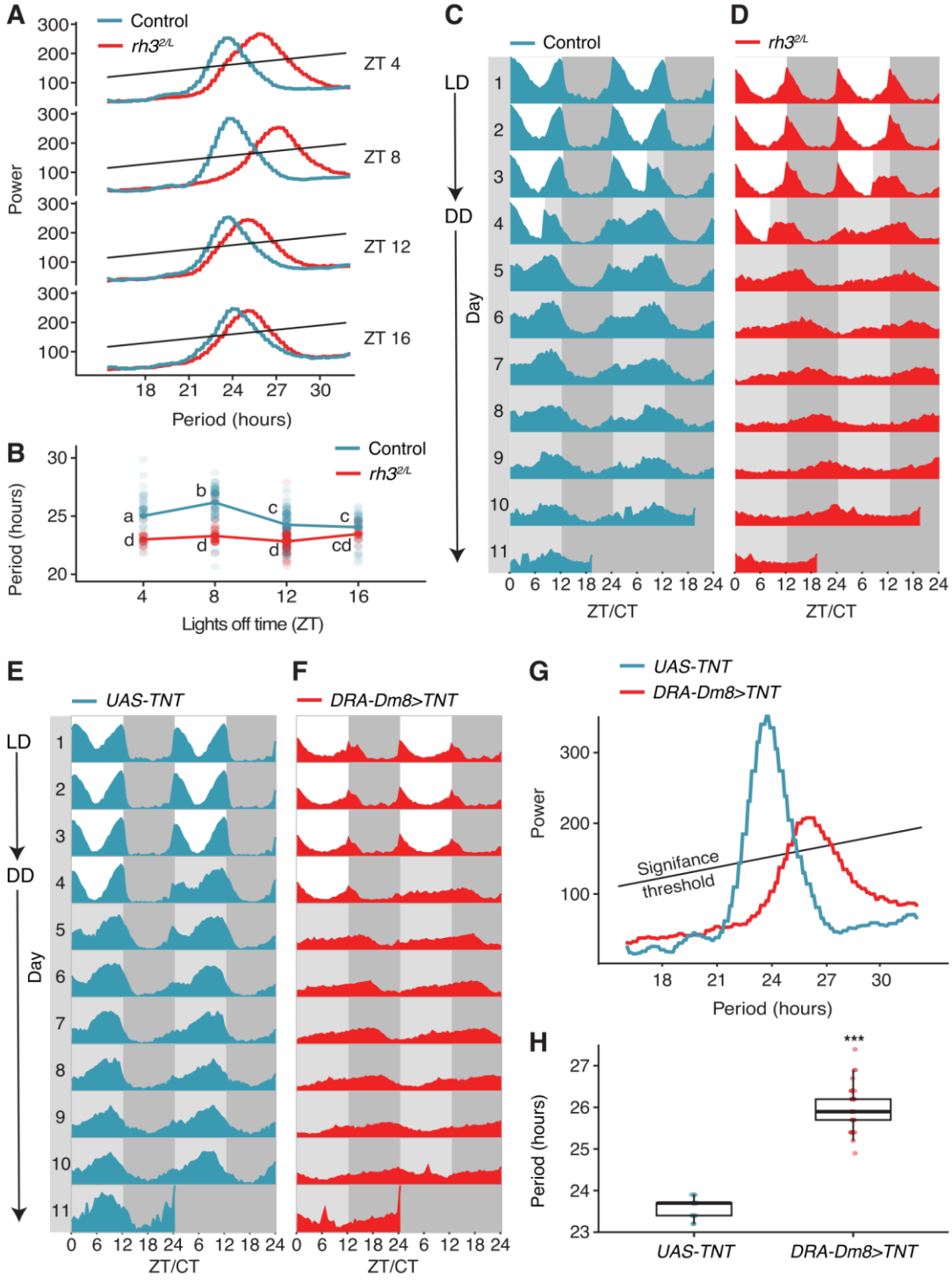
A
Control
rh3²/L
ZT 4
ZT 8
ZT 12
ZT 16
Power
Period (hours)
B
Control
rh3²/L
Period (hours)
Lights off time (ZT)
C
Control
LD
DD
Day
ZT/CT
D
rh3²/L
ZT/CT
E
UAS-TNT
LD
DD
Day
ZT/CT
F
DRA-Dm8>TNT
ZT/CT
G
UAS-TNT
DRA-Dm8>TNT
Power
Signifance threshold
Period (hours)
H
Period (hours)
***
UAS-TNT
DRA-Dm8>TNT

Figure 4. Loss of *rh3* extends circadian periodicity

(A) Periodograms for control (w^+,w^{1118}) and *rh3* mutant flies receiving 4, 8, 12, or 16 hours of light on the day prior to being shifted to dark/dark (DD) conditions.

(B) Relationship between periodicity and lights and lights off time with line passing through each group's median. For the control: n = 27 flies for ZT 4, 65 flies for ZT 8, 272 flies for ZT 12, and 30 flies for ZT 16. For *rh3:* n = 53 flies for ZT 4, 80 flies for ZT 8, 95 flies for ZT 12, and 59 flies for ZT 16. Groups were compared via two-way ANOVA examining the interaction effect between the length of time the last light stimulus (4–16 hours) genotype. Group means were then compared via Tukey's Honest Significant Difference test. Each unique letter (a, b and c) indicates that a group is significantly different ($p \leq 0.05$) from groups labeled with other letters. Groups that share the same letters indicate that there are no significant differences between them.

(C, D, E and F) Double-plotted, representative actograms showing circadian locomotor activity. Circadian time (CT) is a standard unit of time based on the endogenous free-running period of a rhythm. Zeitgeber time (ZT) is a unit of time based on the period of a zeitgeber, such as the 12 h:12 h light/dark cycle. The amplitudes indicate the relative proportion of time that the flies moved during each 30-minute bin. Flies were maintained under 12 h:12 h light/dark cycles (white and dark gray shading, respectively) for three days (C and D, lights off on ZT8 on the fourth day) or four days (E and F) , and then moved to constant darkness for seven days (light gray shading and dark gray shading indicate the subjective days and nights). Each row displays two days of activity. Because these are double-plots, the second day in a given row (on the right), is repeated on the following row (on the left).

(C) Control (w^+,w^{1118}) actogram.

(D) *rh3*$^{2/L}$ actogram.

(E) Actogram showing *UAS-TNT* flies.

(F) Actogram showing flies expressing tetanus toxin under the control of *DRA-Dm8-Gal4* (*DRA-Dm8>TNT)* .

(G) Chi-square periodograms showing free-running (constant darkness) periodicities for the control flies (*UAS-TNT*) and flies expressing tetanus toxin under control of the *DRA-Dm8-Gal4*. Only rhythmic animals were included in the periodicity calculations (peak power with $p<0.05$). Above significance threshold indicates that the power had a p-value ≤ 0.05.

(H) Box and whisker plots comparing the free-running periodicities of control flies (*UAS-TNT*) and *DRA-Dm8>TNT flies.* The boxes display the median, the 25th percentile, and the 75th percentile, with the whiskers representing 1.5 times the interquartile range.

n = 223 flies for control flies, n = 174 for *rh3*$^{2/L}$, n = 64 for *DRA-Dm8>TNT*, and n = 32 for *UAS-TNT*. Student's *t*-test test. ***$p<0.0005$.

Figure 5

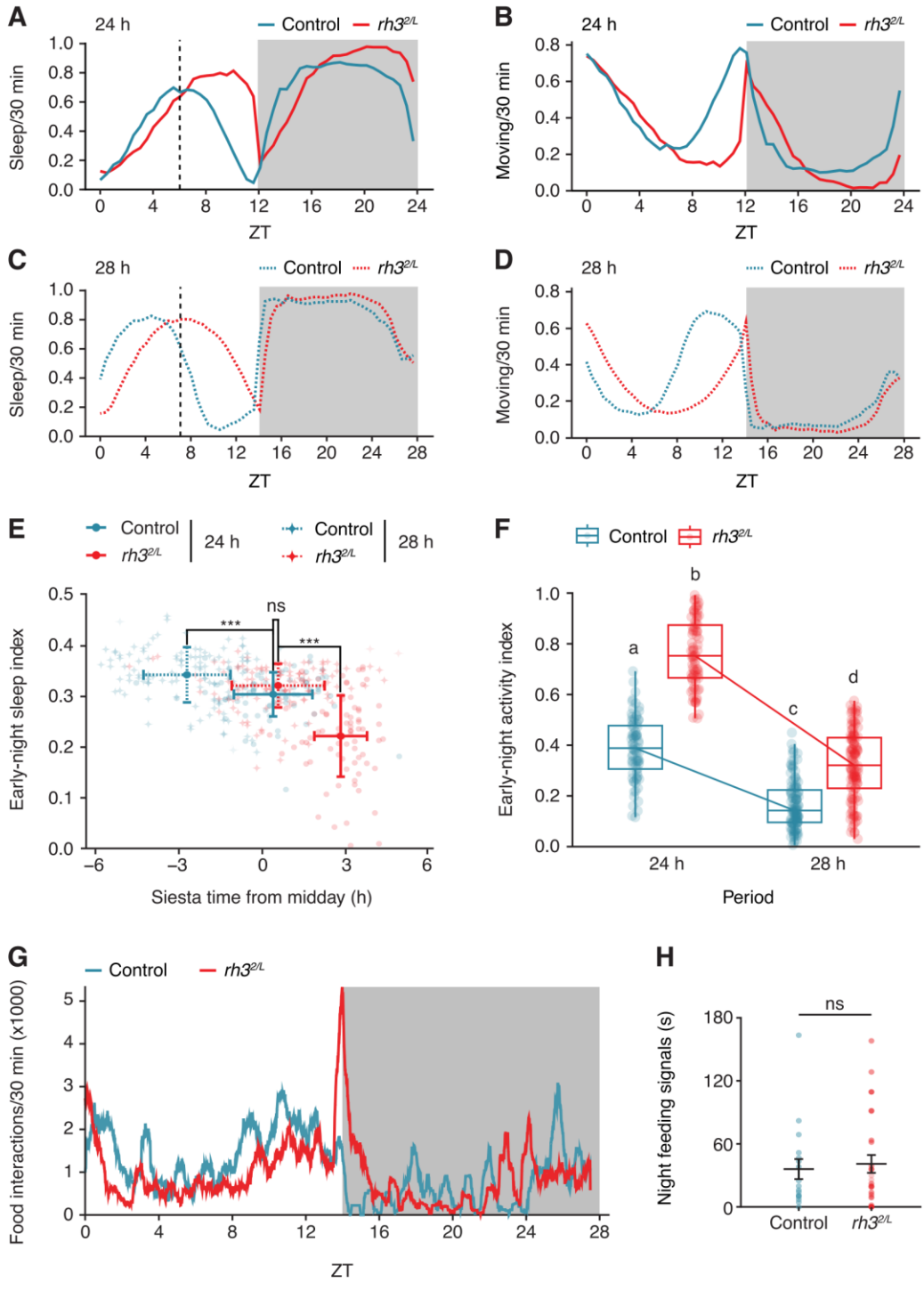
A
24 h
Control
rh3²/L
Sleep/30 min
ZT
B
24 h
Moving/30 min
ZT
C
28 h
Sleep/30 min
ZT
D
28 h
Moving/30 min
ZT
E
Control
rh3²/L
24 h
28 h
Early-night sleep index
ns
***
Siesta time from midday (h)
F
Early-night activity index
a
b
c
d
24 h
28 h
Period
G
Food interactions/30 min (x1000)
ZT
H
Night feeding signals (s)
ns
Control
rh3²/L

Figure 5. Circadian alignment restores the timing of behavior in *rh3* flies

(A) Sleep profiles exhibited by the control (w^+,w^{1118}, blue) and $rh3^{2/L}$ flies (red) under a 12 h:12 h (24 h) light/dark schedule. Profiles represent the average from four days of recordings. The dashed vertical line indicates midday.

(B) Activity profile showing the average of four days of activity data for flies housed under a 12 h:12 h light/dark cycle (24 h).

(C) Sleep profiles of control (blue) and $rh3^{2/L}$ flies (red) under a 14 h:14 h (28 h) light/dark schedule. Profiles represent the average from three days (84 hours) of recordings. The dashed vertical line indicates midday.

(D) Activity profile showing three days (84 hours) of activity data for flies housed under a 14 h:14 h (28 h) light/dark cycle. The Y-axis indicates the proportion of time the flies move in a 30-minute bin.

(E) Bivariate chronotype plot showing early-night sleep indexes, and siesta times from the midday using flies housed under either a 24-h or 28-h light/dark schedules. Statistical significance was determined using pairwise Student's *t*-test with a Bonferroni multiple testing correction.

(F) Early night activity indexes for flies maintained under either a 24-h or 28-h light/dark schedule. Statistical significance was determined using two-way ANOVA followed by a Tukey Honest Significant Difference test. Each unique letter (a, b and c) indicates that a group is significantly different ($p \leq 0.05$) from groups labeled with other letters.

(G) 28-h feeding profile using flies maintained under a 28-h LD schedule.

(H) Nighttime feeding signals (measured using the FLIC assay) exhibited by control and $rh3^{2/L}$ flies and compared using an unpaired Student's *t*-test. ns, not significant.

(A—F), n = 80 for control (24 h), n =116 for control (28 h), n = 78 for *rh3*$^{2/L}$ (24 h), and n = 119 for *rh3*$^{2/L}$ (28 h). For the feeding experiments (G, H), n = 17 for control and n = 27 for *rh3*$^{2/L}$. *** $p<0.0005$.

Figure 6

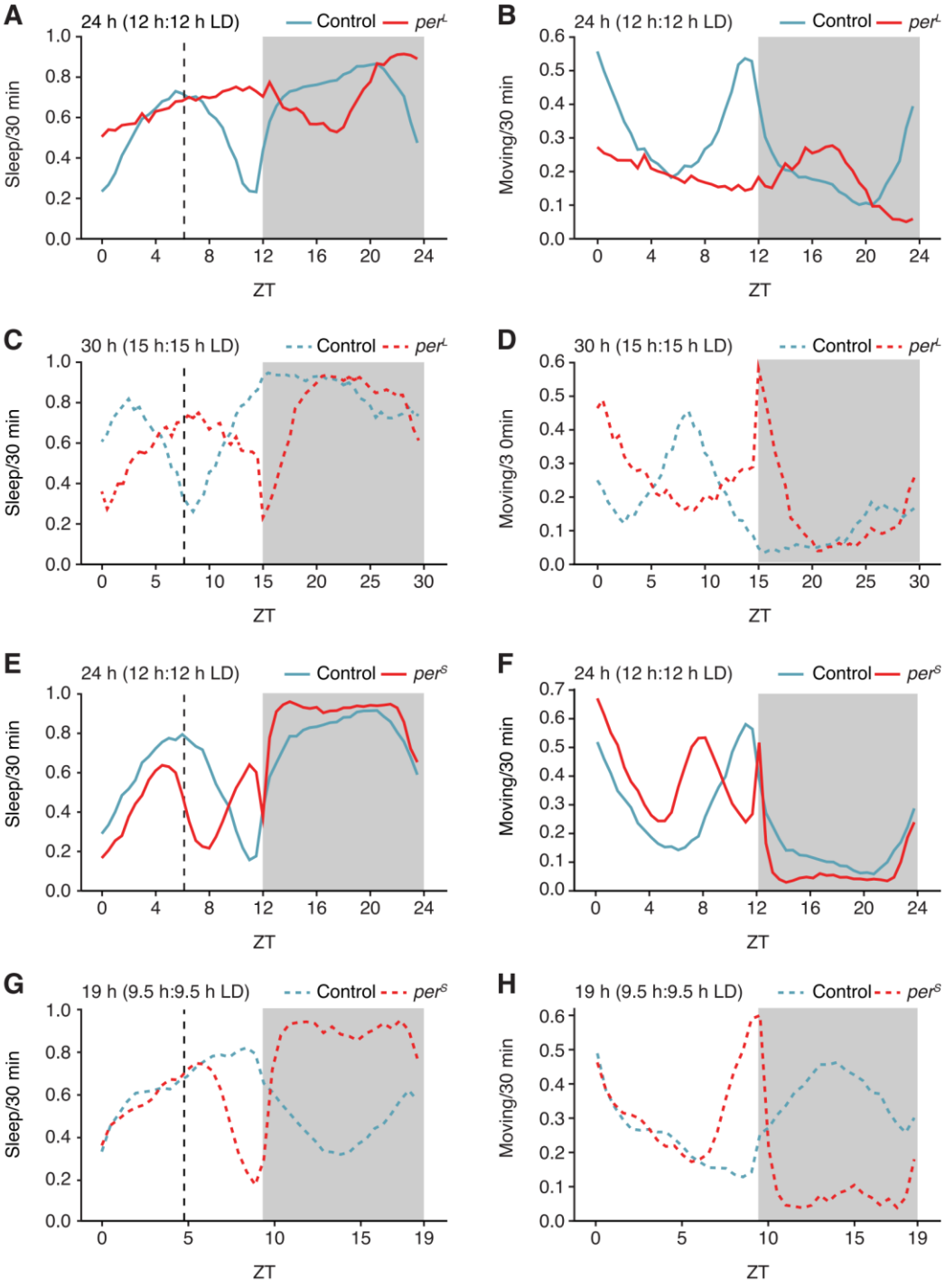
A
24 h (12 h:12 h LD)
Control
perL
Sleep/30 min
ZT
B
24 h (12 h:12 h LD)
Control
perL
Moving/30 min
ZT
C
30 h (15 h:15 h LD)
Control
perL
Sleep/30 min
ZT
D
30 h (15 h:15 h LD)
Control
perL
Moving/3 0min
ZT
E
24 h (12 h:12 h LD)
Control
perS
Sleep/30 min
ZT
F
24 h (12 h:12 h LD)
Control
perS
Moving/30 min
ZT
G
19 h (9.5 h:9.5 h LD)
Control
perS
Sleep/30 min
ZT
H
19 h (9.5 h:9.5 h LD)
Control
perS
Moving/30 min
ZT

Figure 6: Circadian alignment can modify morning and evening chronotypes

(A) Four-day average sleep profile of control (w^{1118}) and per^{L} flies housed under 12 h:12 h light/dark cycles. The dashed line indicates midday.

(B) Four-day average movement profile of control (w^{1118}) and per^{L} flies housed under 12 h:12 h light/dark cycles.

(C) Four-day average sleep profile of control (w^{1118}) and per^{L} flies housed under 15 h:15 h light/dark cycles. The dashed line indicates midday.

(D) Four-day average movement profile of control (w^{1118}) and per^{L} flies housed under 15 h:15 h light/dark cycles.

(E) Average sleep profile of control (w^{1118}) and per^{S} flies housed under 12 h:12 h light/dark cycles. The dashed line indicates midday.

(F) Average sleep profile of control (w^{1118}) and per^{S} flies housed under 12 h:12 h light/dark cycles.

(G) Average sleep profile of control (w^{1118}) and per^{S} flies housed under 9.5 h:9.5 h light/dark cycles. The dashed line indicates midday.

(H) Average movement profile of control (w^{1118}) and per^{S} flies housed under 9.5 h:9.5 h light/dark cycles.

n = 60—96 flies/genotype/condition.

Figure 7

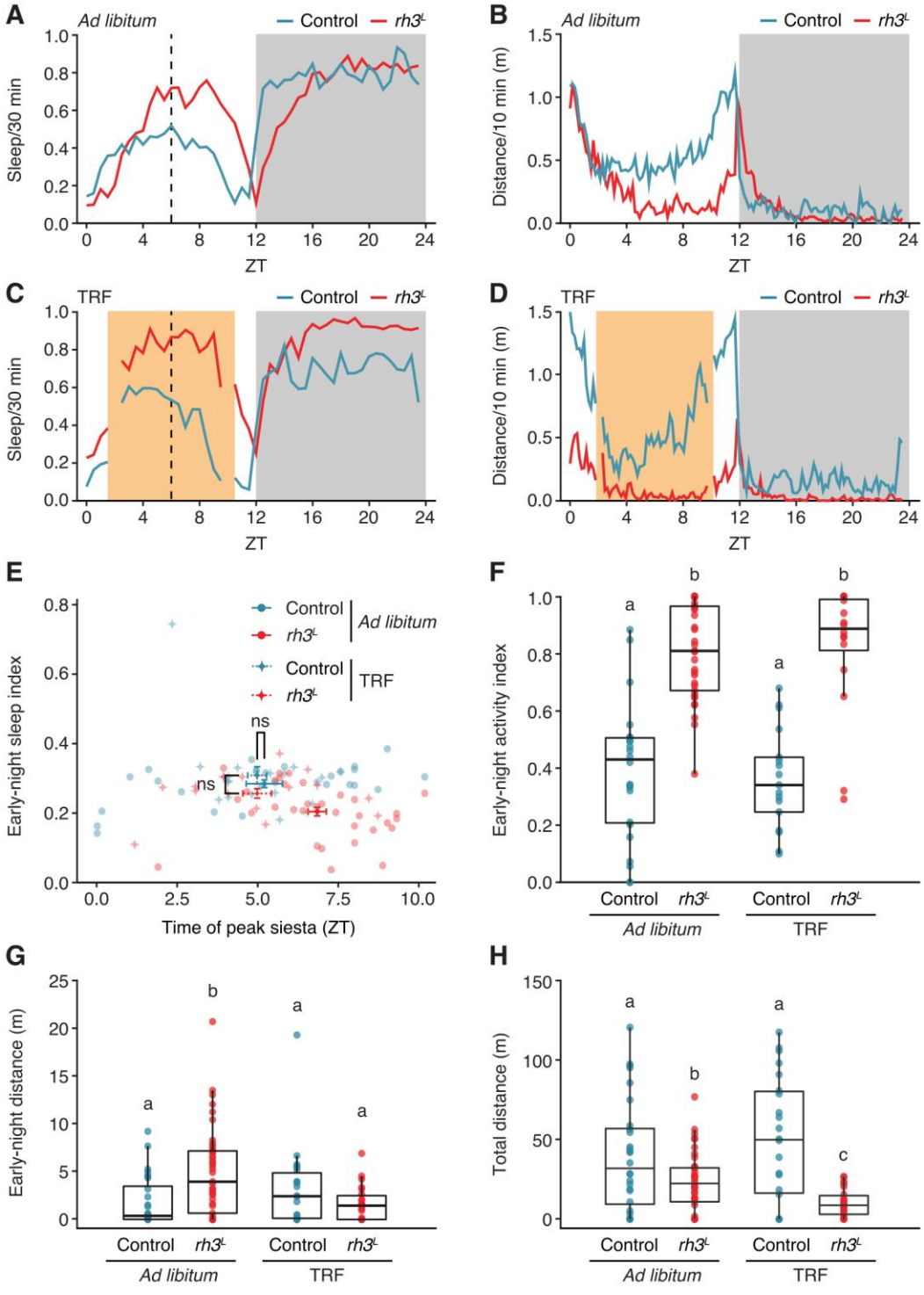
A
Ad libitum
Control
rh3L
Sleep/30 min
ZT
B
Ad libitum
Control
rh3L
Distance/10 min (m)
ZT
C
TRF
Control
rh3L
Sleep/30 min
ZT
D
TRF
Control
rh3L
Distance/10 min (m)
ZT
E
Control
rh3L
Ad libitum
Control
rh3L
TRF
ns
ns
Early-night sleep index
Time of peak siesta (ZT)
F
Early-night activity index
Control
rh3L
Control
rh3L
Ad libitum
TRF
G
Early-night distance (m)
Control
rh3L
Control
rh3L
Ad libitum
TRF
H
Total distance (m)
Control
rh3L
Control
rh3L
Ad libitum
TRF

Figure 7. Time restricted feeding restores a normal chronotype in the *rh3* mutant

(A) Sleep profile of control (w^+,w^{1118}) and *rh3* mutants ($rh3^L$) with *ad libitum* access to food. Sleep (Y-axis) corresponds to the proportion of time asleep in a 30-minute bin from one full day of video tracking.

(B) Activity profile showing one full day recording the movement of flies with *ad libitum* access to food. Y-axis (distance) represents the average movement per fly in a 10-minute bin, assayed using video tracking.

(C) Sleep profile of control (w^+,w^{1118}) and *rh3* mutants ($rh3^L$) with eight-hour restricted access to food. The 30-minute gaps beginning at ZT 2 and 10 are due to the introduction or removal of food, which temporarily interferes with video tracking, and causes movement artifacts.

(D) Activity profile of control (w^+,w^{1118}) and *rh3* mutants ($rh3^L$) with eight-hour restricted access to food. The 10-minute gaps beginning at ZT 2 and 10 are due to the introduction or removal of food, which temporarily interferes with video tracking, and causes movement artifacts.

(E) Bivariate chronotype plots indicating early-night sleep index vs. time of peak siesta for flies with either *ad libitum* access to food or eight-hour restricted access to food. See the STAR Methods for formulas for each parameter.

(F) Early-night activity index for flies with either *ad libitum* feeding or eight-hour restricted access to food. Each unique letter (a, and b) indicates that a group is significantly different ($p \leq 0.05$) from the group labeled with the other letter.

(G) Early-night activity (from ZT 12 to ZT 16) for control and $rh3^L$ flies with either *ad libitum* food access or eight-hour restricted access to food. Each unique letter (a and b) above

the box plots indicates that the group is significantly different ($p \leq 0.05$) from the other group.

(H) Total night activity (from ZT 12 to ZT 24) for control and $rh3^{L}$ mutants with either *ad libitum* access or eight-hour restricted access to food. Each unique letter above the box plots indicates that a group is significantly different ($p \leq 0.05$) from other groups.

n = 18—33 flies/genotype. The p values were calculated using a non-parametric Aligned Rank Transform ANOVA, comparing the factors genotype and diet.

Figure S1

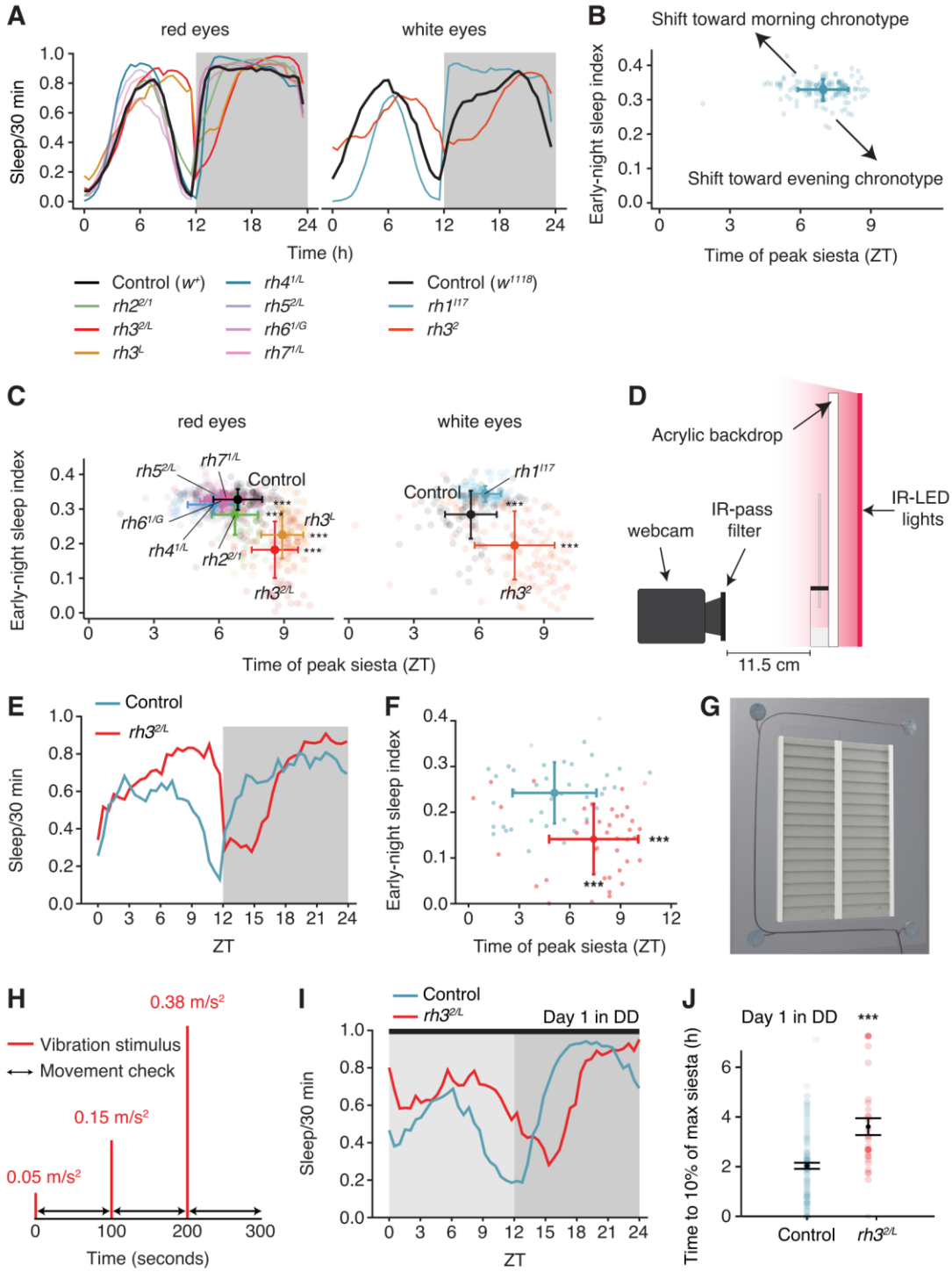
A
red eyes
white eyes
Sleep/30 min
Time (h)
Control (w+)
rh2^2/1
rh3^2/L
rh3^L
rh4^1/L
rh5^2/L
rh6^1/G
rh7^1/L
Control (w^1118)
rh1^I17
rh3^2
B
Shift toward morning chronotype
Shift toward evening chronotype
Early-night sleep index
Time of peak siesta (ZT)
C
red eyes
white eyes
Control
rh5^2/L
rh7^1/L
rh6^1/G
rh3^L
rh4^1/L
rh2^2/1
rh3^2/L
rh1^I17
rh3^2
Early-night sleep index
Time of peak siesta (ZT)
D
Acrylic backdrop
IR-LED lights
webcam
IR-pass filter
11.5 cm
E
Control
rh3^2/L
Sleep/30 min
ZT
F
Early-night sleep index
Time of peak siesta (ZT)
G
H
0.38 m/s²
Vibration stimulus
Movement check
0.15 m/s²
0.05 m/s²
Time (seconds)
I
Control
rh3^2/L
Day 1 in DD
Sleep/30 min
ZT
J
Day 1 in DD
Time to 10% of max siesta (h)
Control
rh3^2/L

Figure S1. Effect of opsins on chronotype

(A) Sleep profiles of control (w^{+}) or (w^{1118}) and opsin mutant flies, separated by eye color. Each profile represents the average from four days of recording. Sleep (Y-axis) corresponds to the proportion of time asleep in a 30-minute bin. Shown are the results compiled from 81–147 flies for each genotype.

(B) Example bivariate chronotype plot showing the early-night sleep index and the time of the daytime siesta from control flies with red eyes. The arrows represent possible shifts towards a morning chronotype (i.e., an increase in early-night sleep index and a decrease in the time of the daytime siesta) or evening chronotype (i.e., a decrease in early-night sleep index and an increase in daytime siesta). The dots represent the means of both parameters and the error bars represent standard deviations. n = 148.

(C) Chronotype plots showing opsin mutants with either red or white eyes. Note, only *rh3* mutants showed a significant, directionally consistent shift in both chronotype parameters, indicating a shift towards evening chronotype. $n \geq 3$ biological replicates for each genotype. Each replicate included 25–32 flies.

Statistical significance was determined using pair-wise Student's *t*-tests with Bonferroni multiple testing corrections. ***$p<0.0005$. *rh3* mutants showed directional changes for both parameters which is defined as an evening chronotype. A complete list of statistics is compiled in Supplementary Table S1.

(D) Single-fly enclosure for video-based motion tracking. Flies were loaded into clear cuvettes with *ad libitum* access to a liquid 5% sucrose food source provided in a 5 μL capillary tube secured at the top of the cuvette. At the bottom of the cuvette is 1.5 mL of

1.5% agar. See STAR Methods for complete protocol detailing the motion-tracking approach.

(E) Sleep profile of control (w^+,w^{1118}) and *rh3* mutants ($rh3^{2/L}$) assayed using video-tracking. Sleep (Y-axis) corresponds to the proportion of time asleep in a 30-minute bin from one full day of recording.

(F) Bivariate chronotype plots indicating early-night sleep index versus time of daytime siesta from video-tracking data. See methods for the formula for each parameter.

n = 39–41 flies/genotype.

(G) Model of sleep arousal behavioral arena.

(H) Vibration stimulus protocol. Flies were exposed to three vibration stimuli (red) that each lasted for three seconds with increasing intensity (measured in acceleration, m/s^2), with a two minute pause before adjacent stimuli. Fly arousal was recorded if a fly that was immobile prior to the vibration stimuli onset moved in the two minutes following the onset of a vibration (movement check, black line with arrows)

(I) Sleep profile of control (w^+,w^{1118}) and *rh3* mutants ($rh3^{2/L}$) in the first subjective day under constant darkness using the DAM system.

(J) Quantification of timing to 10% of maximum siesta for control (w^+,w^{1118}) flies and *rh3* mutants in the first subjective day under constant darkness.

Figure S2

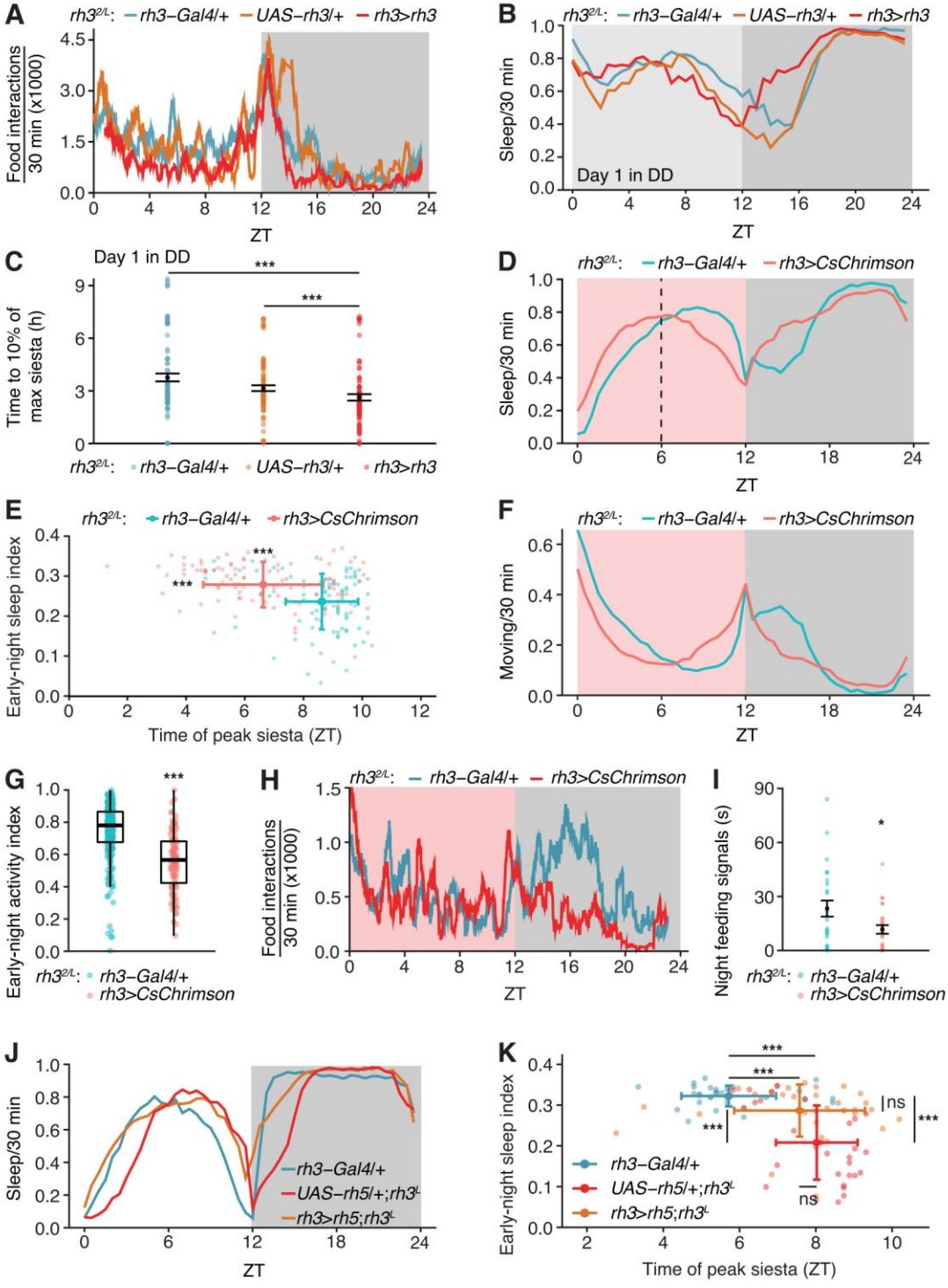
A
rh3²/ᴸ: rh3–Gal4/+ UAS–rh3/+ rh3>rh3
Food interactions 30 min (x1000)
ZT
B
Sleep/30 min
Day 1 in DD
ZT
C
Day 1 in DD
Time to 10% of max siesta (h)
D
rh3²/ᴸ: rh3–Gal4/+ rh3>CsChrimson
Sleep/30 min
ZT
E
Early-night sleep index
Time of peak siesta (ZT)
F
Moving/30 min
ZT
G
Early-night activity index
rh3–Gal4/+
rh3>CsChrimson
H
Food interactions 30 min (x1000)
ZT
I
Night feeding signals (s)
J
Sleep/30 min
rh3–Gal4/+
UAS–rh5/+;rh3ᴸ
rh3>rh5;rh3ᴸ
ZT
K
Early-night sleep index
ns
Time of peak siesta (ZT)

Figure S2. Effect of non-UV light sensors on chronotype

(A) 24-h food-interaction profile (measured using FLIC assays) exhibited by *rh3*$^{2/L}$ mutant flies expressing a wild-type *rh3* transgene (*UAS-rh3*) under control of the *rh3-Gal4* (*rh3>rh3*). n = 21 for *rh3-Gal4*/+;*rh3*$^{2/L}$, n = 17 for *UAS-rh3*/+;*rh3*$^{2/L}$, and n = 26 for *rh3>rh3*;*rh3*$^{2/L}$.

(B) Sleep profile (using the DAM system) of *rh3>rh3* flies during the first subjective day under constant darkness.

(C) Quantification of timing to 10% of the maximum siesta for *rh3>rh3* flies during the first subjective day under constant darkness. ***p<0.0005.

(D) Sleep profile of *rh3*$^{2/L}$ flies expressing *UAS-CsChrimson* under control of the *rh3-Gal4* (*rh3>CsChrimson*;*rh3*$^{2/L}$). The flies were exposed to a 592 nm light during ZT 0–12. Each profile represents the average of four days of recordings. Sleep (Y axis) corresponds to the proportion of inactivity during each 30-minute bin. The dashed vertical line is placed at midday (ZT 6 under a 12 h:12 h light/dark cycle). n = 89 flies for *rh3-Gal4*/+;*rh3*$^{2/L}$ and n = 105 flies for *rh3>CsChrimson*;*rh3*$^{2/L}$.

(E) Bivariate chronotype plots indicating early-night sleep index versus the time of the daytime siesta. n = 89 flies for *rh3-Gal4*/+;*rh3*$^{2/L}$ and n = 105 flies for *rh3>CsChrimson*;*rh3*$^{2/L}$.

(F) Activity profiles showing four days of activity data for flies housed under a 12 h:12 h light/dark cycle. Moving (Y axis) corresponds to the proportion of time the flies moved during each 30-minute bin. n = 89 flies for *rh3-Gal4/+;rh3*$^{2/L}$ and n = 105 flies for *rh3>CsChrimson;rh3*$^{2/L}$.

(G) Reduction in the early-night activity index in *rh3*$^{2/L}$ by light activation of CsChrimson in *rh3*-expressing photoreceptor cells. n = 89 flies for *rh3-Gal4*/+;*rh3*$^{2/L}$ and n = 105 flies for *rh3>CsChrimson*;*rh3*$^{2/L}$. Unpaired Student's *t*-tests. ***p<0.0005.

(H) 24-h food-interaction profile (measured using FLIC assays) due to optogenetic rescue of *rh3* using CsChrimson expressed in *rh3*-expressing photoreceptor cells. n = 25 for *rh3-Gal4*/+;*rh3*$^{2/L}$ and n = 29 for *rh3>CsChrimson*;*rh3*$^{2/L}$.

(I) Night feeding signals in the *rh3*$^{2/L}$ mutant that was activated by CsChrimson in *rh3*-expressing photoreceptor cells. Mean ±SEMs. n = 25 for *rh3-Gal4*/+;*rh3*$^{2/L}$ and n = 29 for *rh3>CsChrimson*;*rh3*$^{2/L}$. Unpaired Student's t-tests. *p <0.05.

(J) Four-day average sleep profile (using DAM assays) showing flies ectopically expressing *rh5* in place of *rh3*.

(K) Bivariate chronotype plots indicating early-night sleep index versus time of daytime siesta. n = 29 flies for *rh3-Gal4*/+, n = 30 flies for *rh3>rh5*;*rh3*$^{2/L}$ n=32 flies, and n = 32 flies for *UAS-rh5*/+;*rh3*$^{2/L}$ flies. Student's *t*-test with Bonferroni multiple testing correction. ***p<0.0005.

Figure S3

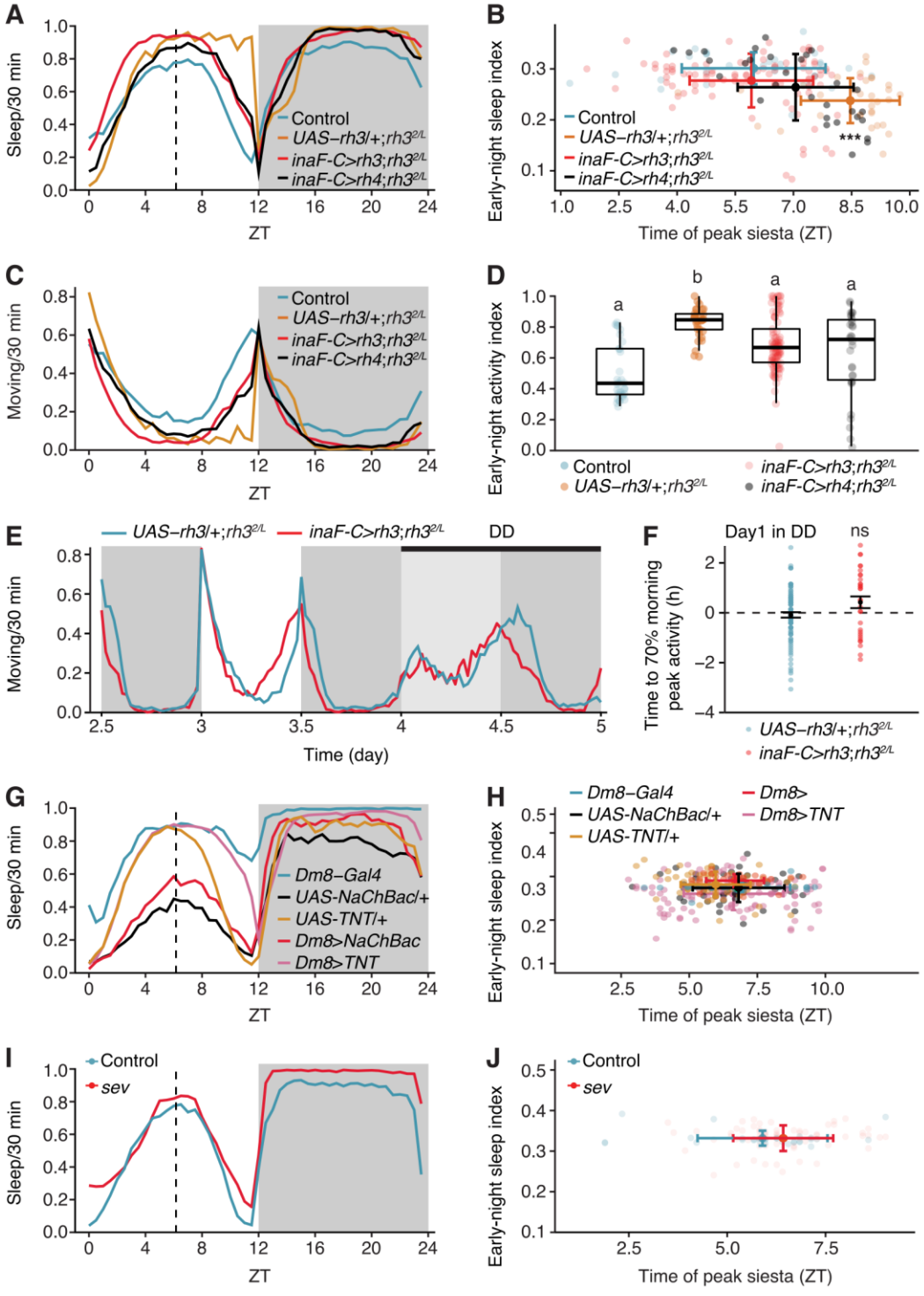
A
Sleep/30 min
ZT
Control
UAS–rh3/+;rh3²/ˡ
inaF-C>rh3;rh3²/ˡ
inaF-C>rh4;rh3²/ˡ
B
Early-night sleep index
Time of peak siesta (ZT)
***
C
Moving/30 min
D
Early-night activity index
a
b
a
a
E
DD
Time (day)
F
Day1 in DD
ns
Time to 70% morning peak activity (h)
G
Dm8–Gal4
UAS-NaChBac/+
UAS-TNT/+
Dm8>NaChBac
Dm8>TNT
H
Dm8–Gal4
UAS-NaChBac/+
UAS-TNT/+
Dm8>
Dm8>TNT
I
sev
J

Figure S3. Rh3 functions in photoreceptors to impact chronotype and *sevenless* locomotor data

(A) Four-day average sleep profile of flies expressing *UAS-rh3* or *UAS-rh4* in R7 photoreceptor cells in the $rh3^{2/L}$ mutant using *inaF-C-Gal4*.

(B) Bivariate chronotype plots indicating early-night sleep indexes versus times of the daytime siesta for flies shown in A. See STAR Methods for the formula for each parameter. Each parameter was compared using a Student's unpaired *t*-test with a Bonferroni multiple testing correction. n = 32 flies for *UAS-rh3/+;*$rh3^{2/L}$; n = 32 flies for control, n = 30 flies for *inaF-C>rh4;*$rh3^{2/L}$; n = 155 flies for *inaF-C>rh3;*$rh3^{2/L}$. ***p<0.0005.

(C) Activity profiles showing four days of activity data for flies housed under a 12 h:12 h light/dark cycle. Moving (Y-axis) corresponds to the proportion of time moving in a 30-minute bin.

(D) Early-night activity index exhibited by $rh3^{2/L}$ flies expressing *UAS-rh3* or *UAS-rh4* in R7 photoreceptor cells under control of the *inaF-C-Gal4* (*inaF-C>rh3;*$rh3^{2/L}$ and *inaF-C>rh4;*$rh3^{2/L}$, respectively). Means ± SEMs. n = 29 flies for *UAS-rh3;*$rh3^{2/L}$; n = 30 flies for *inaF-C>rh4;*$rh3^{2/L}$; n = 155 flies for *inaF-C>rh3;*$rh3^{2/L}$. Each unique letter indicates that a group is significantly different ($p \leq 0.05$) from other groups.

(E) Activity profiles (using the DAM system) for *inaF-C>rh3;*$rh3^{2/L}$ flies transitioning from a 12h:12h light:dark cycle (days 2.5–4) to constant darkness (day 4–5 is the first subjective day under constant darkness).

(F) Quantification of time to 70% of the morning peak activity of the first subjective day under constant darkness.

(G) Four-day average sleep profile of flies with activated (NachBac) or inhibited (TNT) Dm8 neurons. n = 52 flies for *UAS-NachBac/+*, n = 32 flies for *Ort-C2b-Gal4/+*, n = 62 flies for *UAS-TNT/+,* n = 124 flies for *Ort-C2b>TNT,* n = 32 flies for *Ort-C2b>NachBac.*

(H) Bivariate chronotype plot for flies with activated or inhibited Dm8 neurons. See STAR Methods for the formula for each parameter.

(I) Four-day average sleep profile exhibited by control (w^{+},w^{1118}) and *sevenless (sev^{14})* mutant flies. n = 64 control flies and n = 31 *sev^{14}* mutants.

(J) Bivariate chronotype plot for control (w^{+},w^{1118}) and *sevenless (sev^{14})* mutant flies. See STAR Methods for the formula for each parameter.

Figure S4

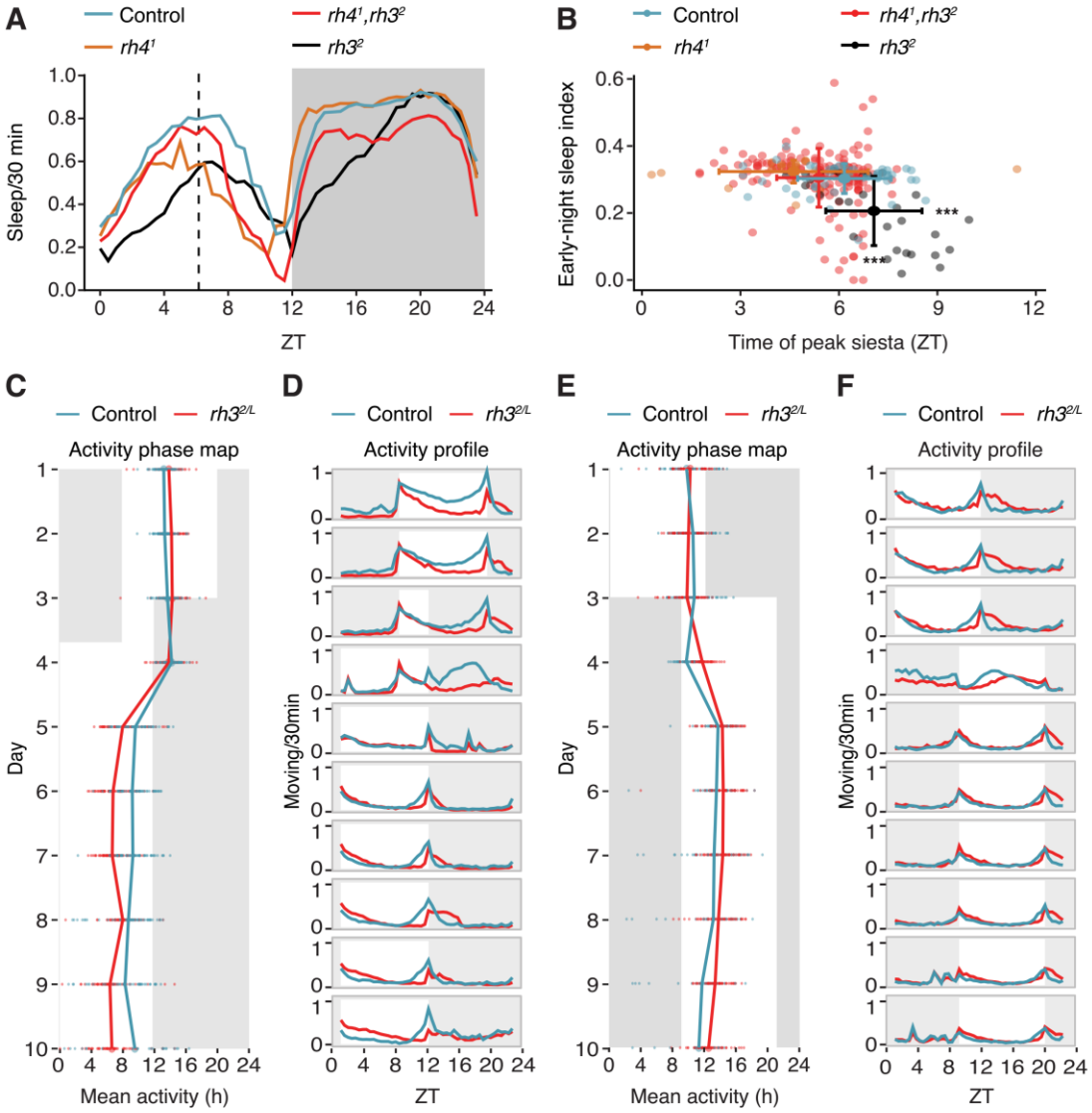
A
Control
rh4¹
rh4¹,rh3²
rh3²
Sleep/30 min
ZT
B
Early-night sleep index
Time of peak siesta (ZT)
***
C
Activity phase map
Day
Mean activity (h)
D
Activity profile
Moving/30min
ZT
E
F
rh3²/L

Figure S4. Flies with a simultaneous loss of *rh3* and *rh4* display a normal chronotype, and phase shifting is not impaired in *rh3* mutants

(A) Four-day average sleep profile of control (w^{1118}), $rh3^{2}$, $rh4^{1}$, and $rh4^{1}$,$rh3^{2}$ flies.

(B) Bivariate chronotype plots for $rh3^{2}$, $rh4^{1}$, and $rh4^{1}$,$rh3^{2}$. n = 30 flies for $rh3^{2}$, n = *19* flies for $rh4^{1}$, n = 154 flies for $rh4^{1}$,$rh3^{2}$. Student's *t*-test with Bonferroni multiple testing correction. ***p<0.0005.

(C) Activity phase plot of control (w^{+},w^{1118}) and $rh3^{2/L}$ mutants following a phase advance. The phase of activity was determined using the weighted mean of activity throughout the span of a day. Flies were maintained in a 12 h:12 h light/dark cycle for three days and allowed 12 hours of free running prior to an 8-h phase advance on day five.

(D) Activity profile of control (w^{+},w^{1118}) and $rh3^{2/L}$ mutant flies following the phase advance shown in the phase map in (C). The Y axis corresponds to the average number of beam breaks per fly/minute in a 30-minute bin.

(E) Activity phase plot of control (w^{+},w^{1118}) and $rh3^{2/L}$ mutants following a phase delay. The phase of activity was determined using the weighted mean of activity throughout the span of a day. Flies were maintained in a 12 h:12 h light/dark cycle for three days and allowed 12 hours of free running prior to an 8-h phase delay on day five.

(F) Activity profile of control (w^{+},w^{1118}) and $rh3^{2/L}$ mutant flies following the phase advance shown in the phase map in (E). Y axis corresponds to the average number of beam breaks per fly/minute in a 30-minute bin. n = 56—62 flies/genotype/condition.

Figure S5

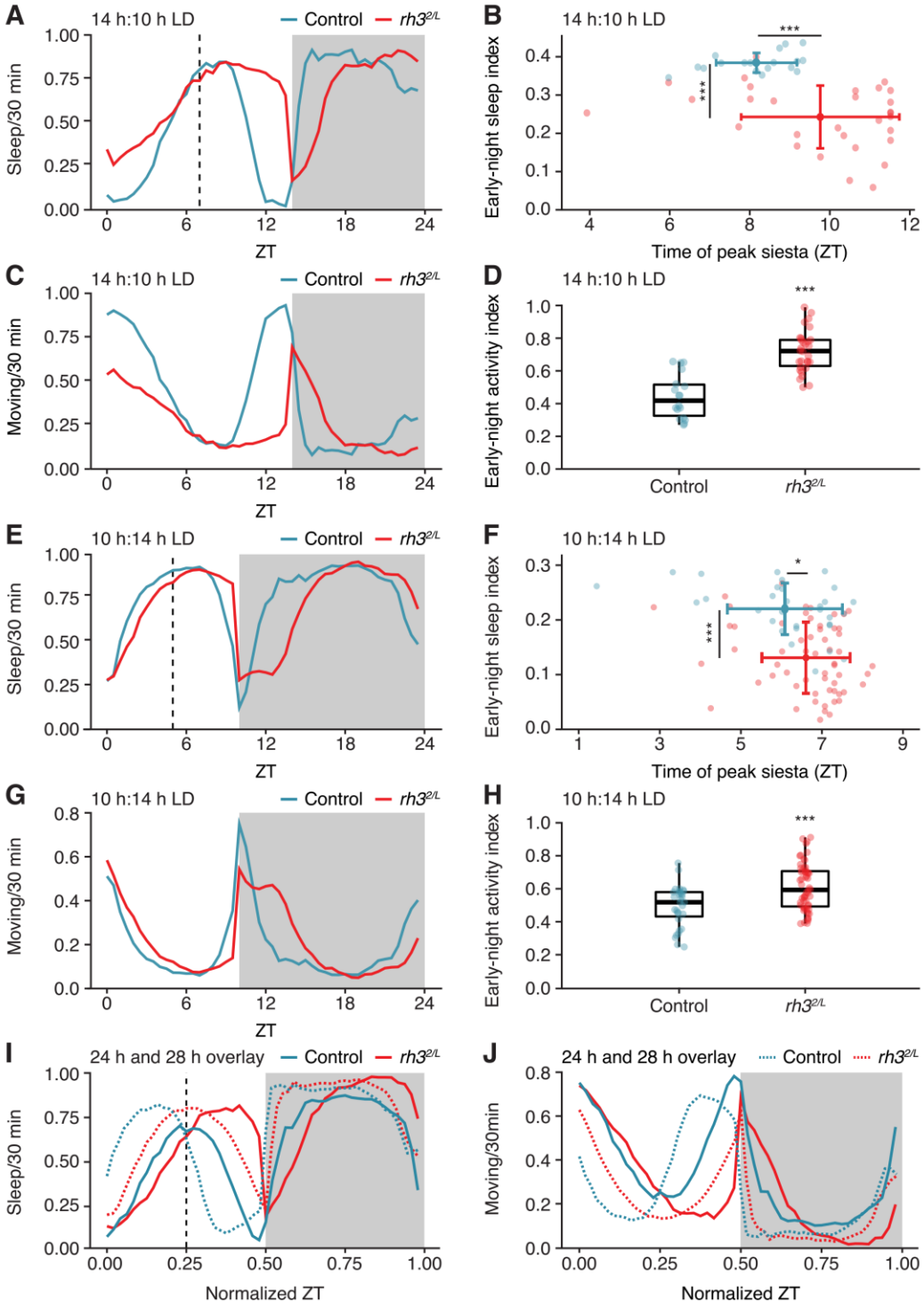
A
14 h:10 h LD
Control
rh3²/L
Sleep/30 min
ZT
B
14 h:10 h LD
Early-night sleep index
Time of peak siesta (ZT)
C
14 h:10 h LD
Moving/30 min
ZT
D
14 h:10 h LD
Early-night activity index
Control
rh3²/L
E
10 h:14 h LD
Sleep/30 min
ZT
F
10 h:14 h LD
Early-night sleep index
Time of peak siesta (ZT)
G
10 h:14 h LD
Moving/30 min
ZT
H
10 h:14 h LD
Early-night activity index
Control
rh3²/L
I
24 h and 28 h overlay
Sleep/30 min
Normalized ZT
J
24 h and 28 h overlay
Moving/30min
Normalized ZT

Figure S5. Modification of the relative lengths of the light or dark phases does not suppress the evening chronotype in *rh3* flies

(A) Four-day average sleep profile from control (w^+,w^{1118}) and $rh3^{2/L}$ flies housed under a 14 h:10 h LD schedule.

(B) Bivariate chronotype plot from flies housed under a 14 h:10 h LD schedule. Each parameter was compared using the Wilcoxon Rank Sum Test.

(C) Four-day average activity profile of control (w^+,w^{1118}) and $rh3^{2/L}$ flies housed under a 14 h:10 h LD cycle.

(D) Early-night activity index for flies under a 14 h:10 h LD cycle.

(E) Four-day average sleep profile from control (w^+,w^{1118}) and $rh3^{2/L}$ flies housed under a 10 h:14 h LD schedule.

(F) Bivariate chronotype plot from flies housed under a 10 h:14 h light/dark schedule. Each parameter was compared using the Wilcoxon Rank Sum Test.

(G) Four-day average activity profile of control (w^+,w^{1118}) and $rh3^{2/L}$ flies housed under a 10 h:14 h light/dark cycle.

(H) Early-night activity index for flies housed under a 10 h:14 h LD cycle.

(I) Overlay of 24 h and 28 h sleep profiles exhibited by control (w^+,w^{1118}) and $rh3^{2/L}$ flies, replotted from Figures 5A–5D with normalized ZTs.

(J) Overlay of 24 h and 28 h activity profiles from control (w^+,w^{1118}) and $rh3^{2/L}$ flies, replotted from Figure 5 with normalized ZTs.

n = 56—64 flies/genotype/condition. *p <0.05. ***p<0.0005.

Figure S6

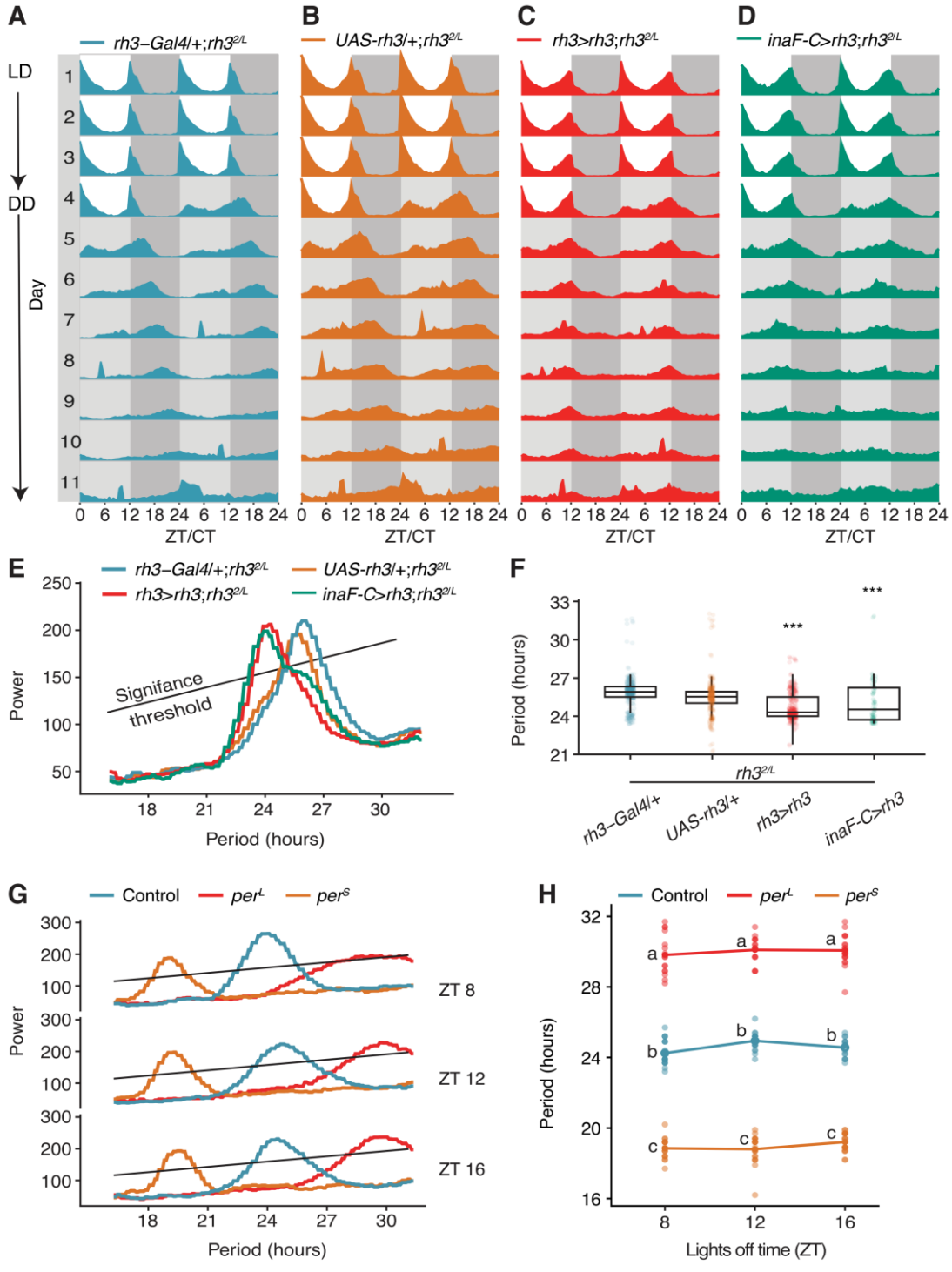
A
B
C
D
rh3–Gal4/+;rh3²/L
UAS-rh3/+;rh3²/L
rh3>rh3;rh3²/L
inaF-C>rh3;rh3²/L
LD
DD
Day
1
2
3
4
5
6
7
8
9
10
11
0 6 12 18 24 6 12 18 24
ZT/CT
E
Power
Signifance threshold
Period (hours)
F
Period (hours)
***
rh3²/L
rh3–Gal4/+
UAS-rh3/+
rh3>rh3
inaF-C>rh3
G
Control
perL
perS
ZT 8
ZT 12
ZT 16
Power
Period (hours)
H
Period (hours)
Lights off time (ZT)

Figure S6. Rh3 functions in the R7 cells to regulate circadian periodicity

(A—D) Double plotted, representative actograms using the indicated flies. The Y-axis corresponds to the proportion of time moving in a 30-minute bin. The flies were maintained under 12 h:12 h light/dark cycles for four days, then moved to constant darkness for seven days to calculate circadian periodicities.

(A) *Gal4* control (*rh3-Gal4*/+;$rh3^{2/L}$).

(B) *UAS* control (*UAS-rh3*/+;$rh3^{2/L}$).

(C) *rh3* rescue (*rh3>rh3;*$rh3^{2/L}$).

(D) Rescue of *rh3* mutant phenotype by expression of *UAS-rh3* in R7 cells (*inaF-C>rh3;*$rh3^{2/L}$).

(E) Chi-square periodogram showing free-running periodicities for the indicated flies.

(F) Box and whisker plots comparing the periodicities for the indicated flies. The box plots display the median, 25th percentile, and 75th percentile. The whiskers indicate 1.5 x the interquartile range or the min/max values if no values surpass 1.5xIQR).

(G) Periodograms for control (w^{1118}), per^S and per^L mutant flies receiving 8, 12, or 16 hours of light on the day prior to being shifted to DD.

(H) Relationship between periodicity and duration of last light stimulus before shifting to DD conditions. The lines pass through each group's median. For the control: n = 64 flies/genotype/condition. Groups were compared using two-way ANOVA examining the interaction effect between duration of last light stimulus and genotype. Group means were compared using Tukey Honest Significant Difference test. Each unique letter indicates that a group is significantly different from other groups.

Figure S7

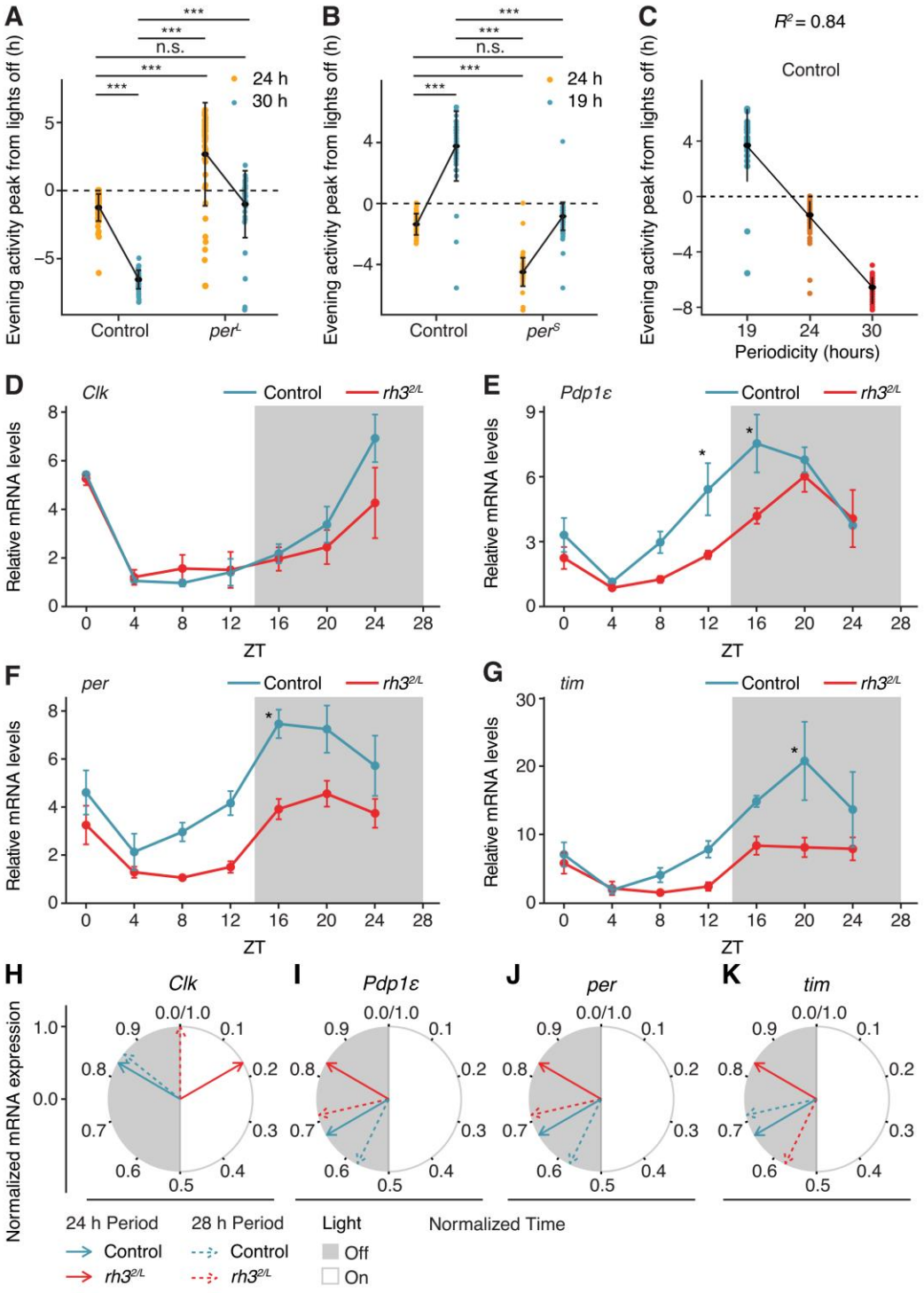
A
B
C
Evening activity peak from lights off (h)
***
n.s.
24 h
30 h
19 h
Control
per^L
per^S
R² = 0.84
Periodicity (hours)
D
E
F
G
Clk
Pdp1ε
per
tim
Control
rh3^2/L
Relative mRNA levels
ZT
H
I
J
K
Normalized mRNA expression
24 h Period
28 h Period
Light
Off
On
Normalized Time

Figure S7. Circadian alignment restores the phase of clock gene expression and chronotype in *per*^{S} and *per*^{L} mutants

(A) Two-way interaction plot indicating the timing of the evening activity peak relative to lights off in control (*w*^{1118}) and *per*^{L} flies housed under a LD cycle with either a 24-h periodicity (12 h:12 h light/dark) or a 30-h periodicity (15 h:15 h light/dark). ***p<0.0005.

(B) Two-way interaction plot indicating the timing of the evening activity peak relative to lights off exhibited by the control (*w*^{1118}) and *per*^{S} flies housed under a LD cycle with either a 24 h periodicity (12 h:12 h light/dark) or a 19 h periodicity (9.5 h:9.5 h light/dark). ***p<0.0005.

(C) Relative timing of the evening activity peak in control (*w*^{1118}) flies housed under a light/dark cycle with a 19-, 24-, or 30-hour periodicity. Statistical significance was determined using two-way ANOVA for S7A and S7B and one-way ANOVA for S7C.

(D—E) Circadian mRNA expression of core-clock genes in control and *rh3* mutant flies, housed under 14 h:14 h (28-h) light/dark cycles. The fold changes were calculated using the ΔΔCT method and were normalized to *rp49*, as well as to the trough of expression for each gene. RNA was extracted from whole-fly homogenates and each data point represents the mean from three independent RNA samples. Error bars represent the mean ± SEM. Statistical significance between each genotype was determined using two-way ANOVA, with Benjamini-Hochberg multiple testing correction.

*p<0.05.

(D) Relative *Clk* mRNA levels.

(E) Relative *Pdp1ε* mRNA levels.

(F) Relative *per* mRNA levels.

(G) Relative *tim* mRNA levels.

(H—K) Circular phase plots of peak core-clock mRNA expression from flies maintained under either a 24-h or 28-h LD cycle. Phase is normalized to the length of each light schedule to 1.0 to facilitate comparisons between 24-h and 28-h conditions (light period is from 0 to 0.5 and the dark period is from 0.5 to 1.0). The mRNA expression peaks are indicated by either solid arrows (24 h periods) or dashed arrows (28 h periods) where blue represents control and red represents *rh3* mutant.

(H) *Clk*.

(I) *Pdp1ε*.

(J) *per*.

(K) *tim*.

Parameter	group1	group2	n1	n2	p	p.signif	p.adj..Bonferroni.	p.adj.signif
Daytime_Siesta	rh1[117]	rh2[2]/rh2[1]	95	81	0.0103	*	0.566	ns
Daytime_Siesta	rh1[117]	rh3[2]	95	147	1.52E-18	***	8.38E-17	***
Daytime_Siesta	rh1[117]	rh3[2]/rh3[lexA]	95	95	2.22E-39	***	1.22E-37	***
Daytime_Siesta	rh1[117]	rh3[lexA]	95	124	4.17E-56	***	2.30E-54	***
Daytime_Siesta	rh1[117]	rh4[1]/rh4[lexA]	95	83	0.0015	**	0.0824	ns
Daytime_Siesta	rh1[117]	rh5[2]/rh5[lexA]	95	96	0.238	ns	1	ns
Daytime_Siesta	rh1[117]	rh6[1]/rh6[G]	95	89	0.373	ns	1	ns
Daytime_Siesta	rh1[117]	rh7[1]/rh7[lexA]	95	84	0.919	ns	1	ns
Daytime_Siesta	rh1[117]	w+,w1118	95	148	0.000146	***	0.00803	**
Daytime_Siesta	rh1[117]	w1118	95	98	7.82E-05	***	0.0043	**
Daytime_Siesta	rh2[2]/rh2[1]	rh3[2]	81	147	1.55E-08	***	8.50E-07	***
Daytime_Siesta	rh2[2]/rh2[1]	rh3[2]/rh3[lexA]	81	95	8.80E-25	***	4.84E-23	***
Daytime_Siesta	rh2[2]/rh2[1]	rh3[lexA]	81	124	3.55E-37	***	1.95E-35	***
Daytime_Siesta	rh2[2]/rh2[1]	rh4[1]/rh4[lexA]	81	83	3.55E-08	***	1.95E-06	***
Daytime_Siesta	rh2[2]/rh2[1]	rh5[2]/rh5[lexA]	81	96	0.000217	***	0.012	*
Daytime_Siesta	rh2[2]/rh2[1]	rh6[1]/rh6[G]	81	89	0.000728	***	0.04	*
Daytime_Siesta	rh2[2]/rh2[1]	rh7[1]/rh7[lexA]	81	84	0.0166	*	0.914	ns
Daytime_Siesta	rh2[2]/rh2[1]	w+,w1118	81	148	0.417	ns	1	ns
Daytime_Siesta	rh2[2]/rh2[1]	w1118	81	98	2.43E-10	***	1.33E-08	***
Daytime_Siesta	rh3[2]	rh3[2]/rh3[lexA]	147	95	1.43E-09	***	7.84E-08	***
Daytime_Siesta	rh3[2]	rh3[lexA]	147	124	8.09E-19	***	4.45E-17	***
Daytime_Siesta	rh3[2]	rh4[1]/rh4[lexA]	147	83	1.42E-31	***	7.79E-30	***
Daytime_Siesta	rh3[2]	rh5[2]/rh5[lexA]	147	96	9.84E-24	***	5.41E-22	***
Daytime_Siesta	rh3[2]	rh6[1]/rh6[G]	147	89	1.34E-21	***	7.39E-20	***
Daytime_Siesta	rh3[2]	rh7[1]/rh7[lexA]	147	84	6.12E-17	***	3.37E-15	***
Daytime_Siesta	rh3[2]	w+,w1118	147	148	8.27E-09	***	4.55E-07	***
Daytime_Siesta	rh3[2]	w1118	147	98	3.99E-38	***	2.20E-36	***
Daytime_Siesta	rh3[2]/rh3[lexA]	rh3[lexA]	95	124	0.0301	*	1	ns
Daytime_Siesta	rh3[2]/rh3[lexA]	rh4[1]/rh4[lexA]	95	83	3.52E-54	***	1.94E-52	***
Daytime_Siesta	rh3[2]/rh3[lexA]	rh5[2]/rh5[lexA]	95	96	8.48E-46	***	4.66E-44	***
Daytime_Siesta	rh3[2]/rh3[lexA]	rh6[1]/rh6[G]	95	89	7.48E-43	***	4.11E-41	***
Daytime_Siesta	rh3[2]/rh3[lexA]	rh7[1]/rh7[lexA]	95	84	1.02E-36	***	5.58E-35	***
Daytime_Siesta	rh3[2]/rh3[lexA]	w+,w1118	95	148	6.32E-28	***	3.47E-26	***
Daytime_Siesta	rh3[2]/rh3[lexA]	w1118	95	98	3.48E-62	***	1.91E-60	***
Daytime_Siesta	rh3[lexA]	rh4[1]/rh4[lexA]	124	83	9.66E-73	***	5.31E-71	***
Daytime_Siesta	rh3[lexA]	rh5[2]/rh5[lexA]	124	96	6.58E-64	***	3.62E-62	***
Daytime_Siesta	rh3[lexA]	rh6[1]/rh6[G]	124	89	7.23E-60	***	3.98E-58	***
Daytime_Siesta	rh3[lexA]	rh7[1]/rh7[lexA]	124	84	4.15E-52	***	2.28E-50	***
Daytime_Siesta	rh3[lexA]	w+,w1118	124	148	2.84E-44	***	1.56E-42	***
Daytime_Siesta	rh3[lexA]	w1118	124	98	2.34E-83	***	1.29E-81	***
Daytime_Siesta	rh4[1]/rh4[lexA]	rh5[2]/rh5[lexA]	83	96	0.0406	*	1	ns
Daytime_Siesta	rh4[1]/rh4[lexA]	rh6[1]/rh6[G]	83	89	0.0233	*	1	ns
Daytime_Siesta	rh4[1]/rh4[lexA]	rh7[1]/rh7[lexA]	83	84	0.00147	**	0.0811	ns
Daytime_Siesta	rh4[1]/rh4[lexA]	w+,w1118	83	148	1.66E-12	***	9.13E-11	***
Daytime_Siesta	rh4[1]/rh4[lexA]	w1118	83	98	0.535	ns	1	ns
Daytime_Siesta	rh5[2]/rh5[lexA]	rh6[1]/rh6[G]	96	89	0.789	ns	1	ns
Daytime_Siesta	rh5[2]/rh5[lexA]	rh7[1]/rh7[lexA]	96	84	0.213	ns	1	ns
Daytime_Siesta	rh5[2]/rh5[lexA]	w+,w1118	96	148	3.44E-07	***	1.89E-05	***
Daytime_Siesta	rh5[2]/rh5[lexA]	w1118	96	98	0.00546	**	0.3	ns
Daytime_Siesta	rh6[1]/rh6[G]	rh7[1]/rh7[lexA]	89	84	0.335	ns	1	ns
Daytime_Siesta	rh6[1]/rh6[G]	w+,w1118	89	148	2.71E-06	***	0.000149	***
Daytime_Siesta	rh6[1]/rh6[G]	w1118	89	98	0.00276	**	0.152	ns
Daytime_Siesta	rh7[1]/rh7[lexA]	w+,w1118	84	148	0.000391	***	0.0215	*
Daytime_Siesta	rh7[1]/rh7[lexA]	w1118	84	98	8.62E-05	***	0.00474	**
Daytime_Siesta	w+,w1118	w1118	148	98	5.12E-16	***	2.82E-14	***
Early_Night_Sleep	rh1[117]	rh2[2]/rh2[1]	95	81	9.71E-12	***	5.34E-10	***
Early_Night_Sleep	rh1[117]	rh3[2]	95	147	1.31E-73	***	7.20E-72	***
Early_Night_Sleep	rh1[117]	rh3[2]/rh3[lexA]	95	95	8.27E-72	***	4.55E-70	***
Early_Night_Sleep	rh1[117]	rh3[lexA]	95	124	8.89E-47	***	4.89E-45	***
Early_Night_Sleep	rh1[117]	rh4[1]/rh4[lexA]	95	83	0.000375	***	0.0206	*
Early_Night_Sleep	rh1[117]	rh5[2]/rh5[lexA]	95	96	0.0381	*	1	ns
Early_Night_Sleep	rh1[117]	rh6[1]/rh6[G]	95	89	0.0112	*	0.619	ns
Early_Night_Sleep	rh1[117]	rh7[1]/rh7[lexA]	95	84	0.133	ns	1	ns
Early_Night_Sleep	rh1[117]	w+,w1118	95	148	0.0322	*	1	ns
Early_Night_Sleep	rh1[117]	w1118	95	98	1.81E-12	***	9.98E-11	***
Early_Night_Sleep	rh2[2]/rh2[1]	rh3[2]	81	147	3.47E-27	***	1.91E-25	***
Early_Night_Sleep	rh2[2]/rh2[1]	rh3[2]/rh3[lexA]	81	95	1.58E-29	***	8.69E-28	***
Early_Night_Sleep	rh2[2]/rh2[1]	rh3[lexA]	81	124	2.61E-12	***	1.44E-10	***
Early_Night_Sleep	rh2[2]/rh2[1]	rh4[1]/rh4[lexA]	81	83	0.00126	**	0.0694	ns
Early_Night_Sleep	rh2[2]/rh2[1]	rh5[2]/rh5[lexA]	81	96	1.05E-06	***	5.79E-05	***
Early_Night_Sleep	rh2[2]/rh2[1]	rh6[1]/rh6[G]	81	89	1.56E-05	***	0.000856	***
Early_Night_Sleep	rh2[2]/rh2[1]	rh7[1]/rh7[lexA]	81	84	1.92E-07	***	1.06E-05	***
Early_Night_Sleep	rh2[2]/rh2[1]	w+,w1118	81	148	4.93E-08	***	2.71E-06	***
Early_Night_Sleep	rh2[2]/rh2[1]	w1118	81	98	0.922	ns	1	ns
Early_Night_Sleep	rh3[2]	rh3[2]/rh3[lexA]	147	95	0.092	ns	1	ns
Early_Night_Sleep	rh3[2]	rh3[lexA]	147	124	1.92E-05	***	0.00106	**
Early_Night_Sleep	rh3[2]	rh4[1]/rh4[lexA]	147	83	1.04E-45	***	5.74E-44	***
Early_Night_Sleep	rh3[2]	rh5[2]/rh5[lexA]	147	96	7.23E-60	***	3.97E-58	***
Early_Night_Sleep	rh3[2]	rh6[1]/rh6[G]	147	89	2.73E-54	***	1.50E-52	***
Early_Night_Sleep	rh3[2]	rh7[1]/rh7[lexA]	147	84	5.83E-59	***	3.21E-57	***
Early_Night_Sleep	rh3[2]	w+,w1118	147	148	1.91E-74	***	1.05E-72	***
Early_Night_Sleep	rh3[2]	w1118	147	98	9.74E-31	***	5.36E-29	***
Early_Night_Sleep	rh3[2]/rh3[lexA]	rh3[lexA]	95	124	5.65E-08	***	3.11E-06	***
Early_Night_Sleep	rh3[2]/rh3[lexA]	rh4[1]/rh4[lexA]	95	83	8.79E-47	***	4.83E-45	***
Early_Night_Sleep	rh3[2]/rh3[lexA]	rh5[2]/rh5[lexA]	95	96	2.24E-59	***	1.23E-57	***
Early_Night_Sleep	rh3[2]/rh3[lexA]	rh6[1]/rh6[G]	95	89	1.66E-54	***	9.15E-53	***
Early_Night_Sleep	rh3[2]/rh3[lexA]	rh7[1]/rh7[lexA]	95	84	6.56E-59	***	3.61E-57	***
Early_Night_Sleep	rh3[2]/rh3[lexA]	w+,w1118	95	148	6.90E-71	***	3.79E-69	***
Early_Night_Sleep	rh3[2]/rh3[lexA]	w1118	95	98	1.03E-32	***	5.65E-31	***
Early_Night_Sleep	rh3[lexA]	rh4[1]/rh4[lexA]	124	83	1.83E-25	***	1.01E-23	***
Early_Night_Sleep	rh3[lexA]	rh5[2]/rh5[lexA]	124	96	1.57E-35	***	8.62E-34	***
Early_Night_Sleep	rh3[lexA]	rh6[1]/rh6[G]	124	89	1.20E-31	***	6.58E-30	***
Early_Night_Sleep	rh3[lexA]	rh7[1]/rh7[lexA]	124	84	9.49E-36	***	5.22E-34	***
Early_Night_Sleep	rh3[lexA]	w+,w1118	124	148	5.13E-44	***	2.82E-42	***
Early_Night_Sleep	rh3[lexA]	w1118	124	98	6.82E-14	***	3.75E-12	***
Early_Night_Sleep	rh4[1]/rh4[lexA]	rh5[2]/rh5[lexA]	83	96	0.116	ns	1	ns
Early_Night_Sleep	rh4[1]/rh4[lexA]	rh6[1]/rh6[G]	83	89	0.29	ns	1	ns
Early_Night_Sleep	rh4[1]/rh4[lexA]	rh7[1]/rh7[lexA]	83	84	0.0447	*	1	ns
Early_Night_Sleep	rh4[1]/rh4[lexA]	w+,w1118	83	148	0.0642	ns	1	ns
Early_Night_Sleep	rh4[1]/rh4[lexA]	w1118	83	98	0.00105	**	0.0575	ns
Early_Night_Sleep	rh5[2]/rh5[lexA]	rh6[1]/rh6[G]	96	89	0.614	ns	1	ns
Early_Night_Sleep	rh5[2]/rh5[lexA]	rh7[1]/rh7[lexA]	96	84	0.614	ns	1	ns
Early_Night_Sleep	rh5[2]/rh5[lexA]	w+,w1118	96	148	0.888	ns	1	ns
Early_Night_Sleep	rh5[2]/rh5[lexA]	w1118	96	98	5.02E-07	***	2.76E-05	***
Early_Night_Sleep	rh6[1]/rh6[G]	rh7[1]/rh7[lexA]	89	84	0.326	ns	1	ns
Early_Night_Sleep	rh6[1]/rh6[G]	w+,w1118	89	148	0.49	ns	1	ns
Early_Night_Sleep	rh6[1]/rh6[G]	w1118	89	98	9.40E-06	***	0.000517	***
Early_Night_Sleep	rh7[1]/rh7[lexA]	w+,w1118	84	148	0.677	ns	1	ns
Early_Night_Sleep	rh7[1]/rh7[lexA]	w1118	84	98	8.62E-08	***	4.74E-06	***
Early_Night_Sleep	w+,w1118	w1118	148	98	1.40E-08	***	7.71E-07	***

Supplemental Table S1. Summary of p-values from the rhodopsin mutant sleep screen

Summary of the pairwise, two-tailed Student's *t*-tests with Bonferroni multiple testing corrections, which were used to examine the effects of various rhodopsin mutations on chronotype. The parameter column refers to either the daytime siesta or Early Night Sleep Index chronotype parameter (see STAR Methods for calculations). The group 1 and group 2 columns indicate the genotypes being compared, and the n1 and n2 columns refer to the number of animals included in each group. The p column displays the unadjusted p value and "p.adj" column displays the p value after a multiple testing correction. *$p<0.05$. **$p<0.005$. ***$p<0.0005$.

METHODS

Key resources table

REAGENT or RESOURCE	SOURCE	IDENTIFIER
Antibodies		
mNeonGreen Tag Antibody	Cell Signaling Technology	Cat #53061
mNeonGreen Tag (E8E3V) Rabbit mAb	Cell Signaling Technology	Cat #55074
Goat anti-rabbit IgG Alexa Fluor 488	Thermo Fisher Scientific/ Invitrogen	Cat #A-11008; RRID: AB_143165
Chemicals, peptides, and recombinant proteins		
Sucrose	Sigma-Aldrich	Cat #S0389
BD Bacto Dehydrated Agar	BD Diagnostics	Cat #214010
UltraPure Agarose	Thermo Fisher Scientific/ Invitrogen	Cat #1650000
LB Broth (Lennox)	Sigma-Aldrich	Cat #L7658
Paraformaldehyde	Electron Microscopy Sciences	N/A
Triton X-100	Sigma-Aldrich	Cat #X100
VECTASHIELD anti-fade mounting media	Vector Labs	Cat #H-1200
Critical commercial assays		
Quick-RNA MiniPrep Kit	Zymo Research	Cat #R1054
iScript Reverse Transcription Supermix	Bio-Rad	Cat #1708841
LightCycler 480 SYBR Green I Master	Roche	Cat #04707516001
Experimental models: Organisms/strains		
Drosophila: w^{1118}	Bloomington Drosophila Stock Center (BDSC)	Cat #BL5905
Drosophila: *Canton S*	Janelia Farm	
Drosophila: $ninaE^{I17}$	BDSC	Cat #BL5701
Drosophila: *rh3-Gal4*	BDSC	Cat #BL7457
Drosophila: sev^{14}; $Ras85D^{e1B}$/TM3, Sb^{1}	BDSC	Cat #BL5689
Drosophila: per^{Long}	BDSC	Cat #BL80918
Drosophila: per^{Short}	BDSC	Cat #BL80919
Drosophila: *DRA-Dm8-Gal4*	BDSC	Cat #BL48565
Drosophila: *UAS-TNT*	BDSC	Cat #BL28838
Drosophila: *UAS-NachBac*	BDSC	Cat #BL9469
Drosophila: *20XUAS-CsChrimson*	BDSC	Cat #BL55135
Drosophila: *Sco/Cyo;MKRS/TM6B*	BDSC	Cat #BL3703
Drosophila: $rh4^{1}$	Laboratory of C. Desplan	N/A
Drosophila: $rh5^{2}$	Laboratory of C. Desplan	N/A
Drosophila: $rh6^{1}$	Laboratory of C. Desplan	N/A
Drosophila: *UAS-rh3*	Laboratory of C. Desplan	N/A
Drosophila: *UAS-rh4*	Laboratory of C. Desplan	N/A
Drosophila: *UAS-rh5*	Laboratory of C. Desplan	N/A
Drosophila: *Ort-C2b-Gal4*	Laboratory of C.-H. Lee	N/A

Drosophila: per::mNeonGreen	Laboratory of S. Yadlapalli	N/A
Drosophila: $rh2^{1}$	Laboratory of C. Montell	N/A
Drosophila: $rh2^{2}$	Laboratory of C. Montell	N/A
Drosophila: $rh3^{2}$	Laboratory of C. Montell	N/A
Drosophila: $rh3^{L}$	This paper	N/A
Drosophila: $rh4^{L}$	Laboratory of C. Montell	N/A
Drosophila: $rh5^{L}$	Laboratory of C. Montell	Cat #BL91221
Drosophila: $rh6^{G}$	Laboratory of C. Montell	Cat #BL66672
Drosophila: $rh7^{1}$	Laboratory of C. Montell	Cat #BL76022
Drosophila: $rh7^{L}$	Laboratory of C. Montell	N/A
Drosophila: *inaF-C-Gal4*	Laboratory of C. Montell	N/A
Drosophila: FM7a;;TM3, Sb^{1}/TM6B, Tb^{1}	Laboratory of C. Montell	N/A
Oligonucleotides		
guide RNA1 primer sequences to target rh3 gene: *rh3*_gRNA_up_FOR: CTTCGCGTTACCGGACTCCATGCTC *rh3*_gRNA_up_REV: AAACGAGCATGGAGTCCGGTAACGC	This paper	N/A
guide RNA2 primer sequences to target rh3 gene: *rh3*_gRNA_down_FOR: CTTCGTTGATGACCAGTATATTGGA *rh3*_gRNA_down_REV: AAACTCCAATATACTGGTCATCAAC	This paper	N/A
rh3 upstream homolog arm primer sequences: $rh3^{LexA}$upstream_FOR: GAAAAGTGCCACCTGACGTCGTTGTCGGCTTTGCCG GG $rh3^{LexA}$upstream_REV: CATTTTGATTGCTAGCGCTCCGGTCTGCGGG	This paper	N/A
rh3 downstream homolog arm primer sequences: $rh3^{LexA}$downstream_FOR: CTAGGCGCGCCCATATGACTGGCTAACTTACCCGGA G $rh3^{LexA}$downstream_REV: GACAAGCCGAACATATGCGAGTTCGTTGCCGTTTCA GT	This paper	N/A
$rh3^{2}$ genotyping primer sequences: $rh3^{2}$_F: TACTGCAACCCAAAATGGTCACTGC $rh3^{2}$_R: CGATTCCACGTTCATCTTCTTGGCC	This paper	N/A
$rh3^{LexA}$ genotyping primer sequences: $rh3^{LexA}$_F: AACCTTCGAAAGAGAACCAACACAA $rh3^{LexA}$_R: CAGTGGCAGGCCCTCTTCCT	This paper	N/A
per^{Logn} genotyping primer sequences: per^{L} _FOR: TCGACAAGACCTGGGAGGCAGG per^{L} _REV: GATCGGAGTGGCGCAGATGACG	This paper	N/A
rp49 RT-qPCR primer sequences: Forward GACGCTTCAAGGGACAGTATCTG Reverse AAACGCGGTTCTGCATGAG	[136]	N/A
Clk RT-qPCR primer sequences: Forward GCAGGAAATCGCGTAATCTCA Reverse ATCGGTGGCCTCATTATGATTTT	[137]	N/A

Pdp1ε RT-qPCR primer sequences: Forward AGGATCATCGGGAACCATGGACAA Reverse TGCCCGAATCATTGCTGCTAACAC	This paper	N/A
per RT-qPCR primer sequences: Forward TGACCGAATCCCTGCTCAAT Reverse CTTTTTATCCCGTGGCCTGG	[137]	N/A
tim RT-qPCR primer sequences: Forward CACTTCCGCAACAACAGAGT Reverse ACTCCGCAGGGTCAGTTTAA	[137]	N/A
Recombinant DNA		
pU6-BbsI-ChiRNA		Addgene Plasmid #45946
pBPLexA::p65Uw		Addgene Plasmid #26231
Software and algorithms		
R (version 4.1.0)		https://www.r-project.org/
MATLAB (version 2021b)		https://www.mathworks.com/products/matlab.html
MATLAB code		https://github.com/Craig-Montell-Lab/Li-and-Meyerhof-et-al.-2023
Other		
Drosophila Activity Monitoring System (DAM2)	TriKinetics	N/A
Drosophila Feeding Monitor (DFM)	[57]	N/A
Glass capillaries	VWR International	Cat #53432-706
Real UV LED light strips (365nm, 1m)	waveform lighting	Cat #PN 7021.65
CENTRIC DAYLIGHT LED Strip Lights for Commercial & Retail 5000K	waveform lighting	Cat #PN 3004.50
SimpleColor Amber LED Strip Lights	waveform lighting	Cat #PN 7041.592

Generation of *rh3^{LexA}* flies

To generate the *rh3^{LexA}* (*rh3^{L}*) flies, we excised nucleotides 1-136 starting from the initiation codon of *rh3*, and inserted the *lexA* gene using CRISPR-HDR. We chose two guide RNAs that target the initiation codon the (5' end) and 136 base pairs downstream (3' end) using the CRISPR Optimal Target Finder: https://flycrispr.org/target-finder/. We annealed the following oligonucleotides to form two primer dimers. Each of the two primer dimers were cloned into the BbsI site of pU6-BbsI-ChiRNA (Addgene #45946) to generate two guide RNA expression plasmids: pU6-BbsI-ChiRNA-rh3_up and pU6-BbsI-ChiRNA-rh3_down.
*rh3*_gRNA_up_FOR: CTTCGCGTTACCGGACTCCATGCTC
*rh3*_gRNA_up_REV: AAACGAGCATGGAGTCCGGTAACGC
*rh3*_gRNA_down_FOR: CTTCGTTGATGACCAGTATATTGGA
*rh3*_gRNA_down_REV: AAACTCCAATATACTGGTCATCAAC
We amplified the *rh3* upstream (1.0 kb) and downstream (1.1 kb) homology arms using the

following primers:
rh3^{LexA}upstream_FOR: GAAAAGTGCCACCTGACGTCGTTGTCGGCTTTGCCGGG
rh3^{LexA}upstream_REV: CATTTTGATTGCTAGCGCTCCGGTCTGCGGG
rh3^{LexA}downstream_FOR: CTAGGCGCGCCCATATGACTGGCTAACTTACCCGGAG
rh3^{LexA}downstream_REV: GACAAGCCGAACATATGCGAGTTCGTTGCCGTTTCAGT

We used the In-Fusion ® HD Cloning Plus (Takara #638910) to insert the upstream and downstream homology arms into the AatII and NdeI sites of pBPLexA::p65Uw (Addgene #26231), respectively, creating the pBPLexA::p65Uw-*rh3*_uparm+downarm plasmid that carries both of the homolog arms. All three plasmids were injected into the BDSC #55821 strain, which provided the source of the Cas9 (Bestgene Inc.)

Primers used for genotyping:
rh3^{2}_F: TACTGCAACCCAAAATGGTCACTGC
rh3^{2}_R: CGATTCCACGTTCATCTTCTTGGCC
rh3^{LexA}_F: AACCTTCGAAAGAGAACCAACACAA
rh3^{LexA}_R: CAGTGGCAGGCCCTCTTCCT

To rule out the possibility that *rh3* mutants' dramatically-extended periodicity resulted from them harboring the *per*^{L} allele, we sequenced a portion of their *per* gene using the following primers: *per*^{L} _FOR: TCGACAAGACCTGGGAGGCAGG and *per*^{L} _REV: GATCGGAGTGGCGCAGATGACG. We found that our wild-type control (*w*$^{+}$,*w*^{1118}), *rh3*^{2}, and *rh3*^{L} stocks encoded a valine at amino acid position 243 in the *per* gene, while our *per*^{L} stock contained a missense mutation (T>A), which changed valine to aspartic acid.

Sleep and locomotor behavioral assays

Flies were raised under 12 h:12 h light/dark cycles at 25 °C in vials with standard molasses-yeast cornmeal food. To measure sleep, 3–7 day-old female flies were individually loaded into clear glass tubes containing 5% sucrose and 1–2% agarose as the food source. Activity was monitored using the *Drosophila* Activity Monitoring System (DAM; TriKinetics).[138] After the flies were loaded into the tubes for the DAM assays, they were allowed to acclimate for 24 hours prior to recording their activity. Locomotor and sleep assays were performed for ≥4 days, and then the average sleep profile was calculated for each fly. Sleep was scored as ≥5 consecutive minutes of inactivity, as reported previously[49] using the Rethomics software package in R.[139] In these assays, flies were housed under full spectrum white lights with an additional UVA light source (Waveform Lighting; 850 lux) at 25 °C, unless indicated otherwise. For the optogenetic experiments, a red-orange LED light (592 nm; 350 lux; Waveform) was used.

Ramping light conditions

For ramping light experiments, an Arduino UNO (Elgoo) controlled by custom Matlab code applied a gradually increasing voltage to a MOSFET transistor gating the power to UV and RGB LED lights, which increased their intensity during the first half of the day and decreased their intensity during the second half. In these experiments, the light intensity followed a sinusoidal wave, with the peak intensity in the middle of the day (ZT 6; 550 lux).

Chronotype analysis

To assay chronotype, two features of sleep were scored for each fly: the timing of the daytime siesta and the early-night sleep index (ENSI). To determine the time of the daytime siesta, we fit a line to the daytime sleep profile of each fly using a generalized additive model via the GAM function (mgcv package; version 1.20.1) in R. This served to smooth the sleep profile of each fly and reduce noise. The daytime siesta for each fly was scored as the time at which the best fit line was at its peak. For instances in which more than one identical peak were found, the timing of the first peak was taken as the daytime siesta. To calculate the ENSI during 12 h:12 h light/dark cycles, each fly's total sleep during the first 4 h after lights off was divided by the total amount of sleep during the first 11.5 h out of the 12 h dark period (sleep during ZT 12—16/sleep during ZT 12—24). ENSI parameters were scaled accordingly for varying LD cycles (e.g., for a 14 h:14 h light/dark cycle, ENSI was calculated as sleep during ZT 14—18.5/sleep during ZT 14—28.)

Free-running periodicity

Circadian periodicity experiments were performed at 25 °C using the DAM system with conditions identical to the sleep assay. First, flies were entrained to 12 h:12 h light/dark cycles for 4 days, and then shifted to constant darkness (DD) for ≥6 days to measure the periodicities. The free-running periodicities under DD cycles were calculated using the chi-squared method using the Rethomics R software package. Dead or sick flies (i.e. flies with <14 beam breaks per day) and arrhythmic flies (chi-square p value >0.05) were excluded from the periodicity calculations.

Fly Liquid Interaction Counter (FLIC) assays

To quantify feeding behavior over time, we used the Fly Liquid Interaction Counter assay (FLIC), which automatically counts interactions between flies and the food.[57] To perform this assay, single flies were aspirated into individual arenas in the *Drosophila* feeding monitor (DFM) providing them *ad libitum* access to a 5% sucrose (Sigma) solution. The flies were allowed to habituate to the DFM for 16–20 h, and then interaction events between the proboscises and the food were recorded for 24 h. To identify food-interaction signals from background noise, we wrote a custom script in Matlab (version 2021b). Briefly, we first fit a smoothing line to the raw DFM signal for each well using a second order Savitzky-Golay filter with a frame length of 2001 readings, which corresponds to ~6 seconds of signal. We then used the difference between this best fit line and the raw DFM signal to eliminate signal drift over the 24 h recording period. Food-interaction events complete an electrical circuit in the DFM, which results in an acute spike in voltage that is then converted into a digital signal read by a microcontroller. We scored food-interaction events as signal spikes that were >40 AU, as described previously.[59] To exclude dead or sick flies, we did not include wells with <50 food interaction events in our analyses. We also excluded wells whose signal was out of the detectable range for >2 minutes. The daily feeding plots were generated by calculating a rolling 30-min average of food interaction events for the population of flies tested.

Time restricted food assays

For time-restricted feeding experiments, we used real-time video tracking to monitor the sleep and activity of individually housed flies with access to a 5% sucrose solution contained in a 5 µL capillary tube (video tracking described in greater detail below). Flies had *ad libitum* access to a 1.5% agar solution at the bottom of their enclosure to prevent desiccation, and were allowed to habituate to their enclosure for 16–20 hours prior to the start of the recording. To maintain an eight-hour feeding window, we manually inserted or removed the capillary tube from each fly enclosure at ZT 2 and 10, respectively. Exchanging capillary tubes produced temporary artifacts in video tracking. To remove these artifacts, we censored the data of activity bins (10 min) and sleep bins (30 min) that fell within the timing of the capillary tube exchange. Censored activity and sleep bins account for the gaps in data present in Figures 7C and 7D. Time-restricted feeding experiments lasted for 48-hours, and the second day of data is shown in Figure 7.

Clock gene expression in peripheral tissue assayed by real-time quantitative PCR

We quantified the mRNA expression of *Clk, per, tim* and *Pdp1ε* from whole flies by real time quantitative PCR (RT-qPCR). To prepare RNA, we collected flies at four-hour intervals over a span of either 24 or 28 hours and flash-froze them on dry ice. We extracted mRNA from whole-fly homogenates using Quick-RNA miniprep kits (ZYMO Research #R1054), and prepared cDNA using iScript Reverse Transcription Supermix kits (BIO-RAD #1708840) with 1 µg of mRNA for each reaction. To perform the RT-qPCR, we amplified the cDNAs for 39 cycles (95 °C, 10 sec; 55 °C, 30 sec; 72 °C, 30 sec) using LightCycler 480 SYBR Green I Master (Roche #04707516001). The fold changes in mRNA expression were quantified via the delta delta CT method, with each sample normalized to the *rp49* gene and to the daily nadir of expression. RT-qPCR experiments were performed with the following primers:
rp49 forward: GACGCTTCAAGGGACAGTATCTG
rp49 reverse: AAACGCGGTTCTGCATGAG
Clk forward: GCAGGAAATCGCGTAATCTCA
Clk reverse: ATCGGTGGCCTCATTATGATTTT
Pdp1ε forward: AGGATCATCGGGAACCATGGACAA
Pdp1ε reverse: TGCCCGAATCATTGCTGCTAACAC
per forward: TGACCGAATCCCTGCTCAAT
per reverse: CTTTTTATCCCGTGGCCTGG
tim forward: CACTTCCGCAACAACAGAGT
tim reverse: ACTCCGCAGGGTCAGTTTAA.

Immunostaining

Drosophila heads from 5–7-day-old adults were fixed in 4% paraformaldehyde in PBS for 20 min at room temperature prior to brain dissections. Samples were then washed in PBST (PBS + 0.1% Triton X-100; 10 min) and blocked with 5% normal goat serum (MP Biomedicals) for 1 hour at room temperature. Next, primary antibodies were added to the blocking buffer for an overnight incubation at 4°C. The samples were washed with PBST (20 min, 3 times) and then incubated with the secondary antibodies in blocking buffer for 2 hours

at room temperature in the dark. The following primary and secondary antibodies were used at the indicated dilutions: mNeonGreen Tag #53061 and #55074 (1:500; Cell Signaling), AlexaFluor 488 goat anti-rabbit IgG (1:200; Thermo Fisher Scientific). After a final PBST wash (10 min, 3 times), the samples were mounted using Vectashield (Vector Laboratory, H-1000) and a coverslip was secured with nail polish.

The samples were imaged using a Zeiss LSM 900 confocal laser scanning microscope using a 40x/1.3 Plan-Apochromat oil DIC objective. Images were processed using the following protocol in ImageJ: A rolling-ball background subtraction (radius 50 pixels) was applied to each Z-stack slice containing fluorescent signal from the lateral pacemaker neurons. The average pixel intensity from each neuron was manually scored from a maximum intensity projection. A custom script in MATLAB (version 2021b) was used to generate heatmaps from max intensity projections (Figures 3F), where images in each panel were normalized to the maximum pixel intensity and then mapped to a custom color palette.

Video tracking for motion detection and sleep

Due to the limited spatial resolution provided by the DAM system, we developed custom motion tracking software with the Computer Vision Toolbox in MATLAB (version 2021b), using a similar approach to what has been described previously.[140,141] For these experiments, flies were individually housed in clear plastic cuvettes (Thomas Scientific #111137) with 1 mL of 1.5% agarose added to the bottom. We provided the flies with access to a 5% sucrose solution contained in a 5 μL capillary tube (VWR #53432-706) that was fitted to the top of the cuvette. Flies were transferred to the cuvette via a mouth pipette and allowed to acclimate for 16–20 hours prior to the start of the experiment. Flies were illuminated using an 850 nm LED infrared light (Waveform #7031), which was placed behind a white acrylic backdrop. Motion was detected in real time using an ELP 2MP webcam, with the infrared filter removed and affixed with an infrared pass filter (Heliopan 850 nm), recording at ~4 frames/sec with a resolution of 1280 x 720 pixels. The webcam was placed 11.5 cm from the backdrop, and the recording lasted for 24–48 hours.

We implemented the following algorithm to track motion (Figure S1D-S1F). We created a dynamic background model by taking the average pixel value from 30 consecutive frames. To reduce noise, each frame was blurred using a Gaussian filter with a standard deviation cutoff of two. Then a test frame was captured, blurred, and subtracted from the background model. Regions with absolute changes in pixel values of ≥5 were considered as possible indications of fly movement. To isolate fly movement, we only considered movement with an area of at least 10 pixels^2 (roughly the size of a fly) that occurred within the cuvette where the fly was housed. The test frame was then added to the background model and this process repeated for the duration of the recording.

Circadian arousal threshold

In order to test the arousal threshold of flies, we 3D printed a custom behavioral arena that individually housed 30 flies, with each in a 45 mm x 6 mm x 6 mm enclosure, where they had *ad libitum* access to a food source consisting 1.5% agarose and 5% sucrose (Figure S1G). Once every two hours, flies were subjected to three vibration stimuli that gradually increased in intensity (Figure S1H). Each stimulus was applied for three seconds followed by

a two-minute pause in which fly movement was assessed. The vibration stimuli were delivered by four, 14 mm shaftless vibration motors affixed to each corner of the behavioral arena. The motors were wired in parallel to an Arduino Uno (Elgoo) which was controlled by custom Matlab software to modulate both the timing and intensity of the vibration stimulus. Arousal to a given stimulus was assigned if an animal was immobile before the start of the stimulus and moved within two minutes of the start of the stimulus. Fly movement was tracked using an identical approach to the one described above.

Estimate of percentage of Rh3-expressing R7 cells in each compound eye

Each ommatidium includes eight photoreceptor cells, six of which (R1-6) extend the full depth of the retina. The remaining two photoreceptor cells (R7 and R8) occupy only the distal and proximal region of the retina, respectively. Thus, relative to the R1-6 cells, the R7 and R8 cells can be counted as 0.5 photoreceptor cells each. Therefore, there are seven photoreceptor cell equivalents and the R1-6 cells comprise ~86% (6/7) of the photoreceptor cell equivalents. The R7 cells constitute ~7.1% (0.5/7) of the photoreceptors per ommatidia. Since only ~30% of the R7 cells express *rh3* [36], then only ~2.1% of all of the photoreceptor cells in each compound eye corresponds to the *rh3*-expressing cells. The rhodopsins and other phototransduction proteins are concentrated in the microvillar structure of the photoreceptor cells—the rhabdomeres. Since the diameters of the R7 cell rhabdomeres (~1 μm) are smaller than the R1-6 rhabdomeres (~1.5 μm), then the *rh3*-expressing R7 cells include only ~1% of the total surface area of the rhabdomeres in each ommatidium.

To estimate the number of DRA ommatidia, we counted the numbers from two publications that labeled these ommatidia, and tabulated 42 [103] and 47 [142] to arrive at an estimate of 45 DRA ommatidia. Since the R7 cells constitute ~7.1% (0.5/7) of the photoreceptors per ommatidia (see above), and ~5.6% of the ommatidia are in the DRA, we estimate that ~0.4% (0.071 x 0.056 x 100) of the R7 photoreceptor cells are in the DRA. All of the R7 cells in the DRA express Rh3. Since the diameter of the R7 cells in the DRA are the same as the outer photoreceptor cells,[142] no further calculations need to be made to account for the smaller rhabdomere diameter of the R7 cells in the DRA.

Quantification and statistical analysis

To analyze sleep behavior, ≥3 independent cohorts of 20–32 flies/genotype/condition were tested, and the sleep parameters of individual flies were quantified independently. The numbers of flies tested (n) were all biological replicates. The (n)s are indicated in all figure legends. Statistics were generated using R (version 4.1.0).

For quantification of mRNA expression based on RT-qPCR, 3 independent RNA extractions were performed on 12–15 flies/genotype/condition and were then compared via two-way ANOVA to test the effect of time and genotype on the fold change in expression. To compare differences in expression at each time point between or among genotypes, we used unpaired, two-tailed Student's *t*-tests with a Bonferroni multiple testing correction.

The statistical methods for comparing chronotype, ENSI, and ENAI are indicated in the figure legends. For groups with normally distributed data, we used a one-way ANOVA for comparison among multiple groups, followed by a pair-wise, unpaired, Student's two-tailed *t*-test with a Bonferroni multiple testing correction.

For behavioral data with a non-normal distribution, and with multiple factors (e.g., genotype and diet) we used an Aligned Rank ANOVA followed by a *post-hoc* test with a Benjamini-Hochberg multiple testing correction from the ARTool R library.[143] Error bars are defined in the corresponding figure legends.

Box plots were generated in R using the ggplot2 graphing package, and display the median, 25th percentile, and 75th percentile. The whiskers indicate 1.5 x the interquartile range or the min/max values if no values surpass 1.5xIQR). * $p<0.05$, ** $p<0.01$, and *** $p<0.001$.

Unique letters used in Figures 3G–3I, 4B, 5F, 7F–7H, S3D and S6H indicate that a group is significantly different from groups labeled with other letters, $p \leq 0.05$. Groups that share the same letters indicate that there are no significant differences between them. (e.g., two groups labeled with "a" are not significantly different from one another but are different from groups labeled "b" or "c" etc.)

II. ACID TASTE IN MOSQUITOES

INTRODUCTION

The threat of Aedes aegypti

The mosquitoes, *Aedes aegypti*, are originally from Africa, however, due to the effects of global warming, increased international travel, and population growth, they have expanded their range to many parts of the world with access to water. [144-146] The hematophagous behavior of female mosquitoes poses a serious threat to global public health, as they can act as vectors for various infectious diseases including dengue, yellow fever and Zika through their blood-feeding processes. Because of their ability to spread deadly diseases, *Aedes aegypti* mosquitoes are among the most dangerous animals in the world. They are responsible for over 1 million deaths every year and put about 3.9 billion people in 128 countries at

risk.[147,148] In October 2020, Santa Barbara County reported its first detection of *Aedes aegypti* invasion. The peril presented by mosquitoes continues to draw nearer to our daily lives. Thus, it is critically important to study how their biology relates to disease transmission, how they develop resistance to insecticides at the molecular level, and how to design and implement genetic methods to control them.

Acid taste in mosquitoes

Generally, mosquitoes detect and locate humans using multiple sensory cues such as CO_2, heat, vision, humidity and human odors.[149-155] However, after landing on a host, mosquitoes will employ their taste organs such as proboscis and tarsi for gustatory discrimination which is essential for their decisions to initiate a bite or not. Mosquitoes are able to make feeding decisions after evaluating the components of a food option.[156] For example, the existence of DEET on human skin is significantly aversive to mosquitoes,[157] thus, it has been used as one of the most effective repellants for mosquitoes.[158] Sweat plays a crucial role in the allure of vertebrates to mosquitoes, and human sweat has a unique chemical composition that explains why some mosquitoes prefer humans over other animals.[159,160] L-Lactic acid is one of the main components in human sweat and there was a positive correlation between the amount of lactic acid found on a person's hand and the number of mosquito bites.[161] Previous research has evidentially proved that the odor of carboxylic acids including lactic acid is attractive to mosquitoes.[162] Yet, little is known about mosquitoes' taste preferences for lactic acid.

In addition, acid is not only a key signal for mosquitoes' blood feeding behavior, but also a common ingredient found in nectar that can have a range of pH from 2 to 8. All male mosquitoes and most female mosquitoes (except when they have fed on blood or are carrying

eggs) get their main energy from plant sugars like nectar, damaged fruits and honeydew during their adult life.[163] However, mosquitoes' taste preferences for these acids are still poorly understood.

In this research, we examined the taste preferences of mated female mosquitoes for various acids including lactic acid, propionic acid, acetic acid, citric acid, glycolic acid and tartaric acid. We found that mated female mosquitoes were attractive to lower concentration of these acid while aversive to high concentrations. And this is potentially due to their preferences for different pH of food.

RESULTS

Acid taste in blood feeding

Lactic acid is one of the key components in human body fluid. Previous research has shown that mosquitoes are attractive to the odor of lactic acid.[162] However, very little is known about mosquitoes' taste preference for lactic acid. To test the lactic acid preferences of *Aedes aegypti*, we performed two-way choice taste assays to compare their preferences for lactic acid plus sucrose versus sucrose only. Surprisingly, we found that mosquitoes were attractive to 0.001mM lactic acid but aversive to high concentrations of lactic acid. (Fig.1A) However, previous research has shown that the concentration of lactate on human skin has a range of 20-60mM. Thus, we propose that the aversion to high concentration of lactic acid could be due to their aversion to low pH food. To test this hypothesis, we first performed two-way choice taste assays to examine their preference for different concentrations of lactate. We adjusted the pH of the solutions with varying amounts of lactate to make them have the same pH in these assays. And we found that the mosquitoes showed attraction to high

concentrations of lactate which is similar to the concentration on human skin. (Fig. 1B) Next, to further test whether their aversion to high concentration of lactic acid is due to aversion to low pH food, we performed two-way choice assays with different concentrations of HCl. Indeed, we found that mosquitoes were aversive to food that has a pH lower than around 3. (Fig.2)

In addition, we next tested mosquitoes' preferences for more acids that exist in human body fluid including propionic acid and acetic acid. We found that mosquitoes are also attractive to 0.001mM propionic acid and aversive to high concentrations of both propionic acid and acetic acid. (Fig.3) In conclusion, mosquitoes could have a general aversion to low pH food but attractive to high concentrations of lactate. We will further test if they are attractive to the carboxylic bones of propionic acid and acetic acid when in solutions that have pH values similar to human sweat.

Acid taste in nectar feeding

Various acids have been found commonly in food resources like nectar and fruit juice that mosquitoes feed which they need to evaluate whether it is beneficial or dangerous. Previously we found that mosquitoes have different preferences towards different pH (Fig. 2). Next, we examined their taste preferences for other acids that can be found in plants. To test this, we performed two-way choice assays using different concentrations of citric acid, glycolic acid or tartaric acid. We found that mated female mosquitoes were aversive to higher concentrations of citric acid and glycolic acid. Interestingly, mosquitoes were attractive to 0.001mM tartaric acid but neutral to higher concentrations of tartaric acid until 1

mM which they were robustly aversive to. This might be because the ability to exchange protons varies depending on the backbone of the molecule. Thus, the future direction of this study would be testing mosquitoes' taste preferences for the carboxylic bones of these acids.

DISCUSSION

In this research, we found that mosquitoes are aversive to higher concentrations of carboxylic acids, which is potentially due to their aversion to low pH food. Additionally, mosquitoes are attractive to higher concentrations of lactate which is similar to the level of human skin.

Generally, the taste receptor cells detect acids and transduces the sour taste signal through ion channels. Previously, *Otop1*, which is a proton-selective ion channel, has been found to be required for acid taste in mice.[164] The homolog of *Otop1* in *Drosophila*, *OtopLA*, is also found to be important for acid preferences in *Drosophila*.[165] Thus, our next step for this research is to look at the *Otop* gene in mosquitoes. There are five isoforms of *Otop* in mosquitoes, among which *OtopA* has the highest homology to *OtopLA* (81%). Additionally, *AeOtopA*, among all five isoforms of *Otop* in mosquitoes has the highest expression in the proboscis.[166] Thus, we will generate null mutants of *AeOtopA* in *Aedes aegypti* and examine whether they have a defect in acid taste preferences. Acids are detected by the taste receptor cells. We can study how responsive taste neurons are by measuring their electrical activity through electrophysiological recording. Thus, we will examine which sensilla on mosquito proboscis is required for acid detection in mosquitoes.

METHODS

Mosquito rearing

The mosquitoes used in this study are WT-Liverpool (Dr. Omar Akbari's lab). Mosquitoes were reared and assayed in chambers at 28° C and 80% humidity under 12h light/12h dark cycles. Eggs are hatched in tanks with RO water with fish food added daily. Mosquito larvae were screened under fluorescent microscope to make sure there was no contamination. Pupae were collected into plastic cups and placed in cages with 10% sucrose solution bottles with wicks. Mosquitoes that were 7-10 days old after eclosion were used for behavior assays. Sheep blood was used for blood feeding and mosquito expansion.

Two-way choice feeding assay

55-60 mosquitoes (aged to 7-10 days) per cage were starved with RO water for 48 hours (female) or 24 hours (males). 96-well plates that contained acid/dye mixtures were put in the cages to allow mosquitoes to feed for 3 hours in the evening. The preference index (PI) was calculated according to the following equation: $(N_{red}-N_{blue})/(N_{red}+N_{blue}+N_{purple})$. We determined the concentrations of the red (Sulforhodamine B; Sigma-Aldrich) and blue (Brilliant Blue FCF; Wako Chemical) food dyes that had no significant effect on food selection by assaying the preference of control mosquitoes to each dye with 20 mM sucrose. Once the concentrations were established that lead to indifference between the two food colorings, different concentrations of different acids or lactate were added in 20mM sucrose solutions to compare with 20mM sucrose only solutions. Sulforhodamine B and Brilliant Blue dyes were switched between test and control solutions for every assay. A PI = 1.0 and −1.0 indicate complete preference for food with sucrose-only and sucrose plus acid or lactate, respectively. A PI = 0 indicated no preference for either food. Trials in which < 40% of the mosquitoes participated were discarded.

ACKNOWLEDGEMENT

Thanks to Ramandeep Singh and Yiqin Shen for helping with the behavior assays.

FIGURES

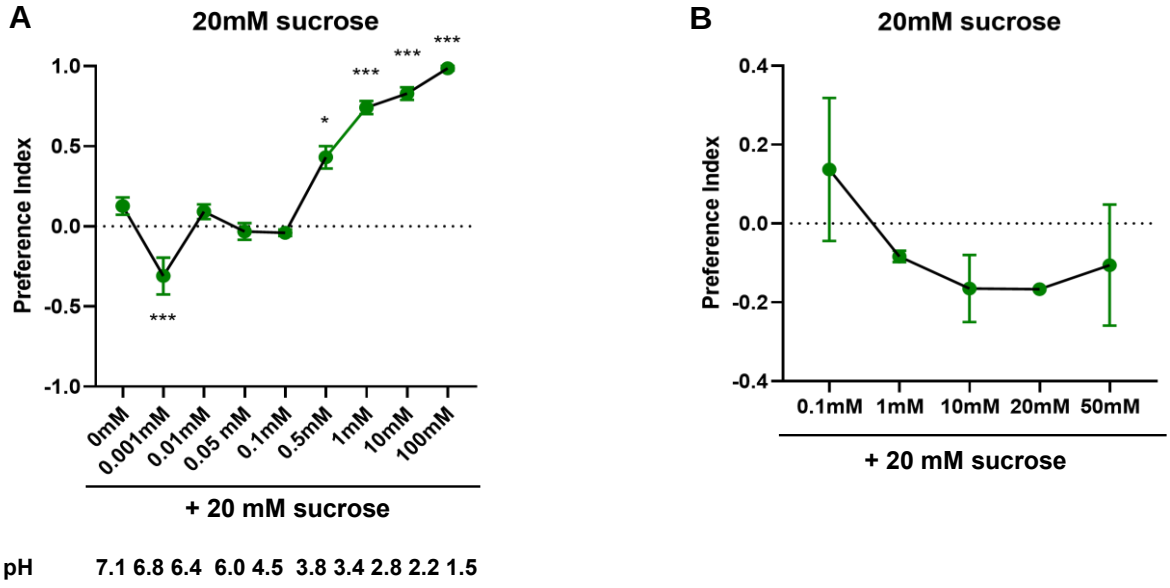

Fig.1 *Aedes aegypti* is aversive to high concentration of lactic acid but prefers higher concentration of lactate. A. Preference index for lactic acid. B. Preference index for lactate.

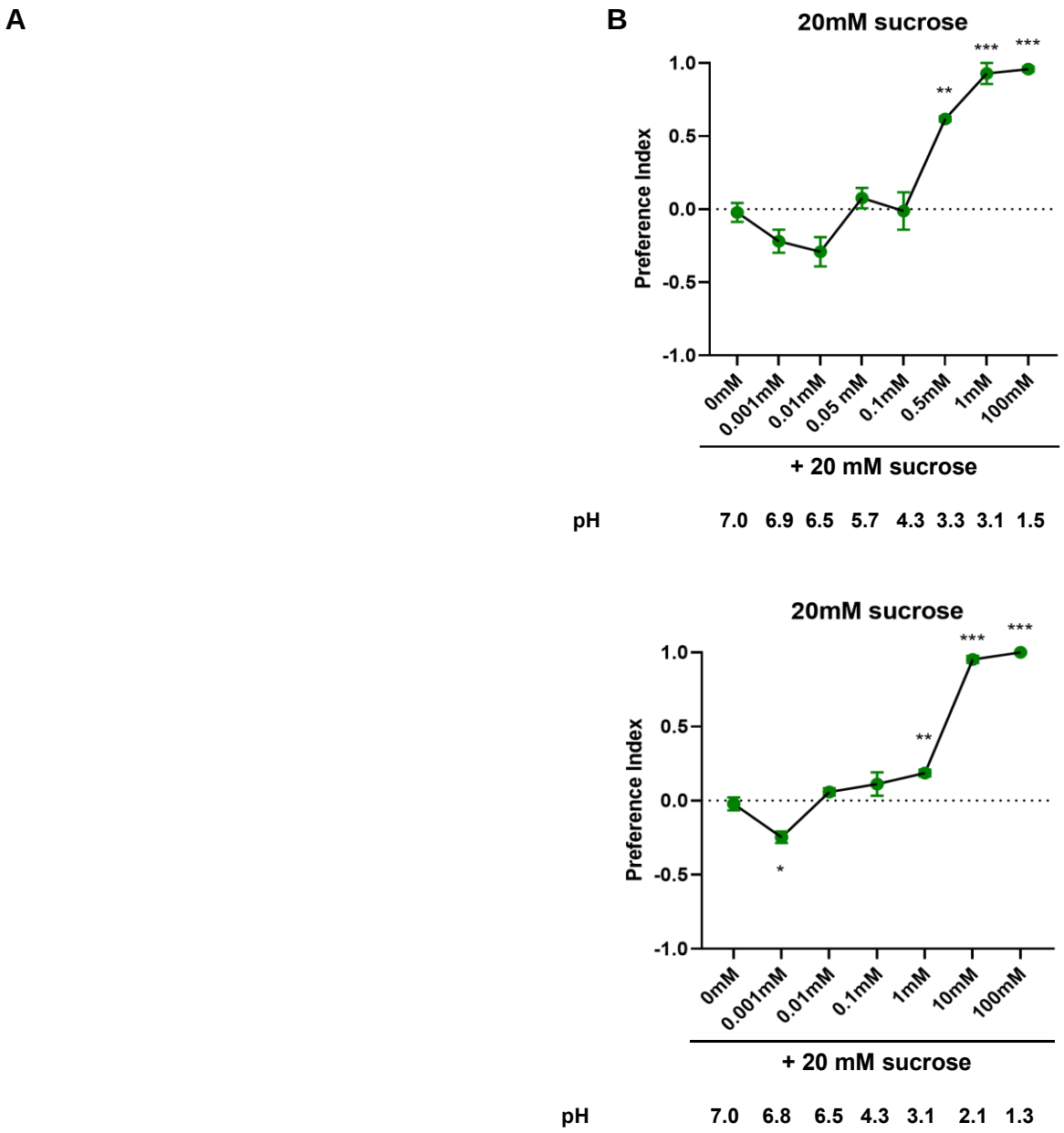

Fig.2 *Aedes aegypti* is aversive to low pH food. A. females. B. males.

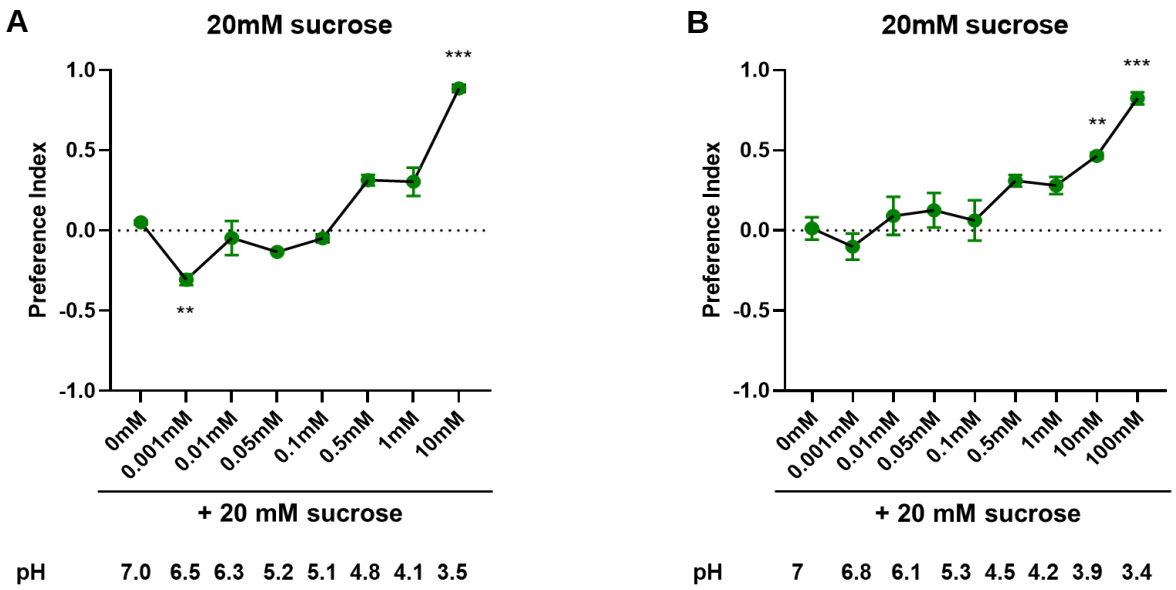

Fig.3 *Aedes aegypti* is aversive to high concentration of propionic acid and acetic acid. A. Preference index for propionic acid. B. Preference index for acetic acid.

A

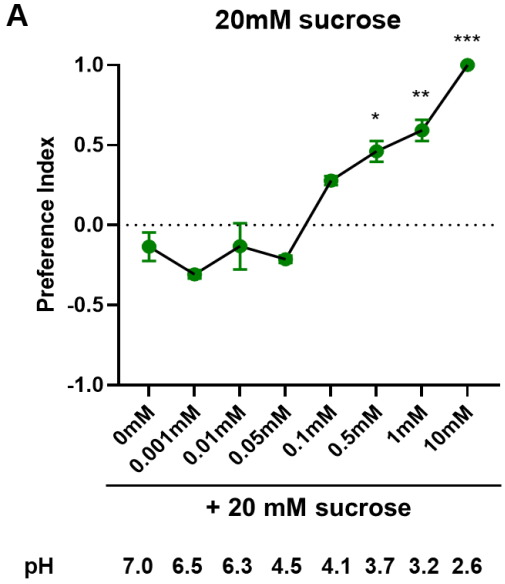
20mM sucrose
Preference Index
1.0
0.5
0.0
-0.5
-1.0
*
**
***
0mM
0.001mM
0.01mM
0.05mM
0.1mM
0.5mM
1mM
10mM
+ 20 mM sucrose
pH 7.0 6.5 6.3 4.5 4.1 3.7 3.2 2.6

B

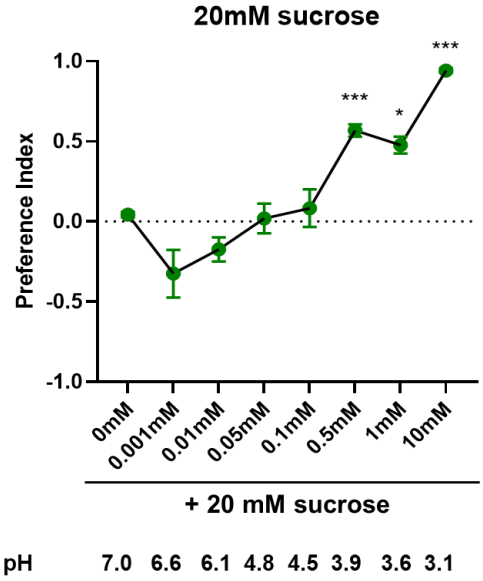
20mM sucrose
Preference Index
1.0
0.5
0.0
-0.5
-1.0
***
*
***
0mM
0.001mM
0.01mM
0.05mM
0.1mM
0.5mM
1mM
10mM
+ 20 mM sucrose
pH 7.0 6.6 6.1 4.8 4.5 3.9 3.6 3.1

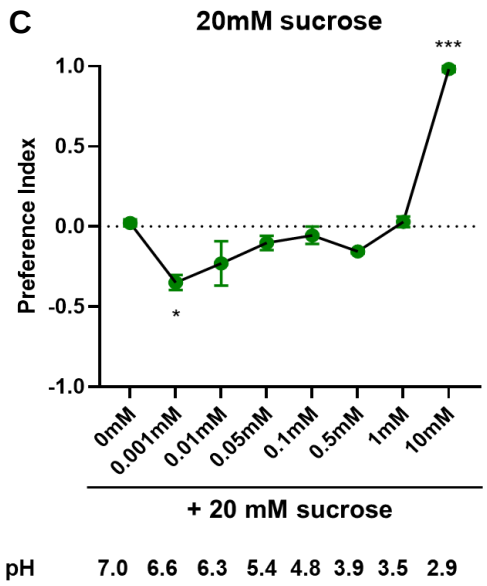

Fig.4 *Aedes aegypti* is aversive to high concentration of citric acid, glycolic acid and tartaric acid. A. Preference index for citric acid. B. Preference index for glycolic acid. C. Preference index for tartaric acid.

III. MECHANOSENSORY IN MOSQUITOES

INTRODUCTION

Mechanosensory in mosquitoes

Mechanical forces are behind many common environmental stimuli, such as a gust of wind follows the subway's swift exit or the touching of a dinosaur egg from 72 million years ago in the American Natural History Museum. All living things share the ability to turn these mechanical changes into electrochemical signals.[167] Mechanosensation enables animals to sense and react to mechanical stimuli like touch, sound, vibration, pressure, and gravity. For mosquitoes, mechanosensation is important for many of their behaviors, including tasting, egg-laying, mating, flying, landing and escaping. They also use mechanosensation to sense air currents, sound waves and gravity, which are crucial for flight and mating. Insects feeding preferences have been shown to correlate with the viscosity of food resources. For example, during nectar feeding, the mosquitoes will decide to drink or not based on the viscosity of nectar.[168] Regardless of the level of sugar, honeybees are drawn to nectar that is warmer and has a lower viscosity.[169] Another study in ants showed that *Camponotus mus* dramatically reduced their pump frequencies when feeding on sucrose with higher viscosity.[170] During blood feeding, after landing on a host, mosquitoes used their tarsi and proboscis to make contact with human skin and look for optimized spot to poke through. Once find the spot, they will retract their proboscis and use the stylets to poke through the skin. These stylets in the skin will move rigorously and look for blood vessels. And this whole process continuously needs mechanosensation and processing of the mechanical signals.[171] However, very little is known about the mechanosensation signaling in this process.

Mechanosensors

Insects have various sensory structures all over their body surface that are connected to specialized neurons that can sense mechanical stimuli. Many of the responses to these mechanical stimuli are mediated by mechanosensors like ion channels, including TRP channels, PIEZO, TMC, NOMPC and TMEM63, etc.[167,172] TMEM63 protein was originally found in plants where it is called OSCA. And TMEM63 is the homolog name of OSCA in animals. The OSCA/TMEM63 family of proteins are conserved across plants, flies, and mammals.[173] TMEM63 has been shown to be important for *Drosophila*'s taste detection of food texture.[174] Mouse TMEM63 proteins could act as an ion channel that senses osmolarity for the detection of osmotic pressure in mammalian cells.[175] In mosquitoes, it is shown that *tmem63* is expressed in mosquito proboscis.[166] Thus, in this research, we tested the role of *tmem63* in mosquitoes' mechanosensation. We generated two null mutants of *tmem63* and verified its protein expressions in the proboscis of mosquitoes. We also tested its function in surface texture detection during blood feeding and found that it is important for mosquitoes to find the ideal spot for poking and blood feeding.

RESULTS

TMEM63 is expressed in the proboscis of mosquitoes

TMEM63 has been shown to be important for *Drosophila*'s taste detection of food texture.[174] However, little is known about whether it is involved in the mechanosensation in mosquitoes. To test this, first we used immunostaining to verify their expression pattern. Previous RNAseq data has shown that *tmem63* is expressed in the mosquito proboscis.[166] To examine this expression pattern from a protein level, we generated *tmem63-QF2* driver line using

CRISPR/Cas9 technique and crossed it with *QUAS-mCD8-GFP*. We found that compared to the control mosquitoes (*QUAS-mCD8-GFP*) which showed no GFP signal, *tmem63>mCD8-GFP* showed GFP signals in the proboscis of both females and males' progeny of the crosses. This evidence validated the expression of *tmem63* in the proboscis of mosquitoes, and also supported our hypothesis about their potential function in blood feeding.

TMEM63 is important for mosquitoes' blood feeding

We next tested whether TMEM63 is involved in blood feeding behavior. To test this, we generated two null mutants for *tmem63*, $tmem63^{GFP}$ mutant and $tmem63^{QF2}$ mutant mosquitoes using CRISPR/Cas9 technique. Generally, we found that wild-type mosquitoes prefer to blood feed on 3% chitosan membranes because the elasticity and hardness of this membrane are similar to human skin. However, we found that $tmem63^{GFP}$ mutant mosquitoes preferred 1.5% chitosan membranes which have decreased hardness. (Fig.2) We also found that $tmem63^{GFP}$ mosquitoes had continuous landings on both membranes, while wild-type mosquitoes had fewer landing occasions after about 6 minutes when most of the mosquitoes landed and initiated blood feeding. (Fig. 3A) The $tmem63^{GFP}$ mutant mosquitoes also had more walking events on the surface of both membranes than wild type which indicated that it potentially took longer time for them to find an ideal location to poke through the membrane and initiate blood feeding. (Fig.3B)

Viscosity preference in mosquitoes

We next examined the mosquitoes' preference for different viscosities of food. Previous research has shown that *Drosophila* prefers a certain viscosity of food.[176] Given that *tmem63*

mutant mosquitoes showed a defect in detecting the surface texture of blood feeding membranes, the next question we asked was that whether *tmem63* is important for mosquitoes to detect different viscosities during general nectar feeding. However, whether mosquitoes have taste preferences for different viscosities of food is not known. To test this, we performed two-way choice assays using 0.5% HPC or. 0% HPC in sucrose. We found that wild-type mosquitoes are aversive to 0.5% HPC. (Fig. 4) Future experiments will be performed with both *tmem63* mutant mosquitoes.

DISCUSSION

In this research, we found that *tmem63* is expressed in the proboscis of *Aedes aegypti*. *tmem63* is also important for mosquitoes to detect the surface texture during blood feeding. Additionally, mosquitoes showed aversion to higher viscosity of food.

To thoroughly test whether and how *tmem63* is required for mosquitoes to detect the surface texture during blood feeding, we established a two-way choice blood feeding assays with video recordings. Next, we will test mosquitoes' preferences to compare membranes with different chitosan concentrations (6%, 3%, 1.5% and 0.75%) used in blood feeding. Through video recording, we plan to test more parameters including number of poking events, average/total waking time before initiating blood feeding and time spend on feeding/engorgement, etc.

To test whether *tmem63* is a direct mechanosensory, we will also test its mechanical response in mammalian HEK293 cells using patch-clamp. We had constructed the plasmid required to express *Aedes tmem63* in mammalian HEK293 cells. We had also successfully transfected

the cells and observed the expression of *tmem63* in the cells. Next, we will examine their electrical response to mechanical stimuli using patch-clamp.

Besides proboscis, mosquitoes also use their tarsi to detect the texture and tastants on the surface of the food resources. Thus, we will also investigate whether *tmem63* is expressed in the tarsi of mosquitoes and whether *tmem63* is functional through tarsi as well.

METHODS

Mosquito rearing

Mosquitoes were reared in chambers at 28° C and 80% humidity under 12h light/12h dark cycles. Eggs are hatched in tanks with RO water with fish food added daily. Mosquito larvae were screened under fluorescent microscope to make sure there was no contamination. Pupae were collected into plastic cups and placed in cages with 10% sucrose solution bottles with wicks. Mosquitoes that were 7-10 days old after eclosion were used for behavior assays. Sheep blood was used for blood feeding and mosquito expansion.

Generation of transgenic strains

To generate the $tmem63^{GFP}$ and $tmem63^{QF2}$ alleles, we selected short-guide RNAs (sgRNAs) that targeted the tmem63 (LOC5573309) loci using the CRISPR Optimal Target Finder (https://flycrispr.org/target-finder/). The target sequences of the sgRNAs used for generating the $tmem63^{GFP}$ and $tmem63^{QF2}$ alleles are as following:

GFP: ATCTTGATTCTACCGTCCCT

QF2: CCTGCTCAATGTCATTGCGT

To generate the *tmem63*^{GFP} and *tmem63*^{QF2} alleles, we created the tmem63-3xP3-GFP and tmem63-3xP3-DsRed-T2A-QF2 DNA constructs for microinjections. To do so, we used the In-Fusion cloning kit (Clontech) to introduce the sgRNAs, and the upstream and downstream homology arms (~1 kb each) into the pAeU6-LgRNA-3xP3-GFP vector or the pAeU6-LgRNA-3xP3-DsRed-T2A-QF2 vector.[153]

All transgenic strains were generated by microinjecting the plasmids into embryos of the transgenic *Aedes aegypti* line that expresses Cas9 under control of the ubiquitin L40 promotor (gift from Dr. Omar Akbari). We collected freshly laid embryos from female mosquitoes, and microinjected the plasmid DNA (~500 ng/μL) into the posterior ends of ~1,000 embryos using a micro-injector (Eppendorf) and a Zeiss Axioplan 2 microscope. We hatched G0 embryos four days after injection, and the adult G0 animals (~100 per injection) were crossed to the opposite sex. The females were blood-fed to generate G1 progeny. We then screened the G1 progeny larvae for expression of the GFP or DsRed fluorescent markers in the eye under a Zeiss SteREO Discovery V8 stereomicroscope. Positive G1 animals were crossed to the wild-type control strain for eight generations after which were used to generated the homozygous lines.

Immunostaining

Dissected proboscis from 5- to 7-day-old adult mosquitoes were fixed in 4% paraformaldehyde in PBS for 2 hours at 4°C. Samples were then washed in PBST (PBS + 0.1% Triton X-100; 10 min) and blocked with block buffer containing 5% normal goat serum (MP Biomedicals) for 1 hour at room temperature. Next, the samples were incubated in primary antibodies overnight at 4°C. Next day, the samples were washed with PBST (20 min,

3 times) and then incubated with the secondary antibodies in blocking buffer overnight at 4°C in the dark. The following primary and secondary antibodies were used at the indicated dilutions: chicken anti-GFP (1:500), AlexaFluor 488 goat anti-chicken IgG (1:250; Thermo Fisher Scientific). After a final PBST wash (10 min, 3 times), the samples were mounted using Vectashield (Vector Laboratory, H-1000) and a coverslip was secured with nail polish. The samples were imaged using a Zeiss LSM 900 confocal laser scanning microscope using a 40x/1.3 Plan-Apochromat oil DIC objective. Images were processed using the following protocol in ImageJ: A rolling-ball background subtraction (radius 50 pixels) was applied to each z-stack slice containing fluorescent signal from the neurons at proboscis. The maximum intensity projection of each channel is merged.

Two-way choice feeding assay

55-60 mosquitoes (aged to 7-10 days) per cage were starved with RO water for 48 hours (female) or 24 hours (males). 96-well plates that contained 0.5% HPC/dye mixtures were put in the cages to allow mosquitoes to feed for 3 hours in the evening. The preference index (PI) was calculated according to the following equation: $(N_{red}-N_{blue})/(N_{red}+N_{blue}+N_{purple})$. We determined the concentrations of the red (Sulforhodamine B; Sigma-Aldrich) and blue (Brilliant Blue FCF; Wako Chemical) food dyes that had no significant effect on food selection by assaying the preference of control mosquitoes to each dye with 20 mM sucrose. Once the concentrations were established that lead to indifference between the two food colorings, 0.5% HPC was added in 20mM sucrose solutions to compare with 20mM sucrose only solutions. Sulforhodamine B and Brilliant Blue dyes were switched between test and control solutions for every assay. A PI = 1.0 and −1.0 indicates complete preference for food

with sucrose-only and sucrose plus 0.5% HPC, respectively. A PI = 0 indicated no preference for either food. Trials in which < 40% of the mosquitoes participated were discarded.

Blood feeding assays

50 mosquitoes (aged to 7-10 days) were put in each cage. Two blood feeders with different chitosan concentrations artificial membranes (3% v.s. 1.5% chitosan) were put in each cage to allow mosquitoes to feed for 30 minutes. Logitech cameras were used to video record the mosquito activities on membranes.

ACKNOWLEDGEMENTS

Thanks to Annalise Bond for gRNA design and Nikola Klier for helping with outcrossing the mutants and generating tmem63 construct used in HEK293 cell transfection.

FIGURES

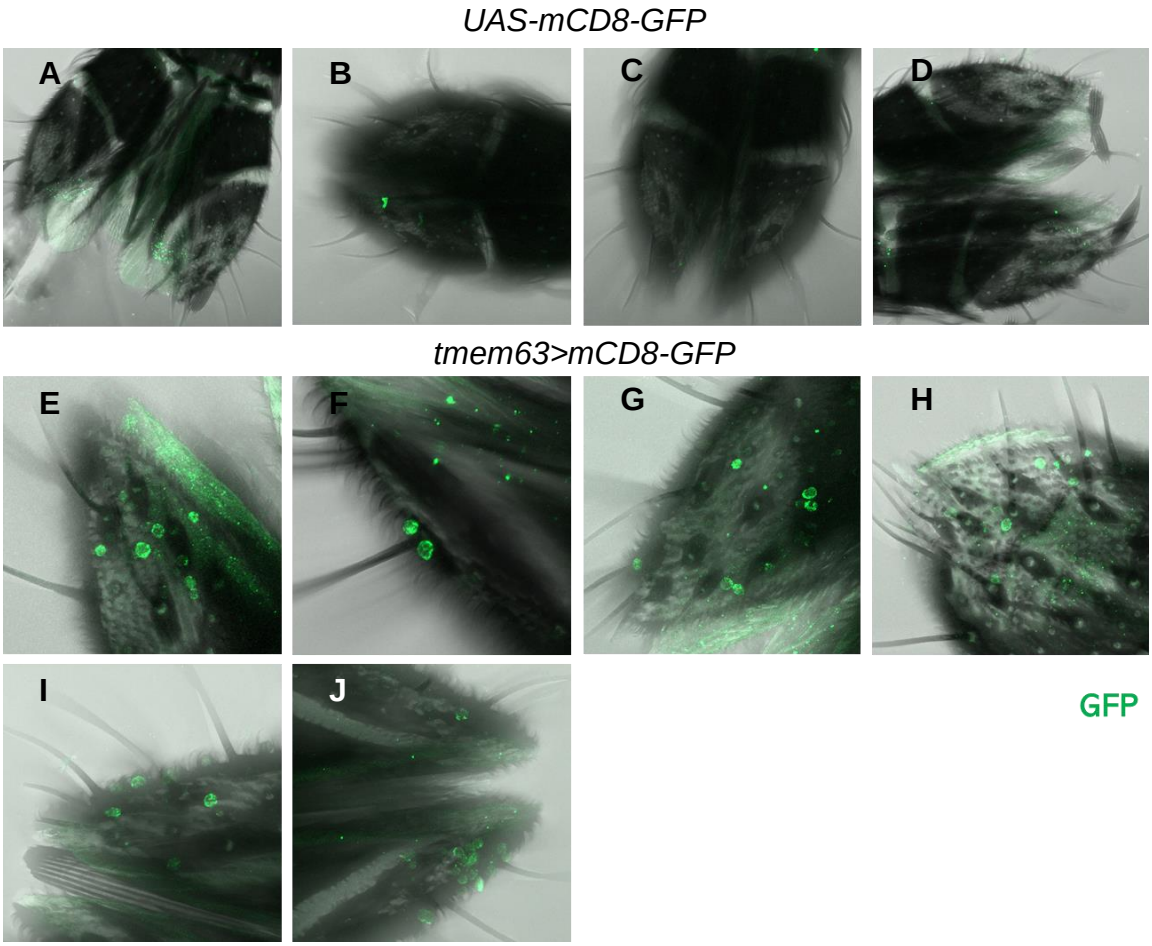

Fig.1 TMEM63 is expressed in the proboscis of Aedes aegypti. (A-D) control (E-H) *tmem63>mCD8-GFP* females (I-J) *tmem63>mCD8-GFP* males

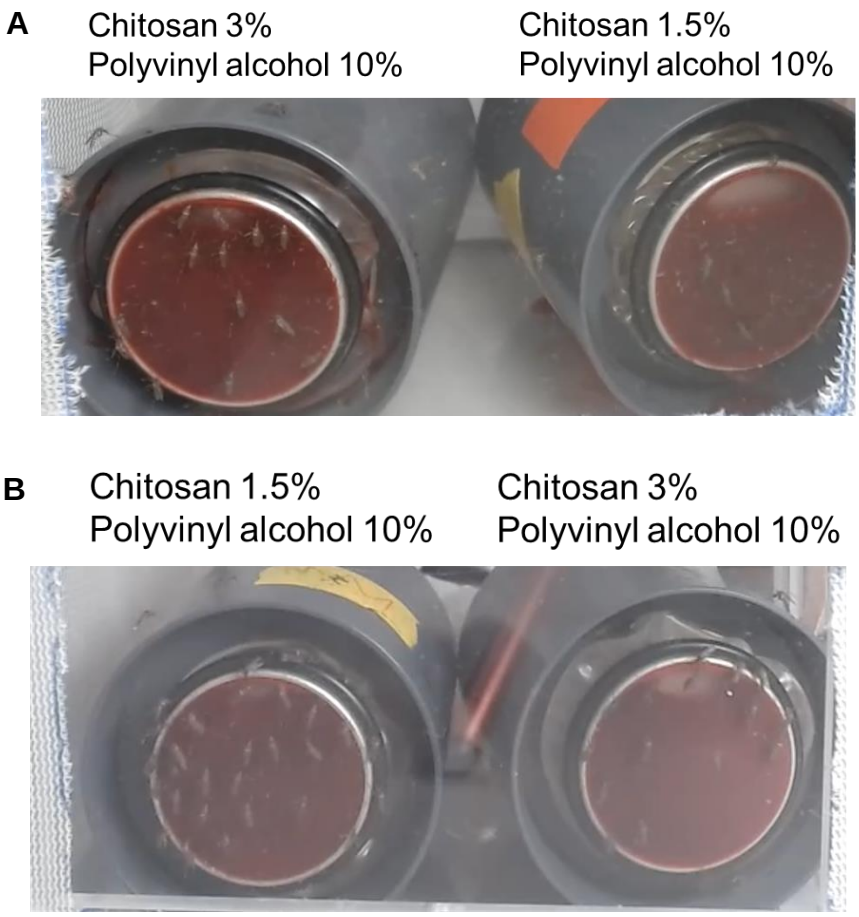

Fig.2 *tmem63* mutant mosquitoes reduces the preference for 3% chitosan. A. control B. *tmem63* mutant

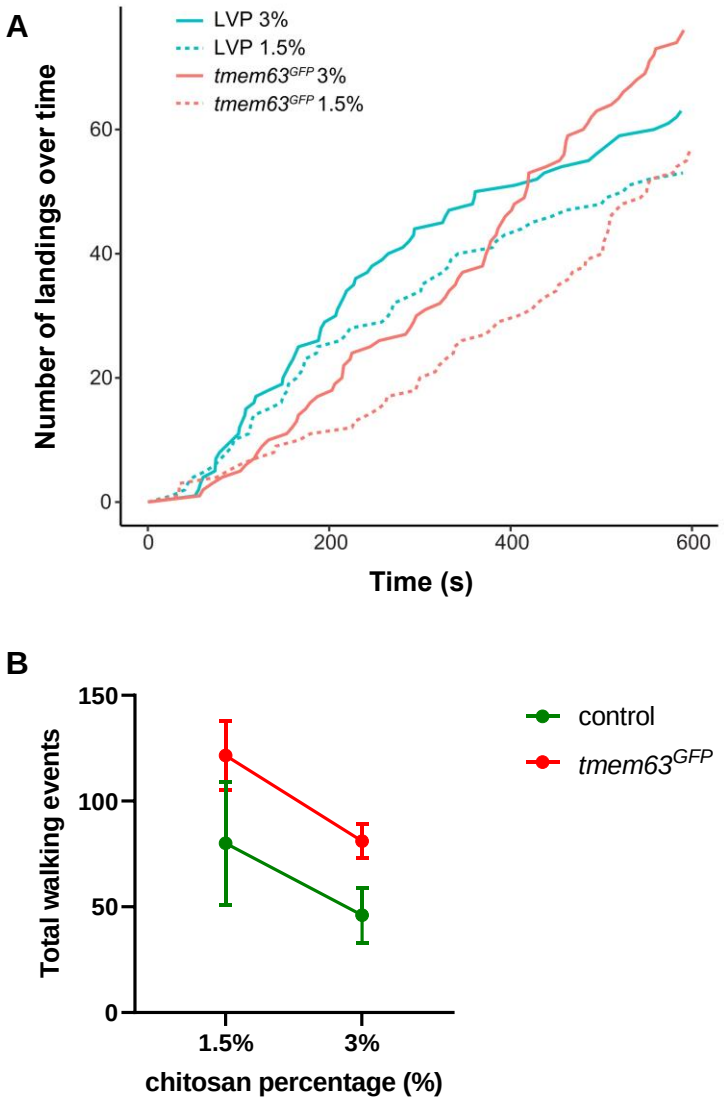

Fig.3 *tmem63* mutant mosquitoes reduces the preference for 3% chitosan. A. number of landings over time B. total walking events

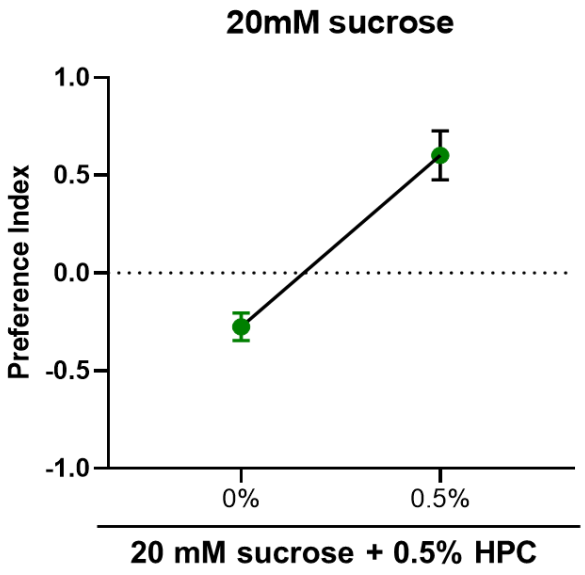

Fig.4 Aedes aegypti is aversive to 0.5% HPC viscosity.

REFERENCES

1. Montaruli, A., Castelli, L., Mulè, A., Scurati, R., Esposito, F., Galasso, L., and Roveda, E. (2021). Biological rhythm and chronotype: new perspectives in health. Biomolecules *11*, 487.
2. Mazri, F.H., Manaf, Z.A., Shahar, S., and Mat Ludin, A.F. (2020). The association between chronotype and dietary pattern among adults: a scoping review. Int. J. Environ. Res. Public Health *17*, 68.
3. Rijo-Ferreira, F., and Takahashi, J.S. (2019). Genomics of circadian rhythms in health and disease. Genome Med. *11*, 82. 10.1186/s13073-019-0704-0.
4. Taylor, B.J., and Hasler, B.P. (2018). Chronotype and mental health: recent advances. Curr. Psychiatry Rep. *20*, 59. 10.1007/s11920-018-0925-8.
5. Vetter, C., Devore, E.E., Ramin, C.A., Speizer, F.E., Willett, W.C., and Schernhammer, E.S. (2015). Mismatch of sleep and work timing and risk of type 2 diabetes. Diabetes Care *38*, 1707-1713. 10.2337/dc15-0302.
6. Dubowy, C., and Sehgal, A. (2017). Circadian rhythms and sleep in *Drosophila melanogaster*. Genetics *205*, 1373-1397. 10.1534/genetics.115.185157.
7. Lee, Y., Field, J.M., and Sehgal, A. (2021). Circadian rhythms, disease and chronotherapy. J. Biol. Rhythms *36*, 503-531. 10.1177/07487304211044301.
8. Pittendrigh, C.S. (1960). Circadian rhythms and the circadian organization of living systems. Cold Spring Harb Symp Quant Biol *25*, 159-184. 10.1101/sqb.1960.025.01.015.
9. Barclay, N.L., Eley, T.C., Buysse, D.J., Archer, S.N., and Gregory, A.M. (2010). Diurnal preference and sleep quality: same genes? A study of young adult twins. Chronobiol. Int. *27*, 278-296. 10.3109/07420521003663801.
10. Hu, Y., Shmygelska, A., Tran, D., Eriksson, N., Tung, J.Y., and Hinds, D.A. (2016). GWAS of 89,283 individuals identifies genetic variants associated with self-reporting of being a morning person. Nat. Commun. *7*, 10448. 10.1038/ncomms10448.
11. Jones, S.E., Lane, J.M., Wood, A.R., van Hees, V.T., Tyrrell, J., Beaumont, R.N., Jeffries, A.R., Dashti, H.S., Hillsdon, M., Ruth, K.S., et al. (2019). Genome-wide association analyses of chronotype in 697,828 individuals provides insights into circadian rhythms. Nat. Commun. *10*, 343. 10.1038/s41467-018-08259-7.

12. Jones, C.R., Campbell, S.S., Zone, S.E., Cooper, F., DeSano, A., Murphy, P.J., Jones, B., Czajkowski, L., and Ptček, L.J. (1999). Familial advanced sleep-phase syndrome: a short-period circadian rhythm variant in humans. Nat. Med. *5*, 1062-1065. 10.1038/12502.
13. Patke, A., Murphy, P.J., Onat, O.E., Krieger, A.C., Özçelik, T., Campbell, S.S., and Young, M.W. (2017). Mutation of the human circadian clock gene *CRY1* in familial delayed sleep phase disorder. Cell *169*, 203-215.e213.
14. Pegoraro, M., Flavell, L.M.M., Menegazzi, P., Colombi, P., Dao, P., Helfrich-Förster, C., and Tauber, E. (2020). The genetic basis of diurnal preference in *Drosophila melanogaster*. BMC Genom. *21*, 596. 10.1186/s12864-020-07020-z.
15. Vink, J.M., Vink, J.M., Groot, A.S., Kerkhof, G.A., and Boomsma, D.I. (2001). Genetic analysis of morningness and eveningness. Chronobiol. Int. *18*, 809-822. 10.1081/CBI-100107516.
16. Toh, K.L., Jones, C.R., He, Y., Eide, E.J., Hinz, W.A., Virshup, D.M., Ptáček, L.J., and Fu, Y.-H. (2001). An h*Per2* phosphorylation site mutation in familial advanced sleep phase syndrome. Science *291*, 1040-1043. 10.1126/science.1057499.
17. Xu, Y., Toh, K.L., Jones, C.R., Shin, J.Y., Fu, Y.H., and Ptáček, L.J. (2007). Modeling of a human circadian mutation yields insights into clock regulation by PER2. Cell *128*, 59-70.
18. Hall, J.C. (2003). Genetics and molecular biology of rhythms in *Drosophila* and other insects. In Adv. Genet., pp. *48. 4*1-280. 10.1016/S0065-2660(03)48000-0.
19. Konopka, R.J., and Benzer, S. (1971). Clock mutants of *Drosophila melanogaster*. Proc. Natl. Acad. Sci. U.S.A. *68*, 2112-2116. 10.1073/pnas.68.9.2112.
20. Pegoraro, M., Picot, E., Hansen, C.N., Kyriacou, C.P., Rosato, E., and Tauber, E. (2015). Gene expression associated with early and late chronotypes in *Drosophila melanogaster*. Front. Neurol. *6*.
21. Rosbash, M. (2021). Circadian rhythms and the transcriptional feedback loop (Nobel lecture). Angew. Chem. Int. Ed. *60*, 8650-8666.
22. Young, M.W. (2018). Time travels: a 40-year journey from Drosophila's clock mutants to human circadian disorders (Nobel lecture). Angew. Chem. Int. Ed. *57*, 11532-11539.

23. Patke, A., Young, M.W., and Axelrod, S. (2020). Molecular mechanisms and physiological importance of circadian rhythms. Nat. Rev. Mol. Cell Biol. *21*, 67-84. 10.1038/s41580-019-0179-2.

24. Ahmad, M., Li, W., and Top, D. (2021). Integration of Circadian Clock Information in the *Drosophila* Circadian Neuronal Network. J. Biol. Rhythms *36*, 203-220. 10.1177/0748730421993953.

25. Schlichting, M. (2020). Entrainment of the *Drosophila* clock by the visual system. Neuroscience Insights *15*. 10.1177/2633105520903708.

26. Li, M.-T., Cao, L.-H., Xiao, N., Tang, M., Deng, B., Yang, T., Yoshii, T., and Luo, D.-G. (2018). Hub-organized parallel circuits of central circadian pacemaker neurons for visual photoentrainment in *Drosophila*. Nat. Commun. *9*, 4247. 10.1038/s41467-018-06506-5.

27. Helfrich-Förster, C. (2020). Light input pathways to the circadian clock of insects with an emphasis on the fruit fly *Drosophila melanogaster*. J. Comp. Physiol. *206*, 259-272. 10.1007/s00359-019-01379-5.

28. Golombek, D.A., and Rosenstein, R.E. (2010). Physiology of circadian entrainment. Physiol. Rev. *90*, 1063-1102. 10.1152/physrev.00009.2009.

29. Saint-Charles, A., Michard-Vanhee, C., Alejevski, F., Chelot, E., Boivin, A., and Rouyer, F. (2016). Four of the six Drosophila rhodopsin-expressing photoreceptors can mediate circadian entrainment in low light. The Journal of comparative neurology *524*, 2828-2844. 10.1002/cne.23994.

30. Ogueta, M., Hardie, R.C., and Stanewsky, R. (2018). Non-canonical Phototransduction Mediates Synchronization of the *Drosophila melanogaster* Circadian Clock and Retinal Light Responses. Curr. Biol. *28*, 1725-1735 e1723. 10.1016/j.cub.2018.04.016.

31. Senthilan, P.R., Grebler, R., Reinhard, N., Rieger, D., and Helfrich-Forster, C. (2019). Role of Rhodopsins as Circadian Photoreceptors in the Drosophila melanogaster. Biology *8*. 10.3390/biology8010006.

32. Ni, J.D., Baik, L.S., Holmes, T.C., and Montell, C. (2017). A rhodopsin in the brain functions in circadian photoentrainment in *Drosophila*. Nature *545*, 340-344. 10.1038/nature22325.

33. O'Tousa, J.E., Baehr, W., Martin, R.L., Hirsh, J., Pak, W.L., and Applebury, M.L. (1985). The Drosophila *ninaE* gene encodes an opsin. Cell *40*, 839-850. 10.1016/0092-8674(85)90343-5.
34. Zuker, C.S., Cowman, A.F., and Rubin, G.M. (1985). Isolation and structure of a rhodopsin gene from D. melanogaster. Cell *40*, 851-858.
35. Montell, C. (2021). *Drosophila* sensory receptors—a set of molecular Swiss Army Knives. Genetics *217*, 1-34. 10.1093/genetics/iyaa011.
36. Montell, C., Jones, K., Zuker, C., and Rubin, G. (1987). A second opsin gene expressed in the ultraviolet-sensitive R7 photoreceptor cells of *Drosophila melanogaster*. J Neurosci *7*, 1558-1566. 10.1523/jneurosci.07-05-01558.1987.
37. Zuker, C., Montell, C., Jones, K., Laverty, T., and Rubin, G. (1987). A rhodopsin gene expressed in photoreceptor cell R7 of the *Drosophila* eye: homologies with other signal-transducing molecules. J Neurosci *7*, 1550-1557. 10.1523/jneurosci.07-05-01550.1987.
38. Chou, W.-H., Hall, K.J., Wilson, D.B., Wideman, C.L., Townson, S.M., Chadwell, L.V., and Britt, S.G. (1996). Identification of a novel Drosophila opsin reveals specific patterning of the R7 and R8 photoreceptor cells. Neuron *17*, 1101-1115.
39. Huber, A., Schulz, S., Bentrop, J., Groell, C., Wolfrum, U., and Paulsen, R. (1997). Molecular cloning of *Drosophila* Rh6 rhodopsin: the visual pigment of a subset of R8 photoreceptor cells. FEBS Lett. *406*, 6-10.
40. Papatsenko, D., Sheng, G., and Desplan, C. (1997). A new rhodopsin in R8 photoreceptors of *Drosophila*: evidence for coordinate expression with Rh3 in R7 cells. Development *124*, 1665-1673.
41. Mismer, D., Michael, W.M., Laverty, T.R., and Rubin, G.M. (1988). Analysis of the promoter of the Rh2 opsin gene in *Drosophila melanogaster*. Genetics *120*, 173-180.
42. Pollock, J.A., and Benzer, S. (1988). Transcript localization of four opsin genes in the three visual organs of *Drosophila*; RH2 is ocellus specific. Nature *333*, 779-782. 10.1038/333779a0.
43. Yasuyama, K., and Meinertzhagen, I.A. (1999). Extraretinal photoreceptors at the compound eye's posterior margin in *Drosophila melanogaster*. J Comp Neurol *412*, 193-202. 10.1002/(SICI)1096-9861(19990920)412:2<193::AID-CNE1>3.0.CO;2-0.

44. Kistenpfennig, C., Grebler, R., Ogueta, M., Hermann-Luibl, C., Schlichting, M., Stanewsky, R., Senthilan, P.R., and Helfrich-Förster, C. (2017). A new rhodopsin influences light-dependent daily activity patterns of fruit flies. J. Biol. Rhythms *32*, 406-422. 10.1177/0748730417721826.
45. Pfeiffenberger, C., Lear, B.C., Keegan, K.P., and Allada, R. (2010). Processing sleep data created with the *Drosophila* Activity Monitoring (DAM) System. Cold Spring Harb. Protoc. *2010*, pdb.prot5520. 10.1101/pdb.prot5520.
46. Pfeiffenberger, C., Lear, B.C., Keegan, K.P., and Allada, R. (2010). Processing circadian data collected from the *Drosophila* Activity Monitoring (DAM) System. Cold Spring Harb. Protoc. *2010*, pdb.prot5519. 10.1101/pdb.prot5519.
47. Cirelli, C., and Bushey, D. (2008). Sleep and wakefulness in *Drosophila melanogaster*. Ann. N. Y. Acad. Sci. *1129*, 323-329. 10.1196/annals.1417.017.
48. Hendricks, J.C., Finn, S.M., Panckeri, K.A., Chavkin, J., Williams, J.A., Sehgal, A., and Pack, A.I. (2000). Rest in *Drosophila* is a sleep-like state. Neuron *25*, 129-138.
49. Shaw, P.J., Cirelli, C., Greenspan, R.J., and Tononi, G. (2000). Correlates of sleep and waking in *Drosophila melanogaster*. Science *287*, 1834-1837. 10.1126/science.287.5459.1834.
50. Huber, R., Hill, S.L., Holladay, C., Biesiadecki, M., Tononi, G., and Cirelli, C. (2004). Sleep homeostasis in *Drosophila melanogaster*. Sleep *27*, 628-639. 10.1093/sleep/27.4.628.
51. Guo, F., Yu, J., Jung, H.J., Abruzzi, K.C., Luo, W., Griffith, L.C., and Rosbash, M. (2016). Circadian neuron feedback controls the *Drosophila* sleep–activity profile. Nature *536*, 292. 10.1038/nature19097
52. Yang, Y., and Edery, I. (2019). *Daywake*, an anti-siesta gene linked to a splicing-based thermostat from an adjoining clock gene. Curr. Biol. *29*, 1728-1734.e1724.
53. Alphen, B.v., Yap, M.H.W., Kirszenblat, L., Kottler, B., and Swinderen, B.v. (2013). A Dynamic Deep Sleep Stage in *Drosophila*. J Neurosci *33*, 6917-6927. 10.1523/jneurosci.0061-13.2013.
54. Faville, R., Kottler, B., Goodhill, G.J., Shaw, P.J., and van Swinderen, B. (2015). How deeply does your mutant sleep? Probing arousal to better understand sleep defects in *Drosophila*. Sci. Rep. *5*, 8454. 10.1038/srep08454.

55. Mrosovsky, N. (1999). Masking: History, Definitions, and Measurement. Chronobiol. Int. *16*, 415-429. 10.3109/07420529908998717.

56. Dreyer, A.P., Martin, M.M., Fulgham, C.V., Jabr, D.A., Bai, L., Beshel, J., and Cavanaugh, D.J. (2019). A circadian output center controlling feeding:fasting rhythms in *Drosophila*. PLoS Genet. *15*, e1008478. 10.1371/journal.pgen.1008478.

57. Ro, J., Harvanek, Z.M., and Pletcher, S.D. (2014). FLIC: high-throughput, continuous analysis of feeding behaviors in *Drosophila*. PloS one *9*, e101107. 10.1371/journal.pone.0101107.

58. Xu, K., Zheng, X., and Sehgal, A. (2008). Regulation of feeding and metabolism by neuronal and peripheral clocks in *Drosophila*. Cell Metab. *8*, 289-300. 10.1016/j.cmet.2008.09.006.

59. May, C.E., Vaziri, A., Lin, Y.Q., Grushko, O., Khabiri, M., Wang, Q.-P., Holme, K.J., Pletcher, S.D., Freddolino, P.L., Neely, G.G., and Dus, M. (2019). High dietary sugar reshapes sweet taste to promote feeding behavior in *Drosophila melanogaster*. Cell Rep. *27*, 1675-1685.e1677.

60. Feiler, R., Bjornson, R., Kirschfeld, K., Mismer, D., Rubin, G., Smith, D., Socolich, M., and Zuker, C. (1992). Ectopic expression of ultraviolet-rhodopsins in the blue photoreceptor cells of *Drosophila*: visual physiology and photochemistry of transgenic animals. J Neurosci *12*, 3862-3868. 10.1523/jneurosci.12-10-03862.1992.

61. Sharkey, C.R., Blanco, J., Leibowitz, M.M., Pinto-Benito, D., and Wardill, T.J. (2020). The spectral sensitivity of *Drosophila* photoreceptors. Sci. Rep. *10*, 18242. 10.1038/s41598-020-74742-1.

62. Leung, N.Y., Thakur, D.P., Gurav, A.S., Kim, S.H., Di Pizio, A., Niv, M.Y., and Montell, C. (2020). Functions of opsins in *Drosophila* taste. Curr. Biol. *30*, 1367-1379.e1366.

63. Li, Q., DeBeaubien, N.A., Sokabe, T., and Montell, C. (2020). Temperature and sweet taste integration in *Drosophila*. Curr. Biol. *30*, 2051-2067.e2055.

64. Senthilan, Pingkalai R., Piepenbrock, D., Ovezmyradov, G., Nadrowski, B., Bechstedt, S., Pauls, S., Winkler, M., Möbius, W., Howard, J., and Göpfert, Martin C. (2012). *Drosophila* auditory organ genes and genetic hearing defects. Cell *150*, 1042-1054. 10.1016/j.cell.2012.06.043.

65. Shen, W.L., Kwon, Y., Adegbola, A.A., Luo, J., Chess, A., and Montell, C. (2011). Function of rhodopsin in temperature discrimination in *Drosophila*. Science *331*, 1333-1336. 10.1126/science.1198904.

66. Sokabe, T., Chen, H.C., Luo, J., and Montell, C. (2016). A switch in thermal preference in *Drosophila* larvae depends on multiple rhodopsins. Cell Rep. *17*, 336-344. 10.1016/j.celrep.2016.09.028.

67. Chen, Z., and Montell, C. (2020). A family of auxiliary subunits of the TRP cation channel encoded by the complex *inaF* locus. Genetics *215*, 713-728. 10.1534/genetics.120.303268.

68. Menon, K.P., Kulkarni, V., Takemura, S.-y., Anaya, M., and Zinn, K. (2019). Interactions between Dpr11 and DIP-γ control selection of amacrine neurons in Drosophila color vision circuits. eLife *8*, e48935. 10.7554/eLife.48935.

69. Sancer, G., Kind, E., Plazaola-Sasieta, H., Balke, J., Pham, T., Hasan, A., Münch, L.O., Courgeon, M., Mathejczyk, T.F., and Wernet, M.F. (2019). Modality-specific circuits for skylight orientation in the fly visual system. Curr. Biol. *29*, 2812-2825.e2814. 10.1016/j.cub.2019.07.020.

70. Wernet, M.F., Mazzoni, E.O., Celik, A., Duncan, D.M., Duncan, I., and Desplan, C. (2006). Stochastic spineless expression creates the retinal mosaic for colour vision. Nature *440*, 174-180. 10.1038/nature04615.

71. Li, Y., Chen, P.-J., Lin, T.-Y., Ting, C.-Y., Muthuirulan, P., Pursley, R., Ilić, M., Pirih, P., Drews, M.S., Menon, K.P., et al. (2021). Neural mechanism of spatio-chromatic opponency in the *Drosophila* amacrine neurons. Curr. Biol. *31*, 3040-3052.e3049. 10.1016/j.cub.2021.04.068.

72. Pagni, M., Haikala, V., Oberhauser, V., Meyer, P.B., Reiff, D.F., and Schnaitmann, C. (2021). Interaction of "chromatic" and "achromatic" circuits in *Drosophila* color opponent processing. Curr. Biol. *31*, 1687-1698.e1684. 10.1016/j.cub.2021.01.105.

73. Nitabach, M.N., Wu, Y., Sheeba, V., Lemon, W.C., Strumbos, J., Zelensky, P.K., White, B.H., and Holmes, T.C. (2006). Electrical hyperexcitation of lateral ventral pacemaker neurons desynchronizes downstream circadian oscillators in the fly circadian circuit and induces multiple behavioral periods. J Neurosci *26*, 479-489. 10.1523/JNEUROSCI.3915-05.2006.

74. Harris, W.A., Stark, W.S., and Walker, J.A. (1976). Genetic dissection of the photoreceptor system in the compound eye of *Drosophila melanogaster*. J Physiol *256*, 415-439. 10.1113/jphysiol.1976.sp011331.

75. Wernet, M.F., Labhart, T., Baumann, F., Mazzoni, E.O., Pichaud, F., and Desplan, C. (2003). Homothorax switches function of *Drosophila* photoreceptors from color to polarized light sensors. Cell *115*, 267-279. 10.1016/s0092-8674(03)00848-1.

76. Courgeon, M., and Desplan, C. (2019). Coordination between stochastic and deterministic specification in the Drosophila visual system. Science *366*, eaay6727. 10.1126/science.aay6727.

77. Ito, C., and Tomioka, K. (2016). Heterogeneity of the peripheral circadian systems in *Drosophila melanogaster*: a review. Front. Physiol. *7*. 10.3389/fphys.2016.00008.

78. Xu, K., DiAngelo, Justin R., Hughes, Michael E., Hogenesch, John B., and Sehgal, A. (2011). The circadian clock interacts with metabolic physiology to influence reproductive fitness. Cell Metab. *13*, 639-654. 10.1016/j.cmet.2011.05.001.

79. Bae, K., Lee, C., Sidote, D., Chuang, K.-y., and Edery, I. (1998). Circadian regulation of a *Drosophila* homolog of the mammalian *Clock* gene: PER and TIM function as positive regulators. Mol. Cell. Biol. *18*, 6142-6151. 10.1128/MCB.18.10.6142.

80. Cyran, S.A., Buchsbaum, A.M., Reddy, K.L., Lin, M.-C., Glossop, N.R.J., Hardin, P.E., Young, M.W., Storti, R.V., and Blau, J. (2003). *vrille, Pdp1,* and *dClock* form a second feedback loop in the *Drosophila* circadian clock. Cell *112*, 329-341.

81. McDonald, M.J., and Rosbash, M. (2001). Microarray analysis and rrganization of circadian gene expression in *Drosophila*. Cell *107*, 567-578.

82. Reddy, P., Zehring, W.A., Wheeler, D.A., Pirrotta, V., Hadfield, C., Hall, J.C., and Rosbash, M. (1984). Molecular analysis of the *period* locus in Drosophila melanogaster and identification of a transcript involved in biological rhythms. Cell *38*, 701-710. 10.1016/0092-8674(84)90265-4.

83. Sehgal, A., Price, J.L., Man, B., and Young, M.W. (1994). Loss of circadian behavioral rhythms and *per* RNA oscillations in the *Drosophila* mutant *timeless*. Science *263*, 1603-1606. 10.1126/science.8128246.

84. Kuintzle, R.C., Chow, E.S., Westby, T.N., Gvakharia, B.O., Giebultowicz, J.M., and Hendrix, D.A. (2017). Circadian deep sequencing reveals stress-response genes that

adopt robust rhythmic expression during aging. Nat. Commun. *8,* 14529. 10.1038/ncomms14529.

85. Xiao, Y., Yuan, Y., Jimenez, M., Soni, N., and Yadlapalli, S. (2021). Clock proteins regulate spatiotemporal organization of clock genes to control circadian rhythms. Proc. Natl. Acad. Sci. U.S.A. *118,* e2019756118. 10.1073/pnas.2019756118.
86. Grima, B., Chélot, E., Xia, R., and Rouyer, F. (2004). Morning and evening peaks of activity rely on different clock neurons of the *Drosophila* brain. Nature *431,* 869-873. 10.1038/nature02935.
87. Renn, S.C.P., Park, J.H., Rosbash, M., Hall, J.C., and Taghert, P.H. (1999). A *pdf* neuropeptide gene mutation and ablation of PDF neurons each cause severe abnormalities of behavioral circadian rhythms in *Drosophila*. Cell *99,* 791-802.
88. Roenneberg, T., Pilz, L.K., Zerbini, G., and Winnebeck, E.C. (2019). Chronotype and social jetlag: a (self-) critical review. Biology *8.* 10.3390/biology8030054.
89. Stanewsky, R., Kaneko, M., Emery, P., Beretta, B., Wager-Smith, K., Kay, S.A., Rosbash, M., and Hall, J.C. (1998). The *cry^{b}* mutation identifies Cryptochrome as a circadian photoreceptor in *Drosophila*. Cell *95,* 681-692. 10.1016/S0092-8674(00)81638-4.
90. Helfrich-Förster, C., Winter, C., Hofbauer, A., Hall, J.C., and Stanewsky, R. (2001). The circadian clock of fruit flies is blind after elimination of all known photoreceptors. Neuron *30,* 249-261. 10.1016/S0896-6273(01)00277-X.
91. Yoshii, T., Hermann-Luibl, C., Kistenpfennig, C., Schmid, B., Tomioka, K., and Helfrich-Förster, C. (2015). Cryptochrome-dependent and -independent circadian entrainment circuits in *Drosophila*. J Neurosci *35,* 6131-6141. 10.1523/jneurosci.0070-15.2015.
92. Alejevski, F., Saint-Charles, A., Michard-Vanhée, C., Martin, B., Galant, S., Vasiliauskas, D., and Rouyer, F. (2019). The HisCl1 histamine receptor acts in photoreceptors to synchronize *Drosophila* behavioral rhythms with light-dark cycles. Nat. Commun. *10,* 252. 10.1038/s41467-018-08116-7.
93. Shawa, N., Rae, D.E., and Roden, L.C. (2018). Impact of seasons on an individual's chronotype: current perspectives. Nat. Sci. Sleep *10,* 345-354. 10.2147/nss.s158596.

94. Leocadio-Miguel, M.A., Louzada, F.M., Duarte, L.L., Areas, R.P., Alam, M., Freire, M.V., Fontenele-Araujo, J., Menna-Barreto, L., and Pedrazzoli, M. (2017). Latitudinal cline of chronotype. Sci. Rep. *7,* 5437. 10.1038/s41598-017-05797-w.

95. Zerbini, G., Winnebeck, E.C., and Merrow, M. (2021). Weekly, seasonal, and chronotype-dependent variation of dim-light melatonin onset. J. Pineal Res. *70,* e12723..

96. Vollmer, C., Randler, C., and Milia, L.D. (2012). Further evidence for the influence of photoperiod at birth on chronotype in a sample of German adolescents. Chronobiol. Int. *29,* 1345-1351. 10.3109/07420528.2012.728656.

97. Duffy, J.F., Rimmer, D.W., and Czeisler, C.A. (2001). Association of intrinsic circadian period with morningness–eveningness, usual wake time, and circadian phase. Behav. Neurosci. *115,* 895-899. 10.1037/0735-7044.115.4.895.

98. Baylies, M.K., Bargiello, T.A., Jackson, F.R., and Young, M.W. (1987). Changes in abundance or structure of the per gene product can alter periodicity of the Drosophila clock. Nature *326,* 390-392. 10.1038/326390a0.

99. Boomgarden, A.C., Sagewalker, G.D., Shah, A.C., Haider, S.D., Patel, P., Wheeler, H.E., Dubowy, C.M., and Cavanaugh, D.J. (2019). Chronic circadian misalignment results in reduced longevity and large-scale changes in gene expression in *Drosophila*. BMC Genom. *20,* 14. 10.1186/s12864-018-5401-7.

100. Fortini, M.E., and Rubin, G.M. (1990). Analysis of cis-acting requirements of the *Rh3* and *Rh4* genes reveals a bipartite organization to rhodopsin promoters in *Drosophila melanogaster*. Genes Dev *4,* 444-463. 10.1101/gad.4.3.444.

101. Weir, P.T., and Dickinson, M.H. (2012). Flying *Drosophila* orient to sky polarization. Curr. Biol. *22,* 21-27. 10.1016/j.cub.2011.11.026.

102. Wernet, M.F., Velez, M.M., Clark, D.A., Baumann-Klausener, F., Brown, J.R., Klovstad, M., Labhart, T., and Clandinin, T.R. (2012). Genetic dissection reveals two separate retinal substrates for polarization vision in *Drosophila*. Curr. Biol. *22*, 12-20. 10.1016/j.cub.2011.11.028.

103. Hardie, R.C. (2012). Polarization vision: *Drosophila* enters the arena. Curr. Biol. *22,* R12-14. 10.1016/j.cub.2011.11.016.

104. Reppert, S.M., Gegear, R.J., and Merlin, C. (2010). Navigational mechanisms of migrating monarch butterflies. Trends in neurosciences *33*, 399-406. 10.1016/j.tins.2010.04.004.

105. Schlichting, M., Menegazzi, P., Rosbash, M., and Helfrich-Forster, C. (2019). A distinct visual pathway mediates high-intensity light adaptation of the circadian clock in *Drosophila*. J Neurosci *39*, 1621-1630. 10.1523/JNEUROSCI.1497-18.2018.

106. Schlichting, M., Grebler, R., Peschel, N., Yoshii, T., and Helfrich-Förster, C. (2014). Moonlight detection by *Drosophila*'s endogenous clock depends on multiple photopigments in the compound eyes. J. Biol. Rhythms *29*, 75-86. 10.1177/0748730413520428.

107. Schlichting, M., Grebler, R., Menegazzi, P., and Helfrich-Förster, C. (2015). Twilight dominates over moonlight in adjusting *Drosophila*'s activity pattern. J. Biol. Rhythms *30*, 117-128. 10.1177/0748730415575245.

108. Berson David, M., Dunn Felice, A., and Takao, M. (2002). Phototransduction by retinal ganglion cells that set the circadian clock. Science *295*, 1070-1073. 10.1126/science.1067262.

109. Panda, S., Provencio, I., Tu Daniel, C., Pires Susana, S., Rollag Mark, D., Castrucci Ana, M., Pletcher Mathew, T., Sato Trey, K., Wiltshire, T., Andahazy, M., et al. (2003). Melanopsin is required for non-image-forming photic responses in blind mice. Science *301*, 525-527. 10.1126/science.1086179.

110. van der Meijden, W.P., Van Someren, J.L., te Lindert, B.H.W., Bruijel, J., van Oosterhout, F., Coppens, J.E., Kalsbeek, A., Cajochen, C., Bourgin, P., and Van Someren, E.J.W. (2016). Individual differences in sleep timing relate to melanopsin-based phototransduction in healthy adolescents and young adults. Sleep *39*, 1305-1310. 10.5665/sleep.5858.

111. Roecklein, K.A., Wong, P.M., Franzen, P.L., Hasler, B.P., Wood-Vasey, W.M., Nimgaonkar, V.L., Miller, M.A., Kepreos, K.M., Ferrell, R.E., and Manuck, S.B. (2012). Melanopsin gene variations interact with season to predict sleep onset and chronotype. Chronobiol. Int. *29*, 1036-1047. 10.3109/07420528.2012.706766.

112. Aschoff, J., and Pohl, H. (1978). Phase relations between a circadian rhythm and its zeitgeber within the range of entrainment. Sci. Nat. *65*, 80-84. 10.1007/BF00440545.

113. Duffy, J.F., and Czeisler, C.A. (2002). Age-related change in the relationship between circadian period, circadian phase, and diurnal preference in humans. Neurosci. Lett. *318*, 117-120.

114. Price, J.L., Blau, J., Rothenfluh, A., Abodeely, M., Kloss, B., and Young, M.W. (1998). *double-time* is a novel *Drosophila* clock gene that regulates PERIOD protein accumulation. Cell *94*, 83-95. 10.1016/S0092-8674(00)81224-6.

115. Fang, Y., Sathyanarayanan, S., and Sehgal, A. (2007). Post-translational regulation of the *Drosophila* circadian clock requires protein phosphatase 1 (PP1). Genes Dev *21*, 1506-1518. 10.1101/gad.1541607.

116. Lim, C., and Allada, R. (2013). ATAXIN-2 activates PERIOD translation to sustain circadian rhythms in *Drosophila*. Science *340*, 875-879. 10.1126/science.1234785.

117. Meyer, N., Harvey, A.G., Lockley, S.W., and Dijk, D.-J. (2022). Circadian rhythms and disorders of the timing of sleep. The Lancet *400*, 1061-1078. 10.1016/S0140-6736(22)00877-7.

118. Pfeffer, M., Korf, H.-W., and von Gall, C. (2015). Chronotype and stability of spontaneous locomotor activity rhythm in BMAL1-deficient mice. Chronobiol. Int. *32*, 81-91. 10.3109/07420528.2014.956218.

119. Pfeffer, M., Wicht, H., von Gall, C., and Korf, H.-W. (2015). Owls and larks in mice. Front. Neurol. *6*. 10.3389/fneur.2015.00101.

120. Ulgherait, M., Midoun, A.M., Park, S.J., Gatto, J.A., Tener, S.J., Siewert, J., Klickstein, N., Canman, J.C., Ja, W.W., and Shirasu-Hiza, M. (2021). Circadian autophagy drives iTRF-mediated longevity. Nature *598*, 353-358. 10.1038/s41586-021-03934-0.

121. Gill, S., Le, H.D., Melkani, G.C., and Panda, S. (2015). Time-restricted feeding attenuates age-related cardiac decline in *Drosophila*. Science *347*, 1265-1269. 10.1126/science.1256682.

122. Stoleru, D., Peng, Y., Agosto, J., and Rosbash, M. (2004). Coupled oscillators control morning and evening locomotor behaviour of *Drosophila*. Nature *431*, 862-868. 10.1038/nature02926.

123. Rieger, D., Shafer, O.T., Tomioka, K., and Helfrich-Förster, C. (2006). Functional Analysis of Circadian Pacemaker Neurons in *Drosophila melanogaster*. J Neurosci *26*, 2531-2543. 10.1523/jneurosci.1234-05.2006.

124. Pendergast, J.S., and Yamazaki, S. (2018). The mysterious food-entrainable oscillator: insights from mutant and engineered mouse models. J. Biol. Rhythms *33*, 458-474. 10.1177/0748730418789043.

125. Richter, C.P. (1922). A behavioristic study of the activity of the rat. Comp. Psychol. Monogr. *1*, *2*, 56-56.

126. Oishi, K., Shiota, M., Sakamoto, K., Kasamatsu, M., and Ishida, N. (2004). Feeding is not a more potent Zeitgeber than the light-dark cycle in *Drosophila*. NeuroReport *15*, 739-743.

127. Singh, V.J., Potdar, S., and Sheeba, V. (2022). Effects of food availability cycles on phase and period of activity-rest rhythm in *Drosophila melanogaster*. J. Biol. Rhythms *37*, 528-544. 10.1177/07487304221111287.

128. Blum, D.J., Hernandez, B., and Zeitzer, J.M. (2023). Early time-restricted eating advances sleep in late sleepers: a pilot randomized controlled trial. J Clin Sleep Med. 10.5664/jcsm.10754.

129. Facer-Childs, E.R., Middleton, B., Skene, D.J., and Bagshaw, A.P. (2019). Resetting the late timing of 'night owls' has a positive impact on mental health and performance. Sleep Med. *60*, 236-247.

130. Lockley, S.W., Arendt, J., and Skene, D.J. (2007). Visual impairment and circadiam rhythm disorders. Dialogues Clin. Neurosci. *9*, 301-314. 10.31887/DCNS.2007.9.3/slockley.

131. Tabandeh, H., Lockley, S.W., Buttery, R., Skene, D.J., Defrance, R., Arendt, J., and Bird, A.C. (1998). Disturbance of sleep in blindness. Am. J. Ophthalmol. *126*, 707-712.

132. Quera Salva, M.A., Hartley, S., Léger, D., and Dauvilliers, Y.A. (2017). Non-24-hour sleep–wake rhythm disorder in the totally blind: diagnosis and management. Front. Neurol. *8*, 686. 10.3389/fneur.2017.00686.

133. Hood, S., and Amir, S. (2017). The aging clock: circadian rhythms and later life. J. Clin. Investig. *127*, 437-446. 10.1172/JCI90328.

134. Zauner, J., Plischke, H., and Strasburger, H. (2022). Spectral dependency of the human pupillary light reflex. Influences of pre-adaptation and chronotype. PloS one *17*, e0253030. 10.1371/journal.pone.0253030.

135. Deibel, S.H., McDonald, R.J., and Kolla, N.J. (2020). Are owls and larks different when it comes to aggression? genetics, neurobiology, and behavior. Frontiers in behavioral neuroscience *14*, 39. 10.3389/fnbeh.2020.00039.

136. Storelli, G., Defaye, A., Erkosar, B., Hols, P., Royet, J., and Leulier, F. (2011). *Lactobacillus plantarum* promotes *Drosophila* systemic growth by modulating hormonal signals through TOR-dependent nutrient sensing. Cell Metab. *14*, 403-414. 10.1016/j.cmet.2011.07.012.

137. Du, X., Yu, L., Ling, S., Xie, J., and Chen, W. (2021). High-salt diet impairs the neurons plasticity and the neurotransmitters-related biological processes. Nutrients *13*. 10.3390/nu13114123.

138. Pfeiffenberger, C., Lear, B.C., Keegan, K.P., and Allada, R. (2010). Locomotor activity level monitoring using the *Drosophila* Activity Monitoring (DAM) System. Cold Spring Harb. Protoc. *2010*, pdb.prot5518. 10.1101/pdb.prot5518.

139. Geissmann, Q., Garcia Rodriguez, L., Beckwith, E.J., and Gilestro, G.F. (2019). Rethomics: an R framework to analyse high-throughput behavioural data. PloS one *14*, e0209331. 10.1371/journal.pone.0209331.

140. Gilestro, G.F. (2012). Video tracking and analysis of sleep in *Drosophila melanogaster*. Nat. Protoc. *7*, 995-1007. 10.1038/nprot.2012.041.

141. Murphy, K.R., Deshpande, S.A., Yurgel, M.E., Quinn, J.P., Weissbach, J.L., Keene, A.C., Dawson-Scully, K., Huber, R., Tomchik, S.M., and Ja, W.W. (2016). Postprandial sleep mechanics in *Drosophila*. eLife *5*, e19334. 10.7554/eLife.19334.

142. Charlton-Perkins, M., and Cook, T.A. (2010). Building a fly eye: terminal differentiation events of the retina, corneal lens, and pigmented epithelia. Current topics in developmental biology *93*, 129-173. 10.1016/B978-0-12-385044-7.00005-9.

143. Wobbrock, J., Findlater, L., Gergle, D., and Higgins, J. (2011). The aligned rank transform for nonparametric factorial analyses using only ANOVA procedures 10.1145/1978942.1978963.

144. Kraemer, M.U.G., Reiner, R.C., Brady, O.J., Messina, J.P., Gilbert, M., Pigott, D.M., Yi, D., Johnson, K., Earl, L., Marczak, L.B., et al. (2019). Past and future spread of the arbovirus vectors Aedes aegypti and Aedes albopictus. Nature Microbiology *4*, 854-863. 10.1038/s41564-019-0376-y.

145. Kraemer, M.U.G., Sinka, M.E., Duda, K.A., Mylne, A.Q.N., Shearer, F.M., Barker, C.M., Moore, C.G., Carvalho, R.G., Coelho, G.E., Van Bortel, W., et al. (2015). The global distribution of the arbovirus vectors Aedes aegypti and Ae. albopictus. eLife *4*, e08347. 10.7554/eLife.08347.

146. Ryan, S.J., Carlson, C.J., Mordecai, E.A., and Johnson, L.R. (2019). Global expansion and redistribution of Aedes-borne virus transmission risk with climate change. PLOS Neglected Tropical Diseases *13*, e0007213. 10.1371/journal.pntd.0007213.

147. Brady, O.J., Gething, P.W., Bhatt, S., Messina, J.P., Brownstein, J.S., Hoen, A.G., Moyes, C.L., Farlow, A.W., Scott, T.W., and Hay, S.I. (2012). Refining the Global Spatial Limits of Dengue Virus Transmission by Evidence-Based Consensus. PLOS Neglected Tropical Diseases *6*, e1760. 10.1371/journal.pntd.0001760.

148. Huang, Y.-J.S., Higgs, S., and Vanlandingham, D.L. (2019). Emergence and re-emergence of mosquito-borne arboviruses. Current Opinion in Virology *34*, 104-109.

149. Tauxe, Genevieve M., MacWilliam, D., Boyle, Sean M., Guda, T., and Ray, A. (2013). Targeting a Dual Detector of Skin and CO2 to Modify Mosquito Host Seeking. Cell *155*, 1365-1379.

150. Matthews, B.J., Younger, M.A., and Vosshall, L.B. (2019). The ion channel ppk301 controls freshwater egg-laying in the mosquito Aedes aegypti. eLife *8*, e43963. 10.7554/eLife.43963.

151. Greppi, C., Laursen, W.J., Budelli, G., Chang, E.C., Daniels, A.M., van Giesen, L., Smidler, A.L., Catteruccia, F., and Garrity, P.A. (2020). Mosquito heat seeking is driven by an ancestral cooling receptor. Science *367*, 681-684. 10.1126/science.aay9847.

152. Younger, M.A., Herre, M., Ehrlich, A.R., Gong, Z., Gilbert, Z.N., Rahiel, S., Matthews, B.J., and Vosshall, L.B. (2020). Non-canonical odor coding ensures

unbreakable mosquito attraction to humans. bioRxiv, 2020.2011.2007.368720. 10.1101/2020.11.07.368720.

153. Zhan, Y., Alonso San Alberto, D., Rusch, C., Riffell, J.A., and Montell, C. (2021). Elimination of vision-guided target attraction in Aedes aegypti using CRISPR. Current Biology *31*, 4180-4187.e4186.

154. Laursen, W.J., Budelli, G., Tang, R., Chang, E.C., Busby, R., Shankar, S., Gerber, R., Greppi, C., Albuquerque, R., and Garrity, P.A. (2023). Humidity sensors that alert mosquitoes to nearby hosts and egg-laying sites. Neuron *111*, 874-887.e878.

155. Corfas, R.A., and Vosshall, L.B. (2015). The cation channel TRPA1 tunes mosquito thermotaxis to host temperatures. eLife *4*, e11750. 10.7554/eLife.11750.

156. Jové, V., Gong, Z., Hol, F.J.H., Zhao, Z., Sorrells, T.R., Carroll, T.S., Prakash, M., McBride, C.S., and Vosshall, L.B. (2020). Sensory Discrimination of Blood and Floral Nectar by Aedes aegypti Mosquitoes. Neuron.

157. Dennis, E.J., Goldman, O.V., and Vosshall, L.B. (2019). Aedes aegypti Mosquitoes Use Their Legs to Sense DEET on Contact. Current Biology *29*, 1551-1556.e1555. 10.1016/j.cub.2019.04.004.

158. Baik, L.S., and Carlson, J.R. (2020). The mosquito taste system and disease control. Proceedings of the National Academy of Sciences *117*, 32848-32856. 10.1073/pnas.2013076117.

159. Smallegange, R.C., Verhulst, N.O., and Takken, W. (2011). Sweaty skin: an invitation to bite? Trends in Parasitology *27*, 143-148.

160. Zhao, Z., Zung, J.L., Hinze, A., Kriete, A.L., Iqbal, A., Younger, M.A., Matthews, B.J., Merhof, D., Thiberge, S., Ignell, R., et al. (2022). Mosquito brains encode unique features of human odour to drive host seeking. Nature *605*, 706-712. 10.1038/s41586-022-04675-4.

161. Acree, F., Turner, R.B., Gouck, H.K., Beroza, M., and Smith, N. (1968). L-Lactic Acid: A Mosquito Attractant Isolated from Humans. Science *161*, 1346-1347. 10.1126/science.161.3848.1346.

162. Raji, J.I., Melo, N., Castillo, J.S., Gonzalez, S., Saldana, V., Stensmyr, M.C., and DeGennaro, M. (2019). Aedes aegypti Mosquitoes Detect Acidic Volatiles Found in Human Odor Using the IR8a Pathway. Current Biology *29*, 1253-1262.e1257.

163. Montell, C., and Zwiebel, L.J. (2016). Chapter Ten - Mosquito Sensory Systems. In Advances in Insect Physiology, A.S. Raikhel, ed. (Academic Press), pp. 293-328.
164. Teng, B., Wilson, C.E., Tu, Y.-H., Joshi, N.R., Kinnamon, S.C., and Liman, E.R. (2019). Cellular and Neural Responses to Sour Stimuli Require the Proton Channel Otop1. Current Biology *29*, 3647-3656.e3645.
165. Ganguly, A., Chandel, A., Turner, H., Wang, S., Liman, E.R., and Montell, C. (2021). Requirement for an Otopetrin-like protein for acid taste in *Drosophila*. Proceedings of the National Academy of Sciences *118*, e2110641118. doi:10.1073/pnas.2110641118.
166. Matthews, B.J., Dudchenko, O., Kingan, S.B., Koren, S., Antoshechkin, I., Crawford, J.E., Glassford, W.J., Herre, M., Redmond, S.N., Rose, N.H., et al. (2018). Improved reference genome of Aedes aegypti informs arbovirus vector control. Nature *563*, 501-507. 10.1038/s41586-018-0692-z.
167. Kefauver, J.M., Ward, A.B., and Patapoutian, A. (2020). Discoveries in structure and physiology of mechanically activated ion channels. Nature *587*, 567-576. 10.1038/s41586-020-2933-1.
168. Kim, B.H., Ha, H., Seo, E.S., and Lee, S.J. (2013). Effect of fluid viscosity on the liquid-feeding flow phenomena of a female mosquito. Journal of Experimental Biology *216*, 952-959. 10.1242/jeb.072710.
169. Nicolson, S.W., de Veer, L., Köhler, A., and Pirk, C.W.W. (2013). Honeybees prefer warmer nectar and less viscous nectar, regardless of sugar concentration. Proceedings of the Royal Society B: Biological Sciences *280*, 20131597. 10.1098/rspb.2013.1597.
170. Lois-Milevicich, J., Schilman, P.E., and Josens, R. (2021). Viscosity as a key factor in decision making of nectar feeding ants. Journal of Insect Physiology *128*, 104164.
171. Choumet, V., Attout, T., Chartier, L., Khun, H., Sautereau, J., Robbe-Vincent, A., Brey, P., Huerre, M., and Bain, O. (2012). Visualizing Non Infectious and Infectious Anopheles gambiae Blood Feedings in Naive and Saliva-Immunized Mice. PloS one *7*, e50464. 10.1371/journal.pone.0050464.
172. Liu, C., and Zhang, W. (2022). Molecular basis of somatosensation in insects. Current opinion in neurobiology *76*, 102592.
173. Murthy, S.E., Dubin, A.E., Whitwam, T., Jojoa-Cruz, S., Cahalan, S.M., Mousavi, S.A.R., Ward, A.B., and Patapoutian, A. (2018). OSCA/TMEM63 are an

evolutionarily conserved family of mechanically activated ion channels. eLife *7*, e41844. 10.7554/eLife.41844.

174. Li, Q., and Montell, C. (2021). Mechanism for food texture preference based on grittiness. Current Biology *31*, 1850-1861.e1856.

175. Zhao, X., Yan, X., Liu, Y., Zhang, P., and Ni, X. (2016). Co-expression of mouse TMEM63A, TMEM63B and TMEM63C confers hyperosmolarity activated ion currents in HEK293 cells. Cell Biochemistry and Function *34*, 238-241.

176. Zhang, Y.V., Aikin, T.J., Li, Z., and Montell, C. (2016). The Basis of Food Texture Sensation in Drosophila. Neuron *91*, 863-877.